The Islamic University Of Gaza

Postgraduate Studies

Faculty of Engineering

Department of Communication Systems Engineering

Master Thesis

Synthesis of Multiplexers Based on Coupled Resonator Structures Using Coupling Matrix Optimization

Prepared by:

Deeb A Tubail

Supervisor

Dr. Talal F. Skaik

A thesis submitted for the Master degree of Science in Communication Engineering

December 2013

1435 هـ

Abstract

In this thesis, design techniques of coupled resonator circuits used in synthesizing two port filters and three port diplexers are developed to synthesize *N* port multiplexers. Novel general structures are proposed here and they can achieve an arbitrary number of channels, different responses and various properties and characteristics. The synthesis of the proposed multiplexers is based on optimization approach where the couplings coefficients between resonators presented by coupling matrix are found from optimization techniques by minimizing a cost function. The cost function which is utilized in this thesis has been used previously in literatures. Scattering parameters formulas are derived to suit the *N* port multiplexers. Different structures with various properties and responses are given and their results prove the ability of the general structure to achieve a massive scale of interesting characteristics and demands. The general structure is a cascade of diplexers which may reduce the complexity of the structure especially during the optimization. This structure has lot of advantages, it has no limits for number of channels and it has no extra resonators or external junctions and power distribution network, also it has a small size.

الملخص

في هذه الرسالة تم تطوير تقنيات تصميم دوائر الرنين المترابطة المستخدمة في تصميم المرشحات ثنائية النوافذ لبناء الأجهزة متعددة المنافذ. وكذلك تم تقديم هيكلية غير مألوفة عامة للأجهزة متعددة المنافذ قادرة على تصميم أي عدد من القنوات باستجابات مختلفة ومواصفات متعددة. تصميم هذه الأجهزة متعددة المنافذ يعتمد على إيجاد أفضل معاملات ترابط بين دوائر الرنين لتحقق أقل قيمة لدائرة الكلفة حيث أن هذه الدالة تم الحصول عليها من دراسات سابقة. معادلات عناصر التبدد تم اشتقاقها لتناسب الأجهزة متعددة المنافذ. تم تقديم أمثلة متنوعة كبرهان على قدرة هذا الهيكل الجديد العام على تحيق الأنواع المختلفة من الاستجابة بمواصفات وخصائص متعددة. الهيكل المقترح يمكن اعتباره عدد متتابع من الأجهزة ثلاثية المنافذ مما يساعد في تقليل تعقيد الهيكل خصوصا في عمليات تحقيق الأمثلية. هذا الهيكل يحقق العديد من المميزات المتمثلة في عدم محدودية عدد القنوات وكذلك عدم وجود أي دائرة رنين إضافية أو وصلة إضافية أو شبكة لتوزيع القدرة وأضف إلى ذلك صغر حجم الهيكل.

Acknowledgment

I would like to thank my supervisor Dr. Talal F. Skaik for his cooperation and support. His ideas and help have been a significant factor for success in my thesis. Also I would like to express my respects to the electrical engineering department at the Islamic university in Gaza. Finally ,I am highly indebted to my family and friends for their encouragements.

Table of Contents

Chapter1

Introduction

1.1 Overview of multiplexers and their applications

The term microwaves may be used to describe electromagnetic (EM) waves with frequencies ranging from 300 MHz to 300 GHz, which correspond to wavelengths (in free space) from 1 m to 1 mm. The EM waves with frequencies above 30 GHz and up to 300 GHz are also called millimeter waves because their wavelengths are in the millimeter range (1–10 mm). Therefore, by extension, the RF/microwave applications can be referred to as communications, radar, navigation, radio astronomy, sensing, medical instrumentation, and others that explore the usage of frequency spectrums in the range of, say, 300 kHz up to 300 GHz. For convenience, some of these frequency spectrums are further divided into many frequency bands. Filters play important roles in many RF/microwave applications. They are used to separate or combine different frequencies. The electromagnetic spectrum is limited and has to be shared; filters are used to select or confine the RF/microwave signals within assigned spectral limits. Emerging applications such as wireless communications continue to challenge RF/microwave filters with ever more stringent requirements—higher performance, smaller size, lighter weight, and lower cost. Depending on the requirements and specifications, RF/microwave filters may be designed as lumped element or distributed element circuits; they may be realized in various transmission line structures, such as waveguide, coaxial line, and microstrip. The recent advance of novel materials and fabrication technologies, including monolithic microwave integrated circuit (MMIC), microelectromechanic system (MEMS), micromachining, high-temperature superconductor (HTS), and low-temperature cofired ceramics (LTCC), has stimulated the rapid development of new microstrip and other filters. In the meantime, advances in computer-aided design(CAD) tools such as full-wave electromagnetic (EM) simulators have revolutionized filter design. Many novel microstrip filters with advanced filtering characteristics have been demonstrated [1].

Multiplexers (MUXs) are used in communication system applications, where there is a need to separate a wideband signal into a number of narrowband signals (RF channels). Channelization of the allocated frequency band allows flexibility for the flow of communication traffic in a multiuser environment. Amplification of individual channels also eases the requirements on the high-power amplifiers (HPAs), enabling them to operate at relatively high efficiency with an acceptable degree of nonlinearity. Multiplexers are also employed to provide the opposite function, that is, to combine several narrowband channels into a single wideband composite signal for transmission via a common antenna. Multiplexers are, therefore, referred to as channelizers or combiners. Due to the reciprocity of filter networks, a MUX can also be configured to separate the transmit and receive frequency bands in a common device, referred to as a duplexer or diplexer. Multiplexers have many applications such as in satellite payloads,

wireless systems, and electronic warfare (EW) systems[2]. Figure (1.1) shows the function of multiplexer in satellite communication as channelizers or combiners[3].

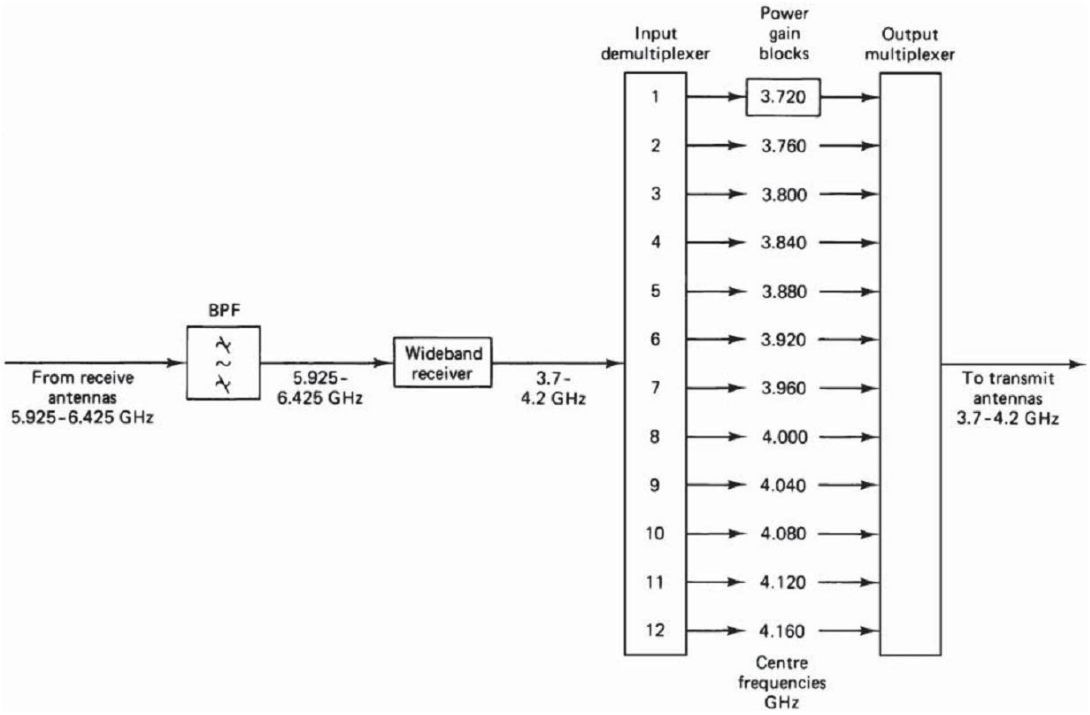

Figure (1.1): Multiplexers in satellite communication .

Conventionally, multiplexer is achieved by using a set of band pass filters (usually known as channel filters), and an energy distribution network. The channel filters pass frequencies within a specified range, and reject frequencies outside the specified boundaries, and the distribution network divides the signal going into the filters, or combines the signals coming from the filters. There are several approaches in designing and implementing multiplexers. The most common configurations are manifold coupled, circulator-coupled, and hybrid-coupled multiplexers [2]. The most commonly used distribution configurations are E- or H-plane *n*-furcated power dividers[4,5], circulators [6] and manifold structures[7,8]. Figure (1.2) shows the configuration of n-channel multiplexer with a 1:*n* divider multiplexing network, and figure (1.3) depicts a circulator configuration, where each channel consists of a band pass filter and a channel-dropping circulator. The power divider configurations can be designed for multiplexers with wideband channels or large channel separation [4]. The circulator configurations have no interaction between channel filters and they are simple to tune. They provide flexibility in adding new channels or replacing the channel filters by different filters without disrupting the whole design. However, they exhibit relatively higher losses since signals pass through the circulators in succession, causing extra loss per trip[2].

In manifold configurations, channel filters are connected by transmission lines: microstrip, coaxial, waveguide, etc. and T-junctions. The configuration of the manifold multiplexer is shown in figure (1.4). Manifold configurations provide low insertion loss and high power handling capability. However, they have complex design, and they do not have the flexibility in adding channels to an existing multiplexer, or

changing a channel since this requires a new design. Also, tuning the whole multiplexer can be time consuming [2].

Other multiplexer configurations based on coupled resonators without external energy distribution networks have also been proposed in literature. Star-junction multiplexers are considered a general approach to the synthesis of microwave multiplexers presenting a star-junction topology (with a resonating junction) [9]. Figure (1.5) shows general architecture of the resonant star-junction multiplexer[9]. Figure (1.6) shows a general four-channel star junction multiplexer topology [10]. The grey circle in Figure (1.6) represents a resonant junction, an extra resonator in addition to the resonators forming the filters. This multiplexer does not include external junctions like the conventional multiplexers, which makes miniaturization possible. Moreover, it has fewer connections to the resonating junction than the star -junction multiplexers [11,12].

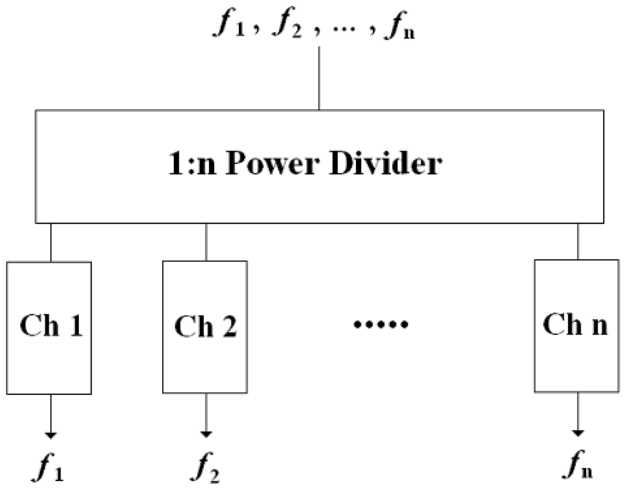

Figure (1.2): Configuration of multiplexer with a 1:*n* divider multiplexing network.

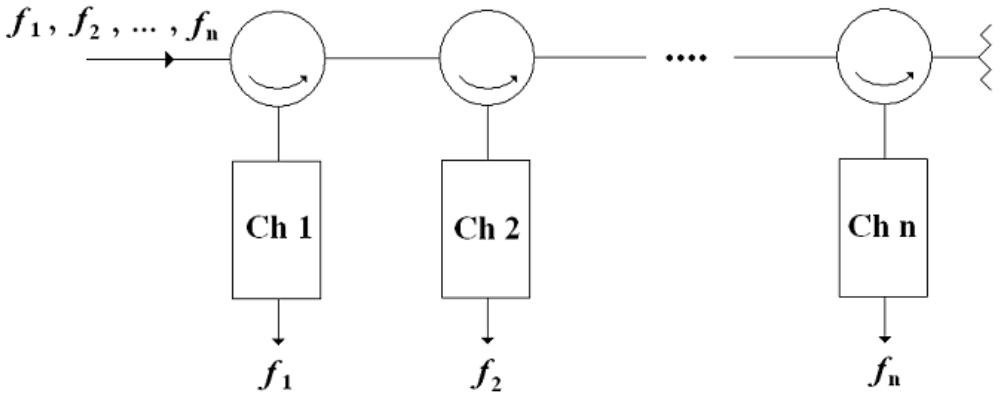

Figure (1.3): Configuration of circulator-coupled multiplexer.

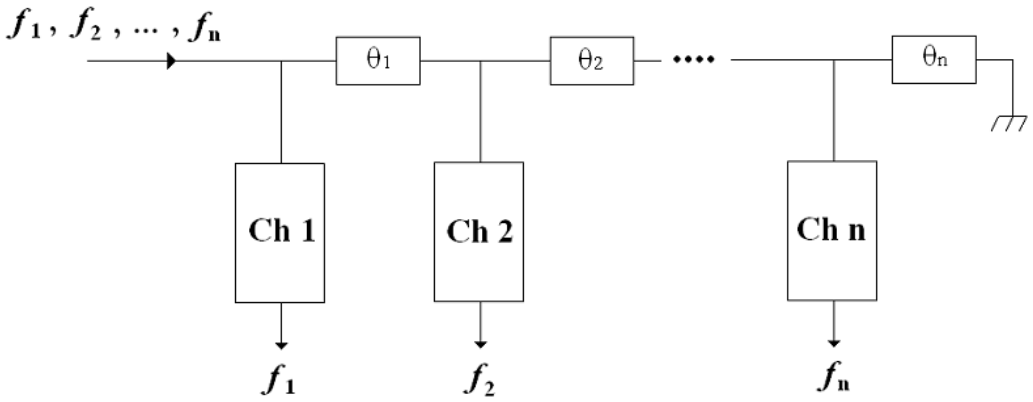

Figure (1.4): Configuration of manifold-coupled multiplexer.

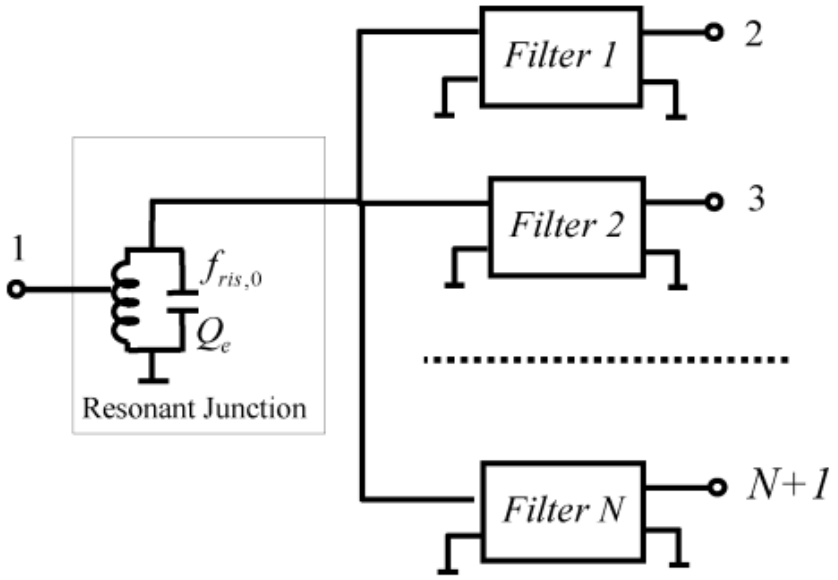

Figure (1.5): General architecture of the resonant star-junction multiplexer.

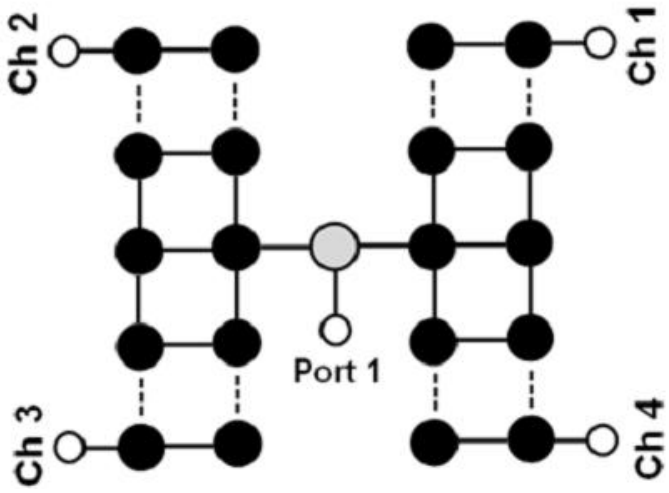

Figure (1.6): General four-channel star-junction multiplexer topology.

1.2 Overview of classical Analog Filters

1.2.1. Butterworth filters

The first family of analog filters are the butter-worth filters which are called maximally flat filters. The butter-worth filter is designed to have as flat a frequency response as possible in the pass-band. A butter-worth filter of order n is a low pass analog filter with the following squared magnitude response [16]. Figure (1.7) present the squared magnitude response of a low pass butter-worth filter.

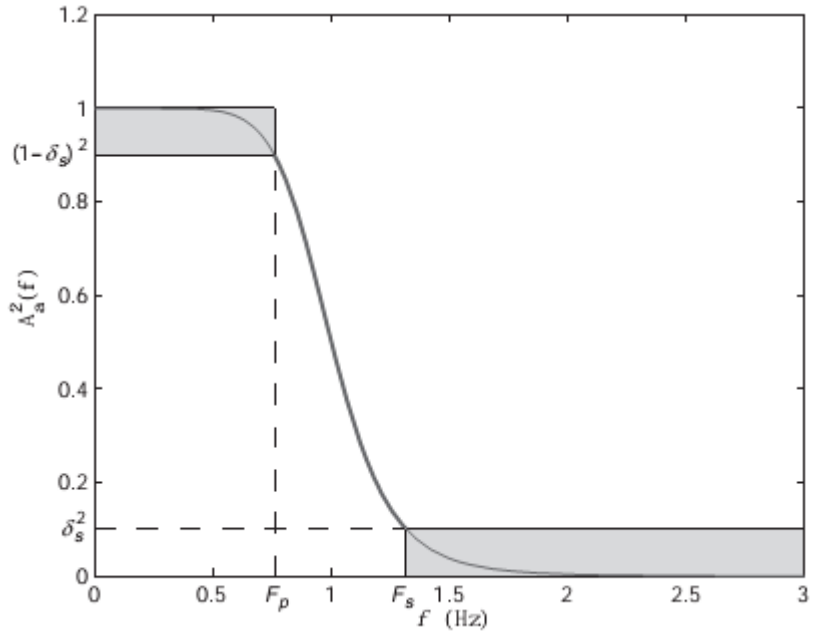

Figure (1.7): Squared Magnitude Response of a Low-pass butterworth Filter.

1.2.2. Chebyshev filter

The magnitude responses of Butterworth filters are smooth and flat because of the maximally flat property. However, a drawback of the maximally flat property is that the transition band of a Butterworth filter is not as narrow as it could be. An effective way to decrease the width of the transition band is to allow ripples or oscillations in the pass-band or the stop-band. They are two types of Chebyshev, when the ripple is in the pass-band, it's called Chebyshev (type I) and when the ripple is in the stop-band, it's called Chebyshev (type II) [16]. Figure (1.8) (a) show Squared Magnitude Responses of a Chebyshev type I and figure (1.8) (b) Squared Magnitude Responses of a Chebyshev type II.

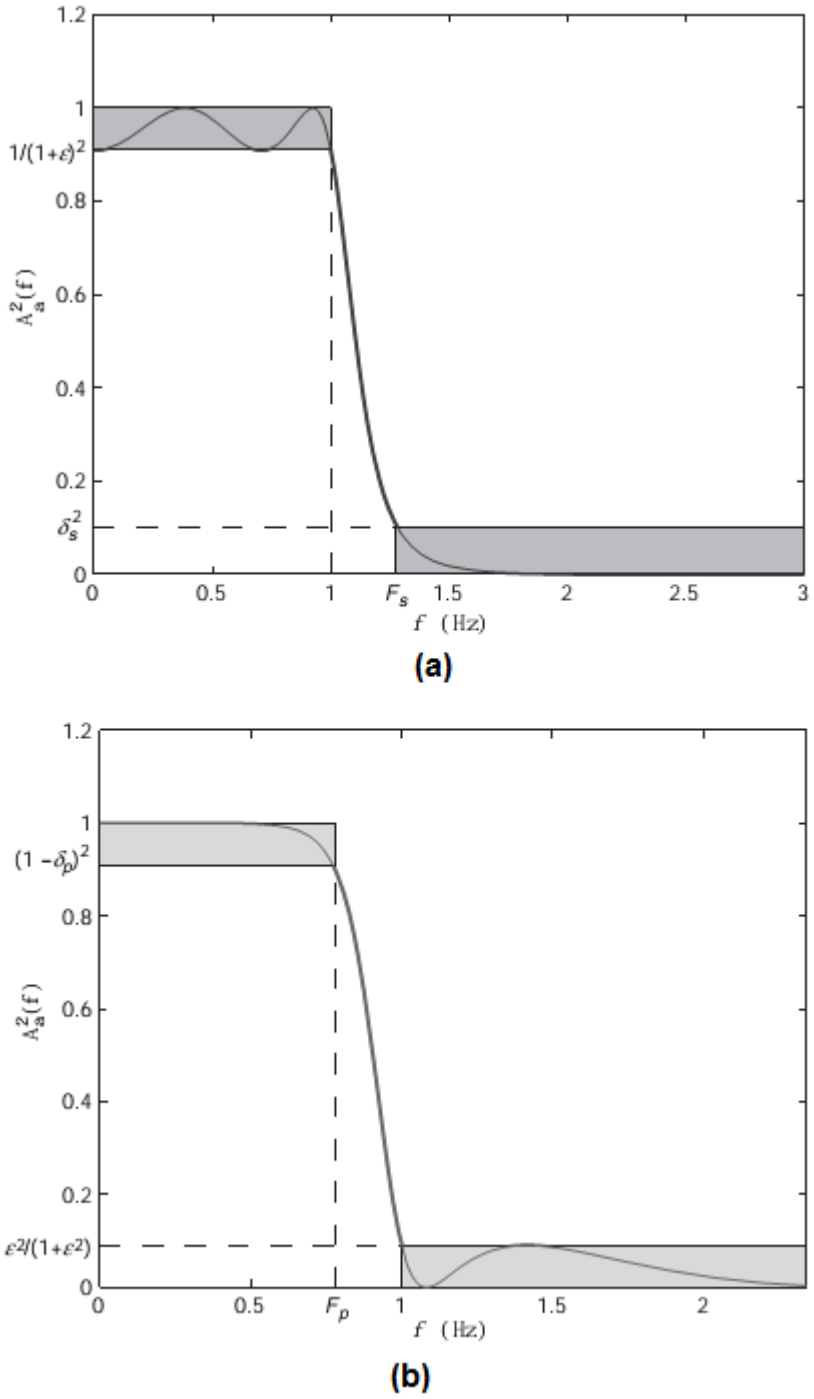

Figure (1.8): (a) Squared Magnitude Responses of a Chebyshev type I.

(b) Squared Magnitude Responses of a Chebyshev type II.

1.2.3. Elliptic filter

The last classical low-pass analog filter is the elliptic or Cauer filter. Elliptic filters are filters that are equiripple in both the pass-band and the stop-band. The elliptic filter has the narrowest transition edge among all types [16]. As the ripple in the stop-band approaches zero, the filter becomes a type I Chebyshev filter. As the ripple in the pass-band approaches zero, the filter becomes a type II Chebyshev filter and finally, as both ripple values approach zero, the filter becomes a Butterworth filter. Figure (1.9) show Squared Magnitude Responses of an elliptic filter.

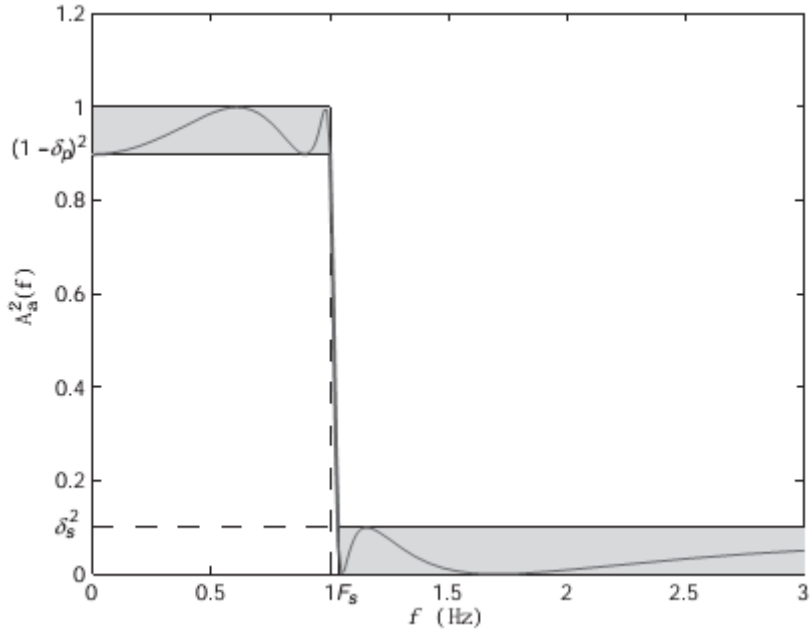

Figure (1.9): Squared Magnitude Response of an elliptic Filter.

1.3 Literature review

There have been several techniques proposed to synthesize multiplexers : classical methods as manifold coupled, circulator-coupled, and hybrid-coupled multiplexers and coupled resonator circuit as modern technique also is used in synthesis of multiplexers.

Here is a list of some previous researches interested in designing multiplexers by coupled resonant circuit as follows:

1. In [9], a novel method for the polynomial synthesis of microwave star junction multiplexers with a resonating junction has been presented. The channel filters can be arbitrarily specified, including the assignment of transmission zeros. An iterative procedure has been developed for the evaluation of the characteristic polynomials of the multiplexer, which are subsequently used for

computing the polynomials associated with the channel filters; these polynomials are then employed for synthesizing the filters like they were detached from the multiplexer. In this way, the results of the synthesis process are not constrained to a specific configuration, which must be only compatible with the assigned transmission zeros. However star junction multiplexer has extra junction in addition to the resonators which construct multiplexer's channel.

2. In [11], the author has presented a novel design of coupled resonator star junction multiplexer which has been designed at the X-band with four non contiguous channels. The multiplexer topology is based on coupled resonator structure, and it consists of thirteen waveguide cavities, one of which serves as a resonating junction. The multiplexer has reduced number of connections to the resonating junction and also has smaller size than other conventional multiplexers, as it does not contain manifolds, circulators ...etc. This design contains extra resonator which isn't used in constructing multiplexer's channel.

3. In [12], the author has proposed novel topologies of star junction multiplexers with resonating junctions. These proposed topologies have an advantage that the number of connections to the resonating junction is reduced and thus allowing multiplexers with more channels to be implemented. An optimization technique is used to synthesize the coupling matrix of the proposed multiplexers in this paper. However the resonating junctions have a fewer connection and it is an extra resonator which increase the size of multiplexer.

4. In [13], the authors have presented a three channel multiplexer formed exclusively by coupled microwave resonators, just like filters but with lager number of ports. This multiplexer only has three channels and this is unsuitable for applications which need more channels.

5. In [14], a novel procedure for synthesizing narrow band triplexers for base station combiners has been presented. The design results have been represented by the coupling coefficients and external Qs of the filters constituting the combiner. The synthesis algorithm is very fast and it allows to obtain a quasi equiripple response in the three pass bands. This multiplexer talks about special case three channels while lots of applications demand larger number of channels.

6. In [15], design techniques used for two-port coupled resonator circuits has been extended to design three-port microwave components such as power dividers with arbitrary power division and diplexers with novel topologies. The synthesis of these devices employs similar coupling matrix optimization techniques to those of coupled resonator filters. The three port devices only has two channel but this isn't suitable for applications that need more channels.

1.4 Thesis motivation

Many techniques have been used in designing multiplexer. Each technique different from others and has some advantages and disadvantages as mentioned in section 1.1. The thesis addresses the development of a general novel topology for *N*-channels multiplexer by coupled resonators circuits without using external distributions networks and hence compact multiplexers cab be designed. Designing multiplexers in conventional techniques is achieved by using a set of band pass filters (usually known as channel filters), and an energy distribution network (junction) which is used to divide the incoming signals into the *N* channels. Extensive work has been reported in literature on miniaturization of multiplexers using specific types of compact resonators or using folded structures. However, the use of external junctions in the structures of these diplexers might involve design complexity. Design techniques for multiplexers based on coupled resonator structures without external junctions have also been presented in literature. These structures are miniaturized since there are no external junctions or extra resonators in addition to the resonators forming filters. Coupled resonator circuits with multiple channels are addressed in this thesis to synthesize compact novel topologies for multiplexers with reduced design complexity and with no practical constraints in realization. Figure (1.10) illustrates a proposed general structure for *N* channel multiplexer without any extra resonator or any extra junction. The isolation between channels changes by changing number of resonators per channel and changing the position of channels.

1.5 Thesis overview

The objective of this research work is synthesis of coupled-resonator circuits with multiple outputs (*N* channels) by extending the design techniques used for three-port coupled resonator diplexers (two channel) proposed in[10,15]. Figure (1.11) shows a topology for a two-channel coupled resonator diplexer, where the circles represent resonators and the lines linking the resonators represent couplings. Synthesis methods of coupled resonator diplexers have been presented in literature. The work in this thesis extends the theory of two-channel coupled resonator diplexer to *N*- channels coupled resonator circuits, such as the general network shown in figure (1.10). This enables synthesis of other passive microwave components made of coupled resonators such as multi channel multiplexers. In this thesis a general novel topology of multiplexer will be presented and multiplexers based on the novel topologies with different number of channels and different number of resonators will be presented.

In chapter two circuits with both electrical and magnetic coupling are presented. A detailed derivation of the coupling matrix of multiple coupled resonators with multiple outputs is also presented. The relations between the scattering parameters for *N* port network in addition to the general coupling matrix are also presented in this chapter. These equations in chapter 2 are used as a basis to the synthesis of *N* channels multiplexers in the next chapters.

In chapter three, frequency transformation, derivation of cost function and optimization are presented. After that in chapter four, various examples for different coupled resonators will be presented whereby the coupling matrix obtained from

optimization will be given as well as the ideal multiplexer response of the scattering parameters. The final chapter provides summary and conclusions drawn from this work.

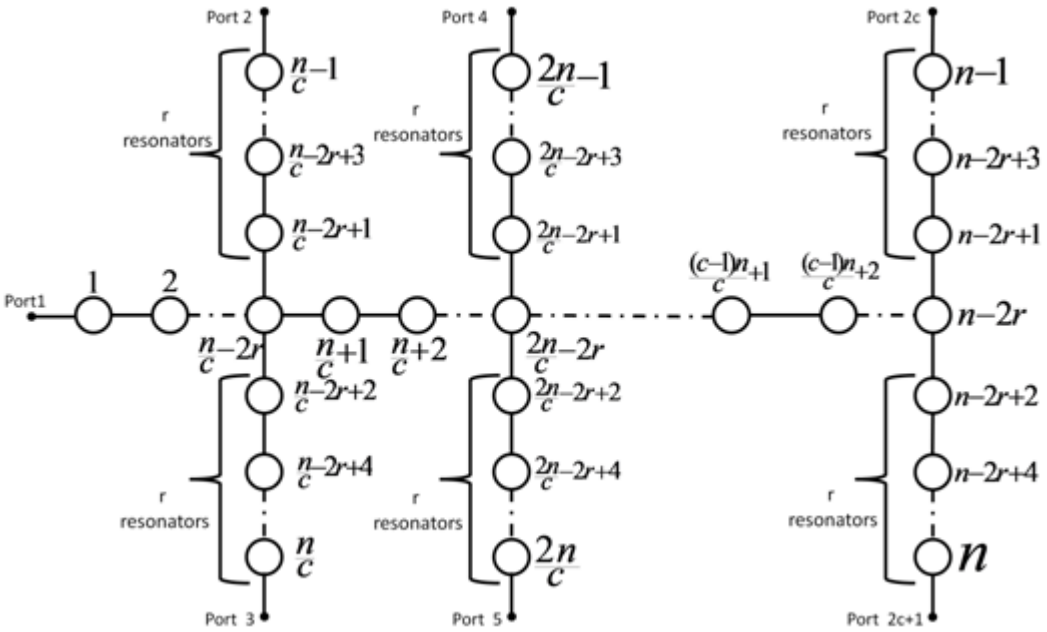

Figure (1.10): A General novel *N* channel multiplexer topology.

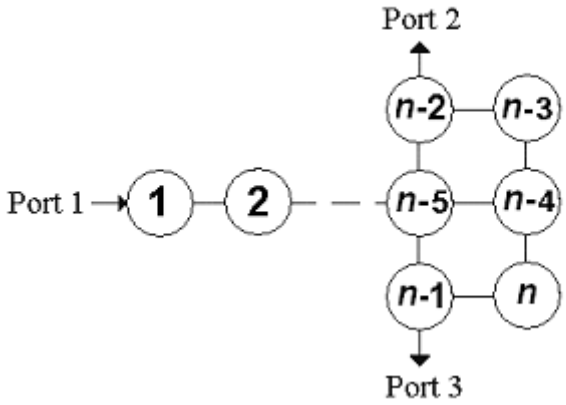

Figure (1.11): The structure of coupled resonators diplexer

REFERENCES

1. J.S. Hong and M.J. Lancaster, "Microstrip filters for RF/microwave applications", Wiley, 2001
2. R. Cameron, C. Kudsia and R. Mansour, "Microwave filters for communication systems", Wiley, 2007.
3. D. Roddy, " Satellite Communications", McGraw-Hill, 2006.
4. J. A. Ruiz-Cruz, J. R. Montejo-Garai, J. M. Rebollar, and S. Sobrino, "Compact full ku-band triplexer with improved E-plane power divider," Progress In Electromagnetics Research, Vol. 86, pp. 39-51, 2008.
5. J. Dittloff, J. Bornemann, and F. Arndt, "Computer aided design of optimum E- or H-plane N-furcated waveguide power dividers," in Proc. European Microwave Conference, Sept. 1987, pp. 181-186.
6. R.R. Mansour, et al., "Design considerations of superconductive input multiplexers for satellite applications," IEEE Transactions on Microwave Theory and Techniques, vol. 44, no. 7, pt. 2, pp. 1213-1229, 1996.
7. J. D. Rhodes and R. Levy, "Design of general manifold multiplexers," IEEE Transactions on Microwave Theory and Techniques, vol. 27, no. 2, pp. 111-123, 1979.
8. R.J. Cameron and M. Yu, "Design of manifold coupled multiplexers," IEEE Microwave Mag., vol. 8, no. 5, pp. 46–59, Oct. 2007.
9. G. Macchiarella and S. Tamiazzo, "Synthesis of star-junction multiplexers", IEEE Transactions on Microwave Theory and Techniques, Vol. 58, No. 12, 3732-3741, 2010.
10. T. Skaik, "Synthesis of Coupled Resonator Circuits with Multiple Outputs using Coupling Matrix Optimization", PhD thesis, University of Birmingham, March 2011.
11. T. Skaik, "Star-Junction X-band Coupled Resonator Multiplexer," Proceedings of the 12th Mediterranean Microwave Symposium, Istanbul, Turkey, Sept 2012.
12. T. Skaik, " Novel Star Junction Coupled Resonator Multiplexer Structures," Progress in Electromagnetics Research Letters, Vol. 31, pp. 113-120, April 2012.
13. A. Garcfa-Lamperez, M. Salazar-Palma, and T. K. Sarkar, "Compact Multiplexer Formed by Coupled Resonators with Distributed Coupling", IEEE Antennas and Propagation Society International Symposium, USA, 2005, pp. 89-92.
14. G. Macchiarella, S. Tamiazzo, "Design of Triplexer Combiners for Base Stations of Mobile Communications", The IEEE MTT-S International Microwave Symposium, USA, May 2010.
15. T. Skaik, M. Lancaster, and F. Huang, “Synthesis of multiple output coupled resonator microwave circuits using coupling matrix optimization,” IET Journal of Microwaves, Antenna & Propagation, vol.5, no.9, pp. 1081-1088, June 2011.
16. R. J. Schilling and S. L. Harris," Fundamentals of Digital Signal Processing Using MATLAB", Cengage Learning,2005.

Chapter 2

Coupled Resonator Circuits

2.1 Introduction

Coupled resonator circuits are of importance for design of RF/microwave filters (and multiplexers), in particular the narrow-band pass filters that play a significant role in many applications. There is a general technique for designing coupled resonator filters in the sense that it can be applied to any type of resonator despite its physical structure. It has been applied to the design of waveguide filters, dielectric resonator filter, ceramic combline filters, microstrip filters, superconducting filters, and micromachined filters. This design method is based on coupling coefficients of inter coupled resonators and the external quality factors of the input and output resonators [1].

The general coupling matrix is of importance for representing a wide range of coupled-resonator filter topologies. It can be formulated either from a set of loop equations or from a set of node equations. This leads to a very useful formula for analysis and synthesis of coupled-resonator filter circuits in terms of coupling coefficients and external quality factors [1].

2.2 Deriving Coupling Matrix of N-port Networks

In a coupled resonator circuit, energy may be coupled between adjacent resonators by a magnetic field or an electric field or both. The coupling matrix can be derived from the equivalent circuit by formulation of impedance matrix for magnetically coupled resonators or admittance matrix for electrically coupled resonators [1]. This approach has been used to derive the coupling matrix of coupled resonator filters, and it is adopted in [2] to derive general coupling matrix of an N-port n-coupled resonators circuit. Magnetic coupling and electric coupling will be considered separately and later a solution will be generalized for both types of couplings [2].

2.2.1. Circuits with magnetically coupled resonators

Considering only magnetic coupling between adjacent resonators, the equivalent circuit of magnetically coupled n-resonators with multiple ports is shown in figure (2.1) [2], where i represents loop current, L, C denote the inductance and capacitance, and R denotes the resistance (represents a port). It is assumed that all the resonators are connected to ports, and the signal source is connected to resonator 1. It is also assumed that the coupling exists between all the resonators.

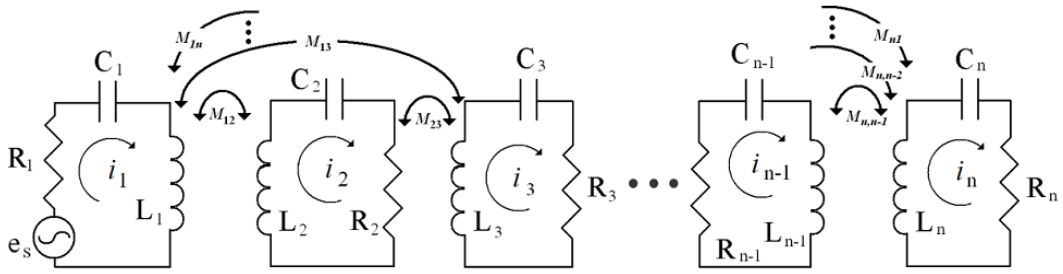

Figure (2.1): Equivalent circuit of magnetically *n*-coupled resonators in *N*-port network

Using Kirchoff's voltage law, the loop equations are derived as follows,

$$\begin{aligned}
&\left(R_1 + j\omega L_1 + \frac{1}{j\omega C_1}\right) i_1 \quad - j\omega L_{12} i_2 \quad \ldots \quad - j\omega L_{1n} i_n \quad = e_s \\
&- j\omega L_{21} i_1 \quad + \left(R_2 + j\omega L_2 + \frac{1}{j\omega C_2}\right) i_2 \quad \ldots \quad - j\omega L_{2n} i_n \quad = 0 \\
&\qquad\qquad \vdots \\
&- j\omega L_{n1} i_1 \quad - j\omega L_{n2} i_2 \quad \ldots \quad + \left(R_n + j\omega L_n + \frac{1}{j\omega C_n}\right) i_n \quad = 0
\end{aligned} \tag{2.1}$$

where $M_{ij} = L_{ij}/L$ and L_{ab}=L_{ba} denotes the mutual inductance between resonators *a* and *b*. The matrix form representation of these equations is as follows,

$$\begin{bmatrix}
R_1 + j\omega L_1 + \frac{1}{j\omega C_1} & - j\omega L_{12} & \cdots & - j\omega L_{1(n-1)} & - j\omega L_{1n} \\
- j\omega L_{21} & R_2 + j\omega L_2 + \frac{1}{j\omega C_2} & \cdots & - j\omega L_{2(n-1)} & - j\omega L_{2n} \\
\vdots & \vdots & \ddots & \vdots & \vdots \\
- j\omega L_{(n-1)1} & - j\omega L_{(n-1)2} & \cdots & R_{n-1} + j\omega L_{n-1} + \frac{1}{j\omega C_{n-1}} & - j\omega L_{(n-1)n} \\
- j\omega L_{n1} & - j\omega L_{n2} & \cdots & - j\omega L_{n(n-1)} & R_n + j\omega L_n + \frac{1}{j\omega C_n}
\end{bmatrix}
\begin{bmatrix} i_1 \\ i_2 \\ \vdots \\ i_{n-1} \\ i_n \end{bmatrix} =
\begin{bmatrix} e_s \\ 0 \\ \vdots \\ 0 \\ 0 \end{bmatrix}$$

(2.2)

or equivalently [Z].[i]=[e], where [Z] is the impedance matrix. Assuming all resonators are synchronized at the same resonant frequency $\omega_0 = \frac{1}{\sqrt{LC}}$, *where* $L = L_1 = L_2 = ... = L_{n-1} = L_n$ and $C = C_1 = C_2 = ... = C_{n-1} = C_n$ the impedance matrix [Z] can be expressed by $[Z] = \omega_0 LFBW.[\overline{Z}]$ where $FBW = \Delta\omega/\omega_0$ is the fractional bandwidth, and $[\overline{Z}]$ is the normalized impedance matrix, given by,

$$[\overline{Z}] = \begin{bmatrix} \frac{R_1}{\omega_0 L(FBW)} + P & \frac{-j\omega L_{12}}{\omega_0 L}\frac{1}{FBW} & \cdots & \frac{-j\omega L_{1(n-1)}}{\omega_0 L}\frac{1}{FBW} & \frac{-j\omega L_{1n}}{\omega_0 L}\frac{1}{FBW} \\ \frac{-j\omega L_{21}}{\omega_0 L}\frac{1}{FBW} & \frac{R_2}{\omega_0 L(FBW)} + P & \cdots & \frac{-j\omega L_{2(n-1)}}{\omega_0 L}\frac{1}{FBW} & \frac{-j\omega L_{2n}}{\omega_0 L}\frac{1}{FBW} \\ \vdots & \vdots & \ddots & \vdots & \vdots \\ \frac{-j\omega L_{(n-1)1}}{\omega_0 L}\frac{1}{FBW} & \frac{-j\omega L_{(n-1)2}}{\omega_0 L}\frac{1}{FBW} & \cdots & \frac{R_{n-1}}{\omega_0 L(FBW)} + P & \frac{-j\omega L_{(n-1)n}}{\omega_0 L}\frac{1}{FBW} \\ \frac{-j\omega L_{n1}}{\omega_0 L}\frac{1}{FBW} & \frac{-j\omega L_{n2}}{\omega_0 L}\frac{1}{FBW} & \cdots & \frac{-j\omega L_{n(n-1)}}{\omega_0 L}\frac{1}{FBW} & \frac{R_n}{\omega_0 L(FBW)} + P \end{bmatrix}$$

(2.3)

where $P = \frac{j}{FBW}\left(\frac{\omega}{\omega_0} - \frac{\omega_0}{\omega}\right)$ is the complex low pass frequency variable.

Defining the external quality factor for resonator i as $Q_{ei} = \omega_0 L/R_i$ and the coupling coefficient as $M_{ij} = L_{ij}/L$, and assuming $\omega/\omega_0 \approx 1$ for narrow band approximation, $[\overline{Z}]$ is simplified to

$$[\overline{Z}] = \begin{bmatrix} \frac{1}{q_{e1}} + P & -jm_{12} & \cdots & -jm_{1(n-1)} & -jm_{1n} \\ -jm_{21} & \frac{1}{q_{e2}} + P & \cdots & -jm_{2(n-1)} & -jm_{2n} \\ \vdots & \vdots & \ddots & \vdots & \vdots \\ -jm_{(n-1)1} & -jm_{(n-1)2} & \cdots & \frac{1}{q_{e(n-1)}} + P & -jm_{(n-1)n} \\ -jm_{n1} & -jm_{n2} & \cdots & -jm_{n(n-1)} & \frac{1}{q_{en}} + P \end{bmatrix}$$

(2.4)

where q_{ei} is the scaled external quality factor $q_{ei} = Q_{ei}.FBW$ and m_{ij} is the normalized coupling coefficient $m_{ij} = M_{ij}/FBW$

The network representation for the circuit in figure (2.1) , considering *N*-ports, is shown in figure (2.2), where a_1, b_1, a_2, b_2, a_3, b_3, a_n and b_n are the wave variables, V_1, I_1, V_2, I_2, V_3, I_3, V_n and I_n are the voltage and current variables and i is the loop current. It is assumed that port 1 is connected to resonator 1, port 2 is connected to resonator 2, port 3 is connected to resonator 3, and port *N* is connected to resonator *N*.

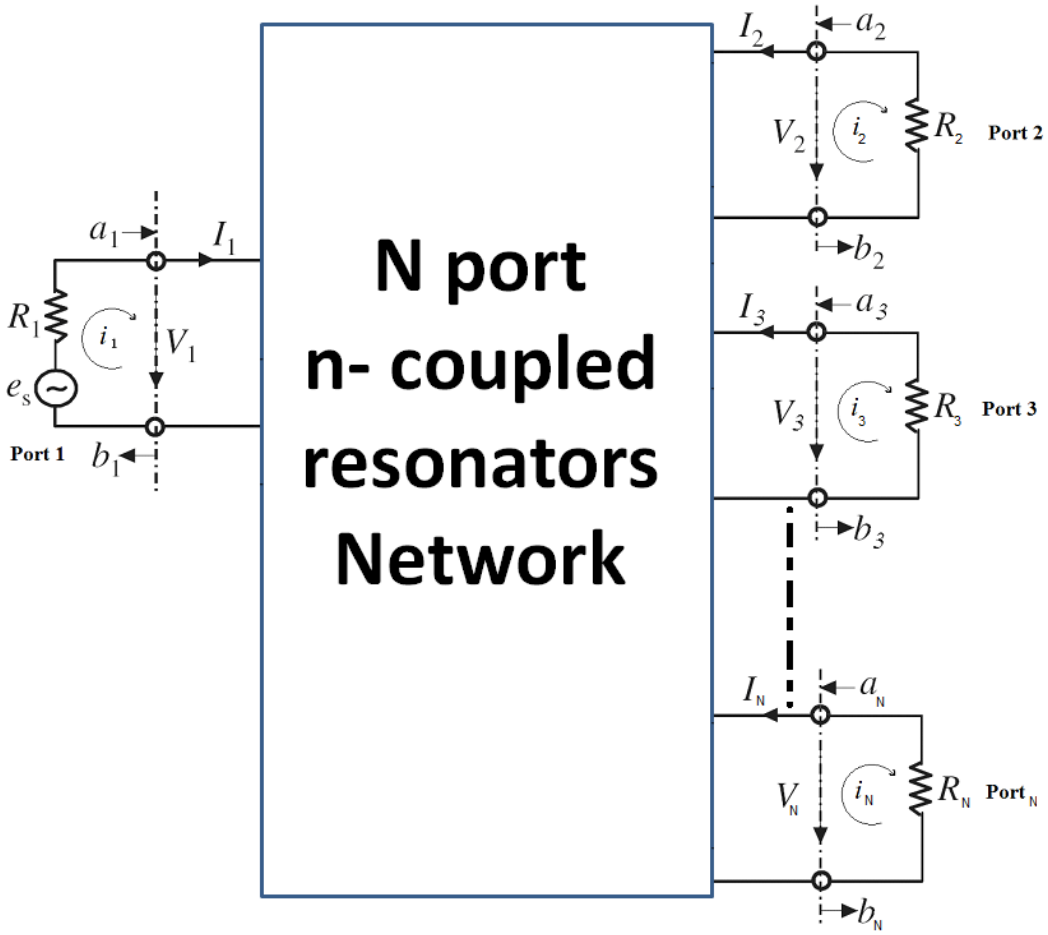

Figure (2.2): Network representation of N-port circuit

The relationships between the voltage and current variables and the wave variables are defined as follows [3],

$$V_N = \sqrt{R}(a_N + b_N) \text{ and } I_N = \frac{1}{\sqrt{R}}(a_N - b_N) \qquad (2.5)$$

Solving the equations (2.5) for a_N and b_N, the wave parameters are defined as follows,

$$a_N = \frac{1}{2}\left(\frac{V_N}{\sqrt{R}} + \sqrt{R} I_N\right) \quad \text{and} \quad b_N = \frac{1}{2}\left(\frac{V_N}{\sqrt{R}} - \sqrt{R} I_N\right) \tag{2.6}$$

where N is the port number, and R corresponds to R_1 for port 1, R_2 for port 2, R_3 for port 3, and R_N for port N. It is noticed in the circuit in figure (2.2) that $I_1=i_1$, $I_2= - i_2$, $I_3= - i_3$, $I_N= - i_N$, and $V_1=e_s-i_1R_1$. Accordingly, the wave variables may be rewritten as follows

$$a_1 = \frac{e_s}{2\sqrt{R_1}} \qquad b_1 = \frac{e_s - 2i_1R_1}{2\sqrt{R_1}}$$

$$a_2 = 0 \qquad b_2 = i_2\sqrt{R_2}$$

$$a_3 = 0 \qquad b_3 = i_3\sqrt{R_3}$$

$$a_N = 0 \qquad b_N = i_N\sqrt{R_N} \tag{2.7}$$

The S-parameters are found from the wave variables as follows,

$$S_{11} = \left.\frac{b_1}{a_1}\right|_{a_2=a_3=.....=a_N=0} = 1 - \frac{2R_1i_1}{e_s}$$

$$S_{21} = \left.\frac{b_2}{a_1}\right|_{a_2=a_3=.....=a_N=0} = \frac{2\sqrt{R_1R_2}\,i_2}{e_s}$$

$$S_{31} = \left.\frac{b_3}{a_1}\right|_{a_2=a_3=.....=a_N=0} = \frac{2\sqrt{R_1R_3}\,i_3}{e_s}$$

$$S_{N1} = \left.\frac{b_N}{a_1}\right|_{a_2=a_3=.....=a_N=0} = \frac{2\sqrt{R_1R_N}\,i_N}{e_s} \tag{2.8}$$

Solving (2.2) for currents loops,

$$i_1 = \frac{e_s}{\omega_0 L.FBW}\left[Z\right]_{11}^{-1}$$

$$i_2 = \frac{e_s}{\omega_0 L.FBW}\left[Z\right]_{21}^{-1}$$

$$i_3 = \frac{e_s}{\omega_0 L.FBW}\left[Z\right]_{31}^{-1}$$

$$i_N = \frac{e_s}{\omega_0 L.FBW}[Z]^{-1}_{N1} \tag{2.9}$$

and by substitution of equations (2.9) into equations (2.8), we have,

$$S_{11} = 1 - \frac{2R_1}{\omega_0 L.FBW}[Z]^{-1}_{11}$$

$$S_{21} = \frac{2\sqrt{R_1 R_2}}{\omega_0 L.FBW}[Z]^{-1}_{21}$$

$$S_{31} = \frac{2\sqrt{R_1 R_3}}{\omega_0 L.FBW}[Z]^{-1}_{31}$$

$$S_{N1} = \frac{2\sqrt{R_1 R_N}}{\omega_0 L.FBW}[Z]^{-1}_{N1} \tag{2.10}$$

In terms of external quality factors $q_{ei} = \frac{\omega_0 L.FBW}{R_i}$, the S-parameters become,

$$S_{11} = 1 - \frac{2}{q_{e1}}[Z]^{-1}_{11}$$

$$S_{21} = \frac{2}{\sqrt{q_{e1} q_{e2}}}[Z]^{-1}_{21}$$

$$S_{31} = \frac{2}{\sqrt{q_{e1} q_{e3}}}[Z]^{-1}_{31}$$

$$S_{N1} = \frac{2}{\sqrt{q_{e1} q_{eN}}}[Z]^{-1}_{N1} \tag{2.11}$$

where q_{e1}, $q_{e2,}$ q_{e3} and q_{eN} are the normalized external quality factors at resonators 1, 2, 3 and N respectively. In case of asynchronously tuned coupled-resonator circuit, resonators may have different resonant frequencies, and extra entries m_{ii} are added to the diagonal entries in $[Z]$ to account for asynchronous tuning as follows,

$$[Z]=\begin{bmatrix} \frac{1}{q_{e1}}+P-jm_{11} & -jm_{12} & \cdots & -jm_{1(n-1)} & -jm_{1n} \\ -jm_{21} & \frac{1}{q_{e2}}+P-jm_{22} & \cdots & -jm_{2(n-1)} & -jm_{2n} \\ \vdots & \vdots & \ddots & \vdots & \vdots \\ -jm_{(n-1)1} & -jm_{(n-1)2} & \cdots & \frac{1}{q_{e(n-1)}}+P-jm_{(n-1)(n-1)} & -jm_{(n-1)n} \\ -jm_{n1} & -jm_{n2} & \cdots & -jm_{n(n-1)} & \frac{1}{q_{en}}+P-jm_{nn} \end{bmatrix} \quad (2.12)$$

2.2.2. Circuits with electrically coupled resonators

The coupling coefficients introduced in the previous section are based on magnetic coupling. This section presents the derivation of coupling coefficients for electrically coupled resonators in an *N*-port circuit, where the electric coupling is represented by capacitors [2]. The normalized admittance matrix $[Y]$ will be derived here in an analogous way to the derivation of the $[Z]$ matrix in the previous section [2].

Shown in figure (2.3) is the equivalent circuit of electrically coupled *n*-resonators in an *N*-port network, where i_s represents the source current, v_i denotes the node voltage, and *G* represents port conductance.

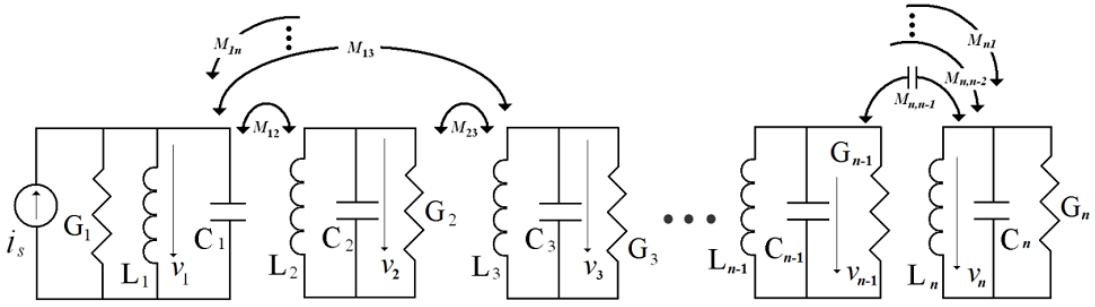

Figure (2.3): Equivalent circuit of electrically n-coupled resonators in N-port network.

It is assumed here that all resonators are connected to ports, and the current source is connected to resonator 1. Also, it is assumed that all resonators are coupled to each other. The solution of this network is found by using Kirchhoff's current law, which states that the algebraic sum of the currents leaving a node is zero. Using this law, the node voltage equations are formulated as follows,

$$\begin{aligned}
&\left(G_1 + j\omega C_1 + \frac{1}{j\omega L_1}\right)v_1 \quad - j\omega C_{12}v_2 \quad \ldots \quad - j\omega C_{1(n-1)}v_{n-1} - j\omega C_{1n}v_n \quad = i_s \\
&- j\omega C_{21}v_1 \quad + \left(G_2 + j\omega C_2 + \frac{1}{j\omega L_2}\right)v_2 \quad \ldots \quad - j\omega C_{2(n-1)}v_{n-1} - j\omega C_{2n}v_n \quad = 0 \\
&\qquad\qquad\qquad\qquad\qquad\qquad\qquad\qquad\qquad\qquad\qquad\qquad\qquad\qquad\qquad\qquad \vdots \\
&- j\omega C_{n1}v_1 \quad - j\omega C_{n2}v_2 \quad \ldots - j\omega C_{n(n-1)}v_{n-1} \quad + \left(G_n + j\omega C_n + \frac{1}{j\omega L_n}\right)v_n \quad = 0
\end{aligned} \tag{2.13}$$

where $M_{ij} = C_{ij}/C$ and $C_{ab}=C_{ba}$ denotes the mutual capacitance between resonators *a* and *b*. The previous equations are represented in matrix form as follows,

$$\begin{bmatrix}
G_1 + j\omega C_1 + \frac{1}{j\omega L_1} & - j\omega C_{12} & \cdots & - j\omega C_{1(n-1)} & - j\omega C_{1n} \\
- j\omega C_{21} & G_2 + j\omega C_2 + \frac{1}{j\omega L_2} & \cdots & - j\omega C_{2(n-1)} & - j\omega C_{2n} \\
\vdots & \vdots & \ddots & \vdots & \vdots \\
- j\omega C_{(n-1)1} & - j\omega C_{(n-1)2} & \cdots & G_{n-1} + j\omega C_{n-1} + \frac{1}{j\omega L_{n-1}} & - j\omega C_{(n-1)n} \\
- j\omega C_{n1} & - j\omega C_{n2} & \cdots & - j\omega C_{n(n-1)} & G_n + j\omega C_n + \frac{1}{j\omega L_n}
\end{bmatrix}
\begin{bmatrix} v_1 \\ v_2 \\ \vdots \\ v_{n-1} \\ v_n \end{bmatrix} =
\begin{bmatrix} i_s \\ 0 \\ \vdots \\ 0 \\ 0 \end{bmatrix} \tag{2.14}$$

or equivalently [Y].[v]=[i], where [Y] is the admittance matrix.

Assuming all resonators are synchronized at the same resonant frequency $\omega_0 = \frac{1}{\sqrt{LC}}$, where $L=L_1=L_2=\ldots=L_{n-1}=L_n$ and $C=C_1=C_2=\ldots=C_{n-1}=C_n$, the admittance matrix [Y] can be expressed by

$$[\mathrm{Y}] = \omega_0 \mathrm{CFBW}.[\mathrm{Y}], \tag{2.15}$$

where $FBW = \Delta\omega/\omega_0$ is the fractional bandwidth, and $[Y]$ is the normalized impedance matrix, given by,

$$[Y]=\begin{bmatrix} \frac{G_1}{\omega_0 C(FBW)}+P & \frac{-j\omega C_{12}}{\omega_0 C}\frac{1}{FBW} & \cdots & \frac{-j\omega C_{1(n-1)}}{\omega_0 C}\frac{1}{FBW} & \frac{-j\omega C_{1n}}{\omega_0 C}\frac{1}{FBW} \\ \frac{-j\omega C_{21}}{\omega_0 C}\frac{1}{FBW} & \frac{G_2}{\omega_0 C(FBW)}+P & \cdots & \frac{-j\omega C_{2(n-1)}}{\omega_0 C}\frac{1}{FBW} & \frac{-j\omega C_{2n}}{\omega_0 C}\frac{1}{FBW} \\ \vdots & \vdots & \ddots & \vdots & \vdots \\ \frac{-j\omega C_{(n-1)1}}{\omega_0 C}\frac{1}{FBW} & \frac{-j\omega C_{(n-1)2}}{\omega_0 C}\frac{1}{FBW} & \cdots & \frac{G_{n-1}}{\omega_0 C(FBW)}+P & \frac{-j\omega C_{(n-1)n}}{\omega_0 C}\frac{1}{FBW} \\ \frac{-j\omega C_{n1}}{\omega_0 C}\frac{1}{FBW} & \frac{-j\omega C_{n2}}{\omega_0 C}\frac{1}{FBW} & \cdots & \frac{-j\omega C_{n(n-1)}}{\omega_0 C}\frac{1}{FBW} & \frac{G_n}{\omega_0 C(FBW)}+P \end{bmatrix}$$

(2.16)

where P is the complex low pass frequency variable.

Defining the external quality factor for resonator i as $Q_{ei}=\omega_0 C/G_i$ and the coupling coefficient as $M_{ij}=C_{ij}/C$, and assuming $\omega/\omega_0 \approx 1$ for narrow band approximation, $[Y]$ is simplified to

$$[Y]=\begin{bmatrix} \frac{1}{q_{e1}}+P & -jm_{12} & \cdots & -jm_{1(n-1)} & -jm_{1n} \\ -jm_{21} & \frac{1}{q_{e2}}+P & \cdots & -jm_{2(n-1)} & -jm_{2n} \\ \vdots & \vdots & \ddots & \vdots & \vdots \\ -jm_{(n-1)1} & -jm_{(n-1)2} & \cdots & \frac{1}{q_{e(n-1)}}+P & -jm_{(n-1)n} \\ -jm_{n1} & -jm_{n2} & \cdots & -jm_{n(n-1)} & \frac{1}{q_{en}}+P \end{bmatrix}$$

(2.17)

where q_{ei} is the scaled external quality factor $q_{ei}=Q_{ei}.FBW$ and m_{ij} is the normalized coupling coefficient $m_{ij}=M_{ij}/FBW$

The network representation for the circuit in figure (2.3), considering *N*-ports, is shown in figure (2.4), where a_1, b_1, a_2, b_2, a_3, b_3, a_n and b_n are the wave variables, V_1, I_1, V_2, I_2, V_3, I_3,V_n and I_n are the voltage and current variables and i is the loop current. It is assumed that port 1 is connected to resonator 1, port 2 is connected to resonator 2, port 3 is connected to resonator 3, and port *N* is connected to resonator *N*.

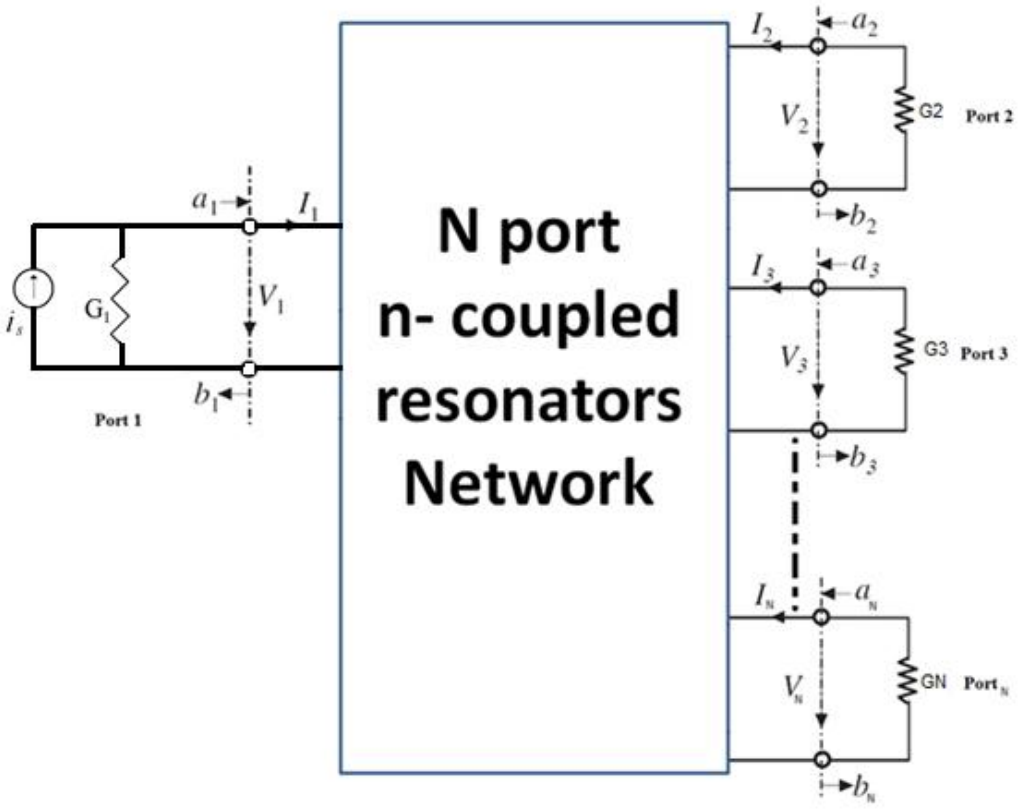

Figure (2.4): Network representation of *N*-port circuit.

It is noticed in the circuit in figure (2.4) that $V_1=v_1$, $V_2=v_2$, $V_3=v_3$, $V_N=V_N$, and $I_1=i_s-v_1G_1$. Accordingly, the wave variables may be rewritten as follows,

$$a_1 = \frac{i_s}{2\sqrt{G_1}} \qquad b_1 = \frac{2v_1G_1 - i_s}{2\sqrt{G_1}}$$

$$a_2 = 0 \qquad b_2 = v_2\sqrt{G_2}$$

$$a_3 = 0 \qquad b_3 = v_3\sqrt{G_3}$$

$$a_N = 0 \qquad b_N = v_N\sqrt{G_N} \qquad (2.18)$$

The S-parameters are found from the wave variables as follows,

$$S_{11} = \left.\frac{b_1}{a_1}\right|_{a_2=a_3=.....=a_N=0} = \frac{2v_1G_1}{i_s} - 1$$

$$S_{21} = \left.\frac{b_2}{a_1}\right|_{a_2=a_3=.....=a_N=0} = \frac{2\sqrt{G_1G_2}v_2}{i_s}$$

$$S_{31} = \left.\frac{b_3}{a_1}\right|_{a_2=a_3=.....=a_N=0} = \frac{2\sqrt{G_1G_3}v_3}{i_s}$$

$$S_{N1} = \left.\frac{b_N}{a_1}\right|_{a_2=a_3=.....=a_N=0} = \frac{2\sqrt{G_1G_N}v_N}{i_s} \tag{2.19}$$

Solving (2.14) for voltage nodes

$$v_1 = \frac{i_s}{\omega_0 C.FBW}[Y]^{-1}_{11}$$

$$v_2 = \frac{i_s}{\omega_0 CFBW}[Y]^{-1}_{21}$$

$$v_3 = \frac{i_s}{\omega_0 C.FBW}[Y]^{-1}_{31}$$

$$v_N = \frac{i_s}{\omega_0 C.FBW}[Y]^{-1}_{N1} \tag{2.20}$$

and by substitution of equations (2.20) into equations (2.19), we have,

$$S_{11} = \frac{2G_1}{\omega_0 C.FBW}[Y]^{-1}_{11} - 1$$

$$S_{21} = \frac{2\sqrt{G_1G_2}}{\omega_0 CFBW}[Y]^{-1}_{21}$$

$$S_{31} = \frac{2\sqrt{G_1G_3}}{\omega_0 C.FBW}[Y]^{-1}_{31}$$

$$S_{N1} = \frac{2\sqrt{G_1G_N}}{\omega_0 C.FBW}[Y]^{-1}_{N1} \tag{2.21}$$

In terms of external quality factors $q_{ei} = \dfrac{\omega_0 CFBW}{G_i}$, the S-parameters become,

$$S_{11} = \frac{2}{q_{e1}}[Y]_{11}^{-1} - 1$$

$$S_{21} = \frac{2}{\sqrt{q_{e1}q_{e2}}}[Y]_{21}^{-1}$$

$$S_{31} = \frac{2}{\sqrt{q_{e1}q_{e3}}}[Y]_{31}^{-1}$$

$$S_{N1} = \frac{2}{\sqrt{q_{e1}q_{eN}}}[Y]_{N1}^{-1} \tag{2.22}$$

To account for asynchronous tuning, the normalized admittance matrix will have extra terms m_{ii} in the principal diagonal, and it will be identical to the normalized impedance matrix in equation (2.12).

2.2.3. General coupling matrix

The derivations in the previous sections show that the normalized admittance matrix of electrically coupled resonators is identical to the normalized impedance matrix of magnetically coupled resonators. Accordingly, a unified solution may be formulated regardless of the type of coupling. In consequence, the S parameters of an *N*-port coupled resonator circuit may be generalized as,

$$S_{11} = 1 - \frac{2}{q_{e1}}[A]_{11}^{-1}$$

$$S_{21} = \frac{2}{\sqrt{q_{e1}q_{e2}}}[A]_{21}^{-1}$$

$$S_{31} = \frac{2}{\sqrt{q_{e1}q_{e3}}}[A]_{31}^{-1}$$

$$S_{N1} = \frac{2}{\sqrt{q_{e1}q_{eN}}}[A]_{N1}^{-1} \tag{2.23}$$

The matrix [A] is given below

$$[A]=\begin{bmatrix} \frac{1}{q_{e1}} & \cdots & 0 & 0 \\ \vdots & \ddots & \vdots & \vdots \\ 0 & \cdots & \frac{1}{q_{e(n-1)}} & 0 \\ 0 & \cdots & 0 & \frac{1}{q_{en}} \end{bmatrix} + P\begin{bmatrix} 1 & \cdots & 0 & 0 \\ \vdots & \ddots & \vdots & \vdots \\ 0 & \cdots & 1 & 0 \\ 0 & \cdots & 0 & 1 \end{bmatrix} - j\begin{bmatrix} m_{11} & \cdots & m_{1(n-1)} & m_{1n} \\ \vdots & \ddots & \vdots & \vdots \\ m_{(n-1)1} & \cdots & m_{(n-1)(n-1)} & m_{(n-1)n} \\ m_{n1} & \cdots & m_{n(n-1)} & m_{nn} \end{bmatrix} \tag{2.24}$$

The formulae in (2.23) and (2.24) will be used as a basis to synthesize *N*-port coupled resonator multiplexer in the next chapters. For completeness, the general formulae of the scattering parameters can be derived analogously to the previous derivations, and they are given by

$$S_{xx} = 1 - \frac{2}{q_{ex}}[A]^{-1}_{xx},$$

$$S_{xy} = \frac{2}{\sqrt{q_{ex}q_{ey}}}[A]^{-1}_{xy}. \tag{2.25}$$

The inverse of the matrix [A] can be described in terms of the adjugate and determinant by employing Cramer‘s rule for the inverse of a matrix,

$$[A]^{-1} = \frac{adj([A])}{\Delta_A}, \qquad \Delta_A \neq 0 \tag{2.26}$$

where $adj([A])$ is the adjugate of the matrix [A], and Δ_A is its determinant. Noting that the adjugate is the transpose of the matrix cofactors, the (x,1) element of the inverse of matrix [A] is:

$$[A]^{-1}_{xy} = \frac{cof_{xy}([A])}{\Delta_A} \tag{2.27}$$

where $cof_{xy}([A])$ is the (x,y) element of the cofactor matrix of [A]. By substitution of (2.27) into (2.25), the following equations are obtained,

$$S_{xx} = 1 - \frac{2}{q_{ex}}\frac{cof_{xx}([A])}{\Delta_A}$$

$$S_{xy} = \frac{2}{\sqrt{q_{ex}q_{ey}}}\frac{cof_{xy}([A])}{\Delta_A} \tag{2.28}$$

The coupled resonator components may be synthesized using different ways: analytic solution to calculate the coupling coefficients, or full synthesis using EM simulation tools, whereby the dimensions of the physical structure are optimized, or optimization techniques to synthesize the coupling matrix [m].The use of full-wave EM simulation is very time consuming when compared to coupling matrix optimization that requires significantly less computational time. Coupling matrix optimization techniques similar to those used to synthesize coupled-resonator filters will be utilized in the current work to produce the coupling matrix entries of the proposed coupled resonator multiplexers. The entries of the coupling matrix [m] are modified at each iteration in the optimization process until an optimal solution is found such that a scalar cost function is minimized. Optimization techniques and cost function formulation will be discussed in Chapter 3.

2.3 Conclusion

The derivation of the coupling matrix of multiple coupled resonators with multiple outputs has been presented. A unified solution has been presented for both electrically and magnetically coupled resonators. The relationships between the scattering parameters and the coupling matrix of an N-port coupled resonator circuit have been formulated. The equations in this chapter will be used as a basis in the synthesis of coupled resonator multiplexers in the next chapters.

REFERENCES

1. J.S. Hong and M.J. Lancaster, "Microstrip filters for RF/microwave applications". New York: Wiley, 2001.
2. T Skaik, "Synthesis of Coupled Resonator Circuits with Multiple Outputs using Coupling Matrix Optimization", PhD thesis, University of Birmingham,2011.
3. M. Radmanesh, RF & Microwave Design Essentials, Authorhouse, 2007.

Chapter 3

Synthesis of Multiplexers using coupling Matrix Optimization

3.1 Introduction

This chapter presents the synthesis of multiplexers using coupling Matrix Optimization. In chapter 1, a general overview has been presented about conventional multiplexers and their advantages and disadvantages. All of these multiplexers have different energy distribution network.

In chapter 2, the theory of coupled resonator circuits for multiple ports has been presented and coupling matrix and scattering parameters for multiple ports network have been derived. In this chapter, frequency transformation is presented, after that based on theory in chapter two, the cost function is formulated to be used in the optimization algorithm. Novel coupled resonator topologies are proposed in this chapter and their synthesis based on coupling matrix optimization will be shown. Numerical examples will be shown in the next chapter.

3.2 Optimization

Optimization theory is a body of mathematical results and numerical methods for finding and identifying the best candidate from a collection of alternatives without having to explicitly enumerate and evaluate all possible alternatives. The process of optimization lies at the root of engineering, since the classical function of the engineer is to design new, better, more efficient, and less expensive systems as well as to devise plans and procedures for the improved operation of existing systems. The power of optimization methods to determine the best case without actually testing all possible cases comes through the use of a modest level of mathematics and at the cost of performing iterative numerical calculations using clearly defined logical procedures or algorithms implemented on computing machines. The development of optimization methodology will therefore require some facility with basic vector matrix manipulations, a bit of linear algebra and calculus, and some elements of real analysis. We use mathematical concepts and constructions not simply to add rigor to the proceedings but because they are the language in terms of which calculation procedures are best developed, defined, and understood. Because of the scope of most engineering applications and the tedium of the numerical calculations involved in optimization algorithms, the techniques of optimization are intended primarily for computer implementation. However, although the methodology is developed with computers in mind, we do not delve into the details of program design and coding. Instead, our emphasis is on the ideas and logic underlying the methods, on the factors involved in selecting the appropriate techniques, and on the considerations important to successful engineering application [1].

The problem of optimization may be formulated as minimization of a scalar objective function $U(\Phi)$, where $U(\Phi)$ is also known as an error function or cost function because it represents the difference between the performance achieved at any stage and the desired specifications. For example, in the case of a microwave filter, the formulation of $U(\Phi)$ may involve the specified and achieved values of the insertion loss and the return loss in the pass band, and the rejection in the stop band. In this thesis, the optimization process aims to minimize the cost function which is specified by the reflection loss, transmission loss and the locations of reflection zeros. The outputs of optimizations are coupling coefficients and the locations of reflection zeros. Optimization problems are usually formulated as minimization of $U(\Phi)$. This does not cause any loss of generality, since the minima of a function $U(\Phi)$ correspond to the maxima of the function $-U(\Phi)$. Thus, by a proper choice of $U(\Phi)$, any maximization problem may be reformulated as a minimization problem. Φ is the set of designable parameters whose values may be modified during the optimization process. In microwave filters, firstly elements of Φ could be the values of capacitors and inductors for a lumped-element or low pass prototype filter, or they could be coupling coefficients for a coupled resonator circuit. But at last, elements of Φ could directly include the physical dimensions of a filter, which are realized using microstrip or other microwave transmission line structures. Usually, there are various constraints on the designable parameters for a feasible solution obtained by optimization. For instance, available or achievable values of lumped elements, the minimum values of microstrip line width, and coupled microstrip line spacing that can be etched. The elements of Φ define a space. A portion of this space where all the constraints are satisfied is called the design space D. In the optimization process, we look for optimum value of Φ inside D [2].

In microwave coupled resonator optimization problems, as well as real world optimization problems, the cost function of many variables will have several local minima, one of them is the global minimum. Local optimization methods are used to find an arbitrary local minimum, which is relatively straightforward. However, finding the global minimum is more challenging and global optimization methods can be used. Local optimization algorithms strongly depend on the initial values of the control parameters. The initial guess should be given as an input to the algorithm that will seek a local minimum within the local neighborhood of the initial guess. However, this local minimum is not guaranteed to be the global minimum. Global optimization algorithms generally do not require initial guess for the control variables, as they generate their own initial values, and they seek the global minimum within the entire search space. In comparison to local methods, global optimization methods are much slower and may take hours or even days to find the optimal solution for problems with tens of variables. Global algorithms tend to be utilized when the local algorithms are not adequate, or when it is of great importance to find the global solution [3].

Lots of optimization methods have been developed for solving constrained and unconstrained optimization problems. Direct Search Optimization is an approach used in solving optimization problems. It makes repeated use of evaluation of the objective function and does not require the derivatives of the objective function. Two typical types of the direct search method are described as follows. Powell's method is a powerful direct search method for multidimensional optimization. A genetic algorithm is the other type of the direct search method which starts with an initial set of random

configurations and uses a process similar to biological evolution to improve upon them. The set of configurations is called the population. During each iteration, called a generation, the configurations in the current population are evaluated using some measure of fitness [2].

The Nelder-Mead simplex algorithm is an enormously popular direct search method for multidimensional unconstrained minimization. It's especially popular in the fields of chemistry, chemical engineering, and medicine. This method attempts to minimize a scalar-valued nonlinear function of real variables using only function values, without any derivative information (explicit or implicit) [4]. This algorithm is applied by using "fminsearch" function available in MATLAB to solve optimization problems in this thesis.

In a gradient-based optimization method, the derivatives of an objective function with respect to the designable parameters are used. The primary reason for the use of derivatives is that at any point in the design space, the negative gradient direction would imply the direction of the greatest rate of decrease of the objective function at that point [2].

Lots of papers talk about synthesizing filters or diplexers using optimization approach. In [6], The authors have used optimization approach in the their paper to synthesize a three channel multiplexer exclusively by coupled microwave resonators.

Also in [7] the authors have synthesized diplexers by applying coupling matrix optimization techniques to those of coupled resonator circuits. After that, in [8] the author proposed novel topologies of star-junction multiplexers with resonating junctions. An optimization technique has been used to synthesize the coupling matrix of the proposed multiplexers in this paper. Also in [9], the author presented a novel design of coupled resonator star-junction multiplexer which was designed at the X-band with four non contiguous channels by optimization method.

Finally in [10], the authors have synthesized filters by optimization a cost function based on the Hausdorff distance between the template sets (the sets of zeros and poles of template filter reflection and transmission characteristics).

3.3 Frequency transformation

The specifications of a multiplexer are usually given in the band-pass frequency domain, in which the real multiplexer operates. As mentioned earlier, the design of the proposed multiplexers takes place in the normalized frequency domain as a low pass prototype. Therefore, a frequency transformation from band pass frequency domain to normalized frequency domain is needed. This section presents frequency transformation formulas of band pass multiplexer with given specification to a low pass prototype. Equation (3.1) is used to calculate the normalized value for each edge in the multiplexer's channels. An illustration of the frequency mapping is shown in figure (3.1). The frequency edges of the bands of the multiplexer are ω_1, ω_2, ω_3,..... and ω_n. These frequencies are mapped into low pass prototype frequencies (x) using the following transformation formula [3,5].

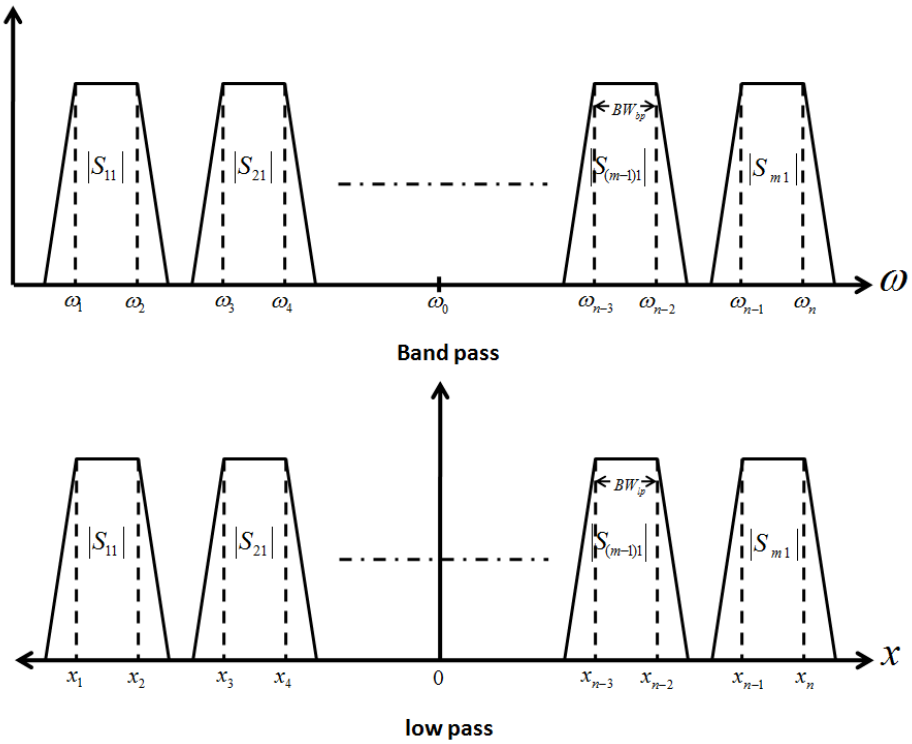

Figure (3.1): Low pass to band pass transformation

$$x_m = \alpha\left(\frac{\omega_m}{\omega_0} - \frac{\omega_0}{\omega_m}\right) \tag{3.1}$$

To map the band edges $x = x_1$ to $\omega = \omega_1$, and $x = x_n$ to $\omega = \omega_n$

$$x_1 = \alpha\left(\frac{\omega_1}{\omega_0} - \frac{\omega_0}{\omega_1}\right) \tag{3.2}$$

$$x_n = \alpha\left(\frac{\omega_n}{\omega_0} - \frac{\omega_0}{\omega_n}\right) \tag{3.3}$$

Solving equations (3.2) and (3.3) yields,

$$\omega_0 = \sqrt{\omega_1 \omega_n} \tag{3.4}$$

$$\alpha = \frac{x_n}{FBW} \quad \text{where } FBW = \frac{\omega_n - \omega_1}{\omega_0} \tag{3.5}$$

The value of the low pass cutoff frequency x_n is normally taken as 2π radian/sec, and the values of x_m can now be found from equation (3.1) [3].

3.4 Derivation of cost function

A cost function that is used in the optimization of the coupling matrix of coupled resonator multiplexer is formulated here. For two ports filter in [11]

$$S_{11}(s)=\frac{F(s)}{E(s)}$$

$$S_{21}(s)=\frac{P(s)/\varepsilon}{E(s)} \tag{3.6}$$

Substituting (3.6) in the energy conservation formula

$$\left|S_{11}\right|^2+\left|S_{21}\right|^2=1 \tag{3.7}$$

and manipulating, the following expression is achieved

$$E^2=F^2+\frac{1}{\varepsilon^2}P^2 \tag{3.8}$$

where *E*, *F* and *P* are all normalized such that their highest degree coefficients are equal to one.

"This shows that apart from the, scaling factor ε , a combination of any two polynomials can completely describe the response. The problem is resolved by analytically calculating the external quality factors. Setting these factors to their correct values at the outset of the optimization cancels the need to invoke the ripple at any stage of the synthesis procedure. Consequently, a combination of any two polynomials can completely determine the response as long as the quality factors are predetermined. As far as speed is concerned, polynomials *F* and *P* prove most efficient to use in the cost function" [11].

The cost function formulated as

$$\Omega=\sum_{i=1}^{R}\left|P_N(S_{ti})\right|^2+\sum_{j=1}^{R}\left|F(S_{rj})\right|^2, \tag{3.9}$$

where *R* is the number of reflection zeros.

This is derived in chapter (4) in [3] for diplexers and utilized here for multiplexers. For a coupled resonator multiplexer, the reflection and transmission functions may be defined in terms of polynomials as follows,

$$S_{11}(s)=\frac{F(s)}{E(s)},$$

$$S_{N1}(s)=\frac{P_N(s)/\varepsilon}{E(s)} \tag{3.10}$$

where the roots of $F(s)$ correspond to the reflection zeros, the roots of $P_N(s)$ correspond to the transmission zeros of the filter frequency response at ports N, ε is a ripple constant, and $E(s)$ roots correspond to the pole positions of the filtering function. The initial cost function may be written in terms of the characteristic polynomials as follows,

$$\Omega=\sum_{N=2}^{M}\sum_{i=1}^{T_N}\left|P_N(S_{ti})\right|^2+\sum_{j=1}^{R}\left|F(S_{rj})\right|^2+\sum_{v=1}^{R-(M-1)}\left|\left|\frac{F(S_{pv})}{E(S_{pv})}\right|-10^{\frac{L_R}{20}}\right|^2 \tag{3.11}$$

where M is the number of ports, S_{ti} are the frequency locations of transmission zeros of S_{N1}, T_N is the number of the transmission zeros of S_{N1}, R is the total number of resonators in the multiplexer, L_R is the desired return loss in dB (L_R<0), and S_{rj} and S_{pv} are the frequency locations of the reflection zeros and the peaks' frequency values of $|S_{11}|$ in the pass band. The last term in the cost function is used to set the peaks of $S_{11}(s)=\frac{F(s)}{E(s)}$ to the required return loss level. It is assumed here that all channels of the multiplexer have the same return loss level.

Recall from section (2.2.3), that for a N-port network of multiple coupled resonators, the scattering parameters are expressed the in terms of the general matrix [A] (equation (2.28)) as follows,

$$\begin{aligned}S_{xx}&=1-\frac{2}{q_{ex}}\frac{cof_{xx}([A])}{\Delta_A}\\ S_{xy}&=1-\frac{2}{\sqrt{q_{ex}q_{ey}}}\frac{cof_{xy}([A])}{\Delta_A}\end{aligned} \tag{3.12}$$

where x is the port connected to resonator x, y is the port connected to resonator y, Δ_A is the determinant of the matrix [A] and cof_{xy} is the cofactor of matrix [A] evaluated by removing the x^{th} row and the y^{th} column of [A].

By equating (3.10) and (3.12), the polynomials $P_1(s)$, $P_2(s)$, $F(s)$ and $E(s)$ are expressed in terms of the general matrix [A] as follows,

$$\frac{P_N(s)}{\varepsilon}=\frac{2.cof_{1N}([A(s)])}{\sqrt{q_{e1}q_{eN}}}$$

$$F(s)=\Delta_A(s)-\frac{2.cof_{11}([A(s)])}{q_{e1}}$$

$$E(s) = \Delta_A(s) \tag{3.13}$$

By substitution of the polynomials in equation (3.13) into equation (3.11), the cost function is now expressed in terms of determinants and cofactors of the matrix [*A*] and the external quality factors as follows,

$$\Omega = \sum_{N=2}^{M}\sum_{i=1}^{T_N}\left|\frac{2.cof_{1N}\left(\left[A(s_{ti})\right]\right)}{\sqrt{q_{e1}q_{eN}}}\right|^2 + \sum_{j=1}^{R}\left|\Delta_A(s_{rj}) - \frac{2.cof_{11}\left(\left[A(s_{rj})\right]\right)}{q_{e1}}\right|^2 + \sum_{v=1}^{R-(M-1)}\left|1 - \frac{2.cof_{11}\left(\left[A(s_{pv})\right]\right)}{q_{e1}.\Delta_A(s_{pv})} - 10^{\frac{L_R}{20}}\right|^2, \tag{3.14}$$

where q_{e1} and q_{eN} are the external quality factors at ports 1 and *N* respectively, $\Delta_A(S=x)$ is the determinant of the matrix [*A*] evaluated at the frequency variable *x*, and cof_{ab} ($[A(s=v)]$) is the cofactor of matrix [*A*] evaluated by removing the a^{th} row and the b^{th} column of [*A*] and finding the determinant of the resulting matrix at the frequency variable $s=v$.

The first term in the cost function is used if the multiplexer characteristics contain transmission zeros. However, for a Chebyshev response, this term may be used to minimize the transmission of each channel at the pass band of the other channel, thus increasing the isolation between channel ports. Consequently, the frequency locations s_{ti} are chosen to be the band edges of the channel at port *m*. In another word, this term is used in Chebyshev when much steeper edges of the channels are needed.

The low pass frequency positions of the reflection zeros of the multiplexer are initially set to be equally spaced in the optimization algorithm, and later these positions are moved until equiripple level at specified insertion loss is achieved.

The initial guess of the locations of reflection zeros within a multiplexer channel is presented here. For a multiplexer channel with edges of (x_1,x_2) Hz, the leftmost reflection zero is located at (x_1+0.02)*i* Hz, and the rightmost reflection zero is located at (x_2-0.02)*i* Hz. The other reflection zeros are equally spaced between (x_1+0.02)i and (x_2-0.02)i with frequency spacing as follows:

$$\frac{(x_2 - x_1 - 0.04)}{(m-1)}, \tag{3.15}$$

where *m* is the total number of reflection zeros within a multiplexer channel.

The values of the external quality factors are numerically calculated, and their values are set at the beginning of the algorithm This reduces the optimization parameters set and improves the convergence time.

The normalized external quality factors of these filters are related by:

$$q_{ex_1x_2} = \frac{2}{x_2 - x_1} q_{e\pm1}$$

$$\frac{1}{q_{e1}} = \sum_{i=1}^{N} \frac{1}{q_{ei}}$$

$$q_{e1} = \frac{q_{ex_1x_2}}{m} \tag{3.16}$$

where $q_{ex_1x_2}$ is the normalized external quality factor of the filter with edges of x_1 and x_2, N is total number of channels and $q_{e\pm1}$ is the normalized external quality factor of the filter with edges of ±1, that can be calculated from the g-values.

For a symmetrical multiplexer with channel edges (x_1,x_2), the normalized external quality factor at port (m) are calculated from first equation in equation (3.16), and the normalized external quality factor at the common port 1 is calculated from second equation in equation (3.16).

The variables that need to be optimized in the optimization algorithm are the coupling coefficients and also the frequency locations of the reflection zeros.

3.5 Multiplexer with the novel topology

Two general coupled resonator multiplexer topologies are proposed here. They are shown in figures (3.2) and (3.3) and they can achieve Chebyshev and quasi-elliptic responses respectively. Firstly, the design started with simple structure for four Chebyshev channels and it was consisted of eight resonators and one resonator per channel, then the total number of resonators was increased by increasing the number of resonators per channels. After that, quasi-elliptic responses was achieved. Finally, the number of channels was increased and six channels multiplexer was given as an example.

As shown in figure (3.2) and figure (3.3) where figure (3.2) represents a general structure proposed for multiplexer having Chebyshev response and figure (3.3) represents a general structure proposed for multiplexer having quasi elliptic response, the multiplexer consists of n resonators where n is the total number of resonators, and c is the number of the upper arms or lower arms. These resonators are distributed on 2c channel. The lower arms are mirror of the upper arms (symmetrical channels) and each arm represents a channel consisted of r resonators. In figure (3.4), the channels in the positive side are from upper arms and the channels in the negative side are from lower arms.

Figure (3.4) shows that in this topology the number of channels can be an arbitrary number which is dependent on the number of arms meaning that it can be

increased by increasing the number of arms. Also the number of resonators per arm r can change the isolation between channels and improve the selectivity. In other words increasing the number of resonators per arm increases the isolation.

Resonators in each arm should have different self-resonant frequencies (M_{ii}) to separate the multiplexer channels from each other. The resonators in the vertical branch should have different self-resonant frequencies to achieve disjoint frequency bands at the different channels. Consequently, for the high frequency channels to be at upper arms (ports), the resonators above the junction resonator should have positive frequency offsets ($M_{ii} > 0$), and for the low frequency channel to be at lower arms (ports), the resonators below the junction resonator should have negative frequency offsets ($M_{ii} < 0$). This is supposed to reduce the complexity by achieving symmetry but in general channels' self resonant frequencies may be interchanged between some channels to achieve some advantages such as interchanging the positions of channels to improve the isolation.

It should be noted that the work on novel multiplexer topologies started from a simple eight resonator structure, with $n = 8$ and $r = 1$, followed by other experiments on adding arms to increase channels, also followed by other experiments on adding resonators to the vertical arms until arriving to the generalized topology given in figure (3.2). The junction resonator takes important part in power distribution and also it contributes to the filter transfer function.

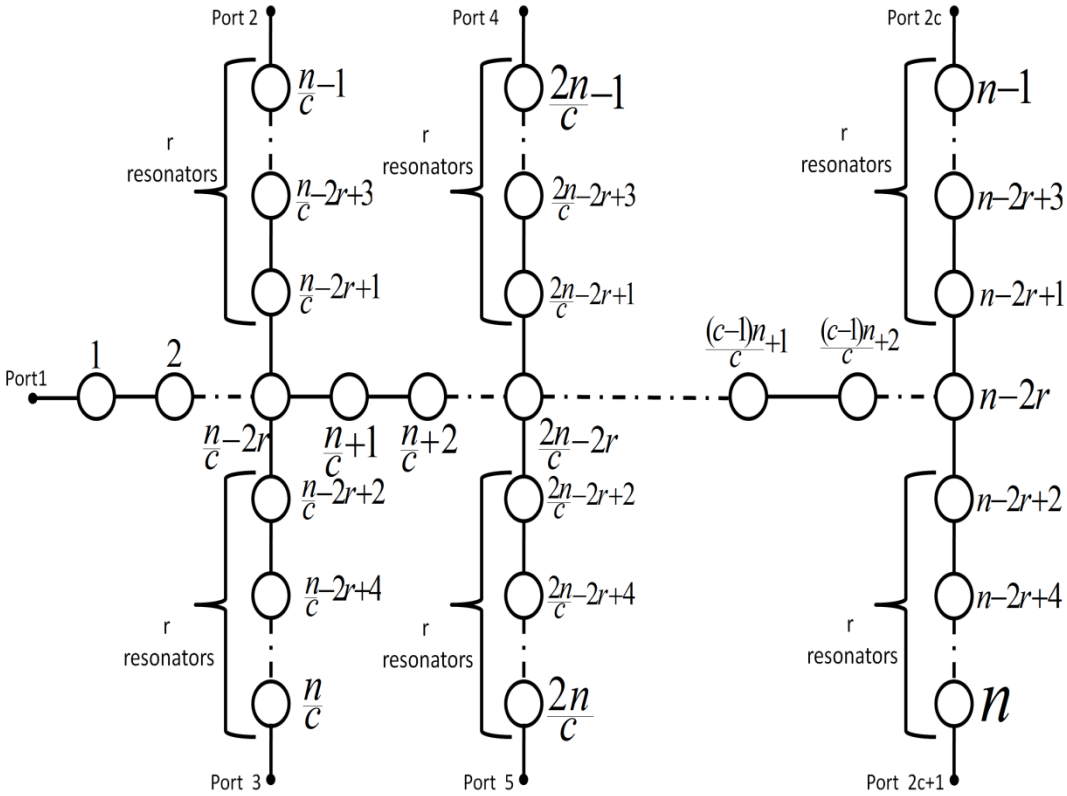

Figure (3.2): general structure proposed for multiplexer having Chebyshev response

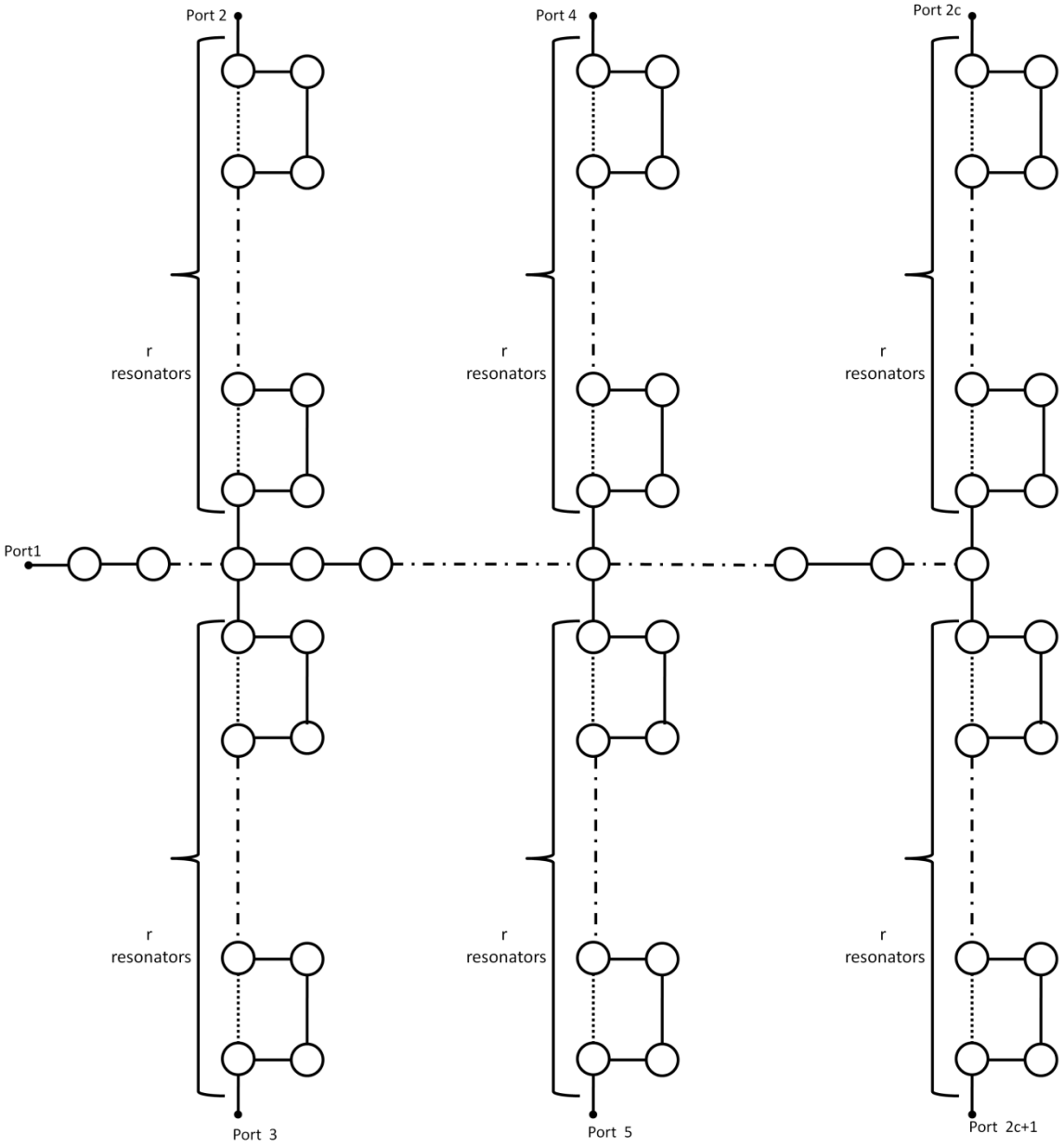

Figure (3.3): general structure proposed for multiplexer having quasi elliptic response

The topology of the multiplexer has been enforced in the optimization algorithm, and the following conditions for coupling coefficients have been applied to simplify the optimization problem:

1. The self-resonant frequencies (M_{ii}) in the lower arm are the negative of the self-resonant frequencies (M_{ii}) in the upper arms as below

$$M_{\frac{n}{c}-1,\frac{n}{c}-1} = -M_{\frac{n}{c},\frac{n}{c}} \quad , \qquad M_{\frac{n}{c}-2r+3,\frac{n}{c}-2r+3} = -M_{\frac{n}{c}-2r+4,\frac{n}{c}-2r+4}$$
$$,\ldots\ldots\ldots\ldots\ldots\ldots\ldots\ldots, M_{n-1,n-1} = -M_{n,n}$$

2. The self-resonant frequencies (M_{ii}) for resonators in the horizontal line equal zero.

$$M_{1,1} = M_{2,2} = M_{\frac{n}{c}+1,\frac{n}{c}+1} = \ldots\ldots\ldots\ldots\ldots = M_{n-2r,n-2r} = 0$$

3. The coupling coefficients between the resonators in upper arms are equal to those in lower arms as below

$$M_{\frac{n}{c}-2r+1,\frac{n}{c}-2r+3} = M_{\frac{n}{c}-2r+2,\frac{n}{c}-2r+4} \ ,\ldots\ldots\ldots\ldots\ldots\ldots\ldots\ldots, M_{n-1,n-3} = M_{n-2,n}$$

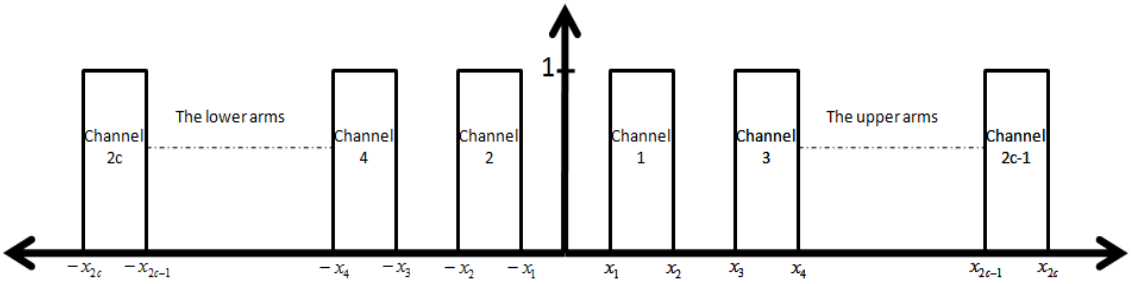

Figure (3.4): Channels in low pass prototype

The bandwidth of each channel can be determined by choosing the values of edges of channels x_1, x_2, x_3, x_4,……,x_{2c-1} and x_{2c}. Channels may have different characteristics, some of them have Chebyshev responses and others have elliptic response.

3.6 Conclusion

In this chapter, the synthesis procure of coupled resonator multiplexers is presented. Frequency transformation formulas as well as cost function have been shown. An overview of number of optimization methods and algorithms in general have been presented. The frequency transformation from band pass to low pass for multiplexers has been derived, also the derivation of cost function used in multiplexer synthesis has been declared. Finally the proposed topologies for multiplexer with both Chebyshev and elliptic response were introduced to be used in the next chapter. Numerical examples will be presented in the next chapter.

REFERENCES

1. A. Ravindran , K. M. Ragsdell and G. V. Reklaitis, "Engineering Optimization Methods and Applications",Wiley,2006.
2. J.S. Hong and M.J. Lancaster, "Microstrip filters for RF/microwave applications". New York: Wiley, 2001.
3. T. F. Skaik, "Synthesis of Coupled Resonator Circuits with Multiple Outputs using Coupling Matrix Optimization", PhD thesis, the University of Birmingham, 2011.
4. J.C. Lagarias, J. A. Reeds, M. H. Wright, and P. E. Wright, "Convergence Properties of the Nelder-Mead Simplex Method in Low Dimensions," SIAM Journal of Optimization, Vol. 9 Number 1, pp. 112-147, 1998.
5. I. Hunter, "Theory and Design of Microwave Filters", the IEEE, London, UK, 2001
6. A. Garcfa-Lamperez, M. Salazar-Palma, and T. K. Sarkar, "Compact Multiplexer Formed by Coupled Resonators with Distributed Coupling", IEEE Antennas and Propagation Society International Symposium, USA, 2005, pp. 89-92.
7. T. Skaik, M. Lancaster, and F. Huang, "Synthesis of multiple output coupled resonator microwave circuits using coupling matrix optimization," *IET Journal of Microwaves, Antenna & Propagation*, vol.5, no.9, pp. 1081-1088, June 2011.
8. T. Skaik, "Novel Star Junction Coupled Resonator Multiplexer Structures", *Progress in Electromagnetics Research Letters*, Vol. 31, pp. 113-120, April 2012.
9. T. Skaik, "Star-Junction X-band Coupled Resonator Multiplexer", Proceedings of the 12th Mediterranean Microwave Symposium, Istanbul, Turkey, Sept 2012.
10. T. Kacmajor, J. J. Michalski, J. Gulgowski, " Filter Tuning and Coupling Matrix Synthesis by Optimization with Cost Function Based on Zeros, Poles and Hausdorff Distance ", The IEEE MTT-S International Microwave Symposium, Canada, June 2012.
11. A. B. Jayyousi and M. J. Lancaster, "A gradient-based optimization technique employing determinants for the synthesis of microwave coupled filters," IEEE MTT-S International Microwave Symposium, USA, 2004, pp 1369-1372.

Chapter 4

Numerical Examples for Coupled Resonator Multiplexers

4.1 Examples of multiplexers with novel Topology

In this chapter, nine examples of multiplexers with the proposed novel topologies are given where each example has different characteristics from others and each example with different characteristics gives a proof for validity of the new topology. The first example is the simplest example which consists of minimum number of resonators in the simplest image to construct four channels multiplexer. In the next example the number of resonators per arm is increased and thus the total number of resonators is increased which declares that the isolation between each channel can be improved by this way. The third example is as the previous one, but it has wider bandwidth than the second example. All the first three examples have Chebyshev response, however in the fourth example Quasi-Elliptic responses are achieved. The isolation in example number four is better than isolation in example three because the number of resonators in example four is larger than that in example three, and the channels are sharper than channels in third example due to quasi elliptic response in example four. In the fifth example both the Chebyshev and Quasi elliptic response are achieved in the same structure, where two channels have Chebyshev response and the other two channels have Quasi elliptic response. In all previous examples the frequency locations of reflection zeros were not optimized , but only were the coupling coefficients. But in sixth example, both the coupling coefficient and frequency location of reflection zeros are optimized to get equal S_{11} peaks with -20 dB return loss. In the seventh example the number of channels is increased to six channels by increasing number of arms. In the eighth example the isolation is improved by interchanging the position of channels as another way to improve the isolation. Finally, in ninth example the two inner channels have a different order and number of resonators from the two outer channels and the validity of the results have been checked . All previous examples show that the number of channels can be controlled by number of arms, and number of resonators can be changed to get different characteristics, also any type of responses can be achieved, all that based on coupled resonators circuits.

The synthesis procedure starts with frequency transformation from band pass to low pass prototype using normalization equations or transformation equations (3.1-3.5). After that using equations (3.15, 3.16) the initial frequency location reflection zeros and external quality factors are calculated. Finally the initial frequency location reflection zeros, initial coupling coefficient , return loss, external coupling factors and transmission zeros are entered as parameters of cost function equation (3.14) to be optimized using optimization algorithms. The results obtained from optimization processes are coupling coefficients and frequency locations of reflection zeros.

4.1.1. Example 1: Non-contiguous narrow band four channels multiplexer with $n = 8$, $r = 1$, $x_1 = 0.8$, $x_2 = 0.9$, $x_3 = 1.5$, $x_4 = 1.6$.

The multiplexer consists of four non contiguous channels as shown in figure (4.1), the simplest structure, and it has eight resonators in total with one resonator per arm. The specified return loss is 20 dB. The channels have an equal bandwidth and they are separated by unequal guard bands. The edges of channels 1, 2, 3 and 4 are {-1.6,-1.5},{-0.9,-0.8},{0.8,0.9},{1.5,1.6}, respectively. The normalized external quality factors are numerically calculated using equation (3.16) as $q_{e3} = q_{e4} = q_{e7} = q_{e8} = 13.2960$ and $q_{e1} = 3.3240$. The locations of return zeros are calculated using equation (3.15) as $\pm 0.8200i, \pm 0.8800i, \pm 1.5200i$ and $\pm 1.5800i$. These locations are the initial locations and they may need optimization as in some next examples.

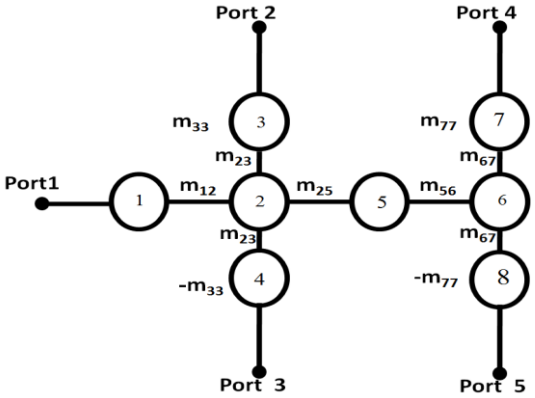

Figure (4.1): Structure of multiplexer one.

Table (4.1): The general coupling matrix of the above structure.

Resonators	1	2	3	4	5	6	7	8
1	0	m_{12}	0	0	0	0	0	0
2	m_{12}	0	m_{23}	m_{23}	m_{25}	0	0	0
3	0	m_{23}	m_{33}	0	0	0	0	0
4	0	m_{23}	0	$-m_{33}$	0	0	0	0
5	0	m_{25}	0	0	0	m_{56}	0	0
6	0	0	0	0	m_{56}	0	m_{67}	m_{67}
7	0	0	0	0	0	m_{67}	m_{77}	0
8	0	0	0	0	0	m_{67}	0	$-m_{77}$

The coupling coefficients between any adjacent resonators m_{ij} and frequency offsets m_{ii} are optimized using cost function in equation (3.14) to have final values $m_{12} = 1.2471$, $m_{23} = 0.2198$, $m_{25} = 0.6350$, $m_{33} = 0.8411$, $m_{56} = 1.0964$, $m_{67} = 0.2165$, $m_{77} = 1.5005$. For symmetry, some conditions were taken in account to simplify the optimization, these conditions are $m_{23} = m_{24}$, $m_{67} = m_{68}$, $m_{33} = -m_{44}$ and $m_{77} = -m_{88}$.

The optimization started with ten initial values {0.1,0.2,.....,1} to get the best result to be optimized to get final values. This means that the initial values were put in loop to get the correct beginning. In this example only the second term in the cost

function in equation (3.14), the term related to return zeros, was used in optimization and the others were neglected. Table (4.1) is the general optimization matrix of the structure in figure (4.1). The numerical optimized coupling matrix is given in table (4.2) and the multiplexer prototype response is depicted in figure (4.2). Table (4.3) displays the realized values that are achieved by optimization versus the targets.

Table (4.2): The optimized coupling matrix of multiplexer one.

Resonators	1	2	3	4	5	6	7	8
1	0	1.2471	0	0	0	0	0	0
2	1.2471	0	0.2198	0.2198	0.6350	0	0	0
3	0	0.2198	0.8411	0	0	0	0	0
4	0	0.2198	0	-0.8411	0	0	0	0
5	0	0.6350	0	0	0	1.0964	0	0
6	0	0	0	0	1.0964	0	0.2165	0.2165
7	0	0	0	0	0	0.2165	1.5005	0
8	0	0	0	0	0	0.2165	0	-1.5005

Table (4.3): The Realized values versus the targets.

Item		Target	Realized values	Percentage of error
Return loss(L_R) in db		-20	-21.84	9.2%
boundaries	x_1	0.8	0.718	10.3%
	x_2	0.9	0.934	3.8%
	x_3	1.5	1.43	4.7%
	x_4	1.6	1.646	2.9%

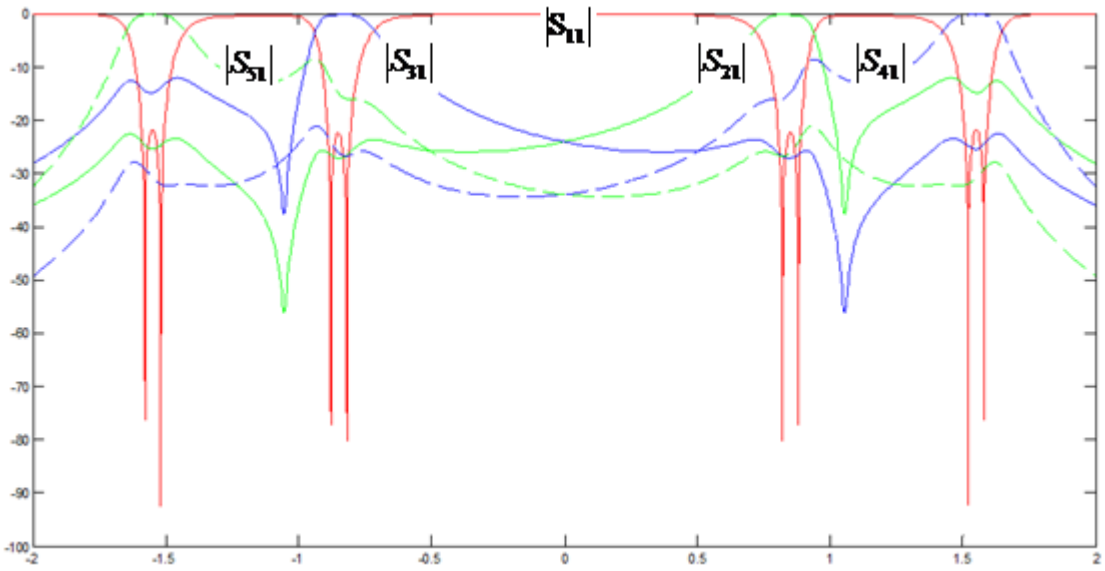

Figure (4.2): The theoretical response of multiplexer one.

4.1.2. Example 2: Non-contiguous narrow band four channels multiplexer with $n = 12$, $r = 2$, $x_1 = 0.4$, $x_2 = 0.55$, $x_3 = 1.35$, $x_4 = 1.5$.

The multiplexer consists of four non contiguous channels as shown in figure (4.3), and it has twelve resonators in total with two resonators per arm. The specified return loss is 20 dB. The channels have an equal bandwidth and they are separated by equal guard bands. The edges of channels 1,2,3 and 4 are {-1.5,-1.35}, {-0.55,-0.4},{0.4,0.55},{1.35,1.5} respectively. The normalized external quality factors are numerically calculated using equation (3.16) as $q_{e5} = q_{e6} = q_{e11} = q_{e12} = 11.3547$ and $q_{e1} = 2.8387$. The locations of return zeros are calculated using equation (3.15) as $\pm$ 0.4200i, $\pm$ 0.4750i, $\pm$ 0.5300i, $\pm$ 1.3700i, $\pm$ 1.4250i and $\pm$ 1.4800i. These locations are the initial locations and they may need optimization as in some next examples.

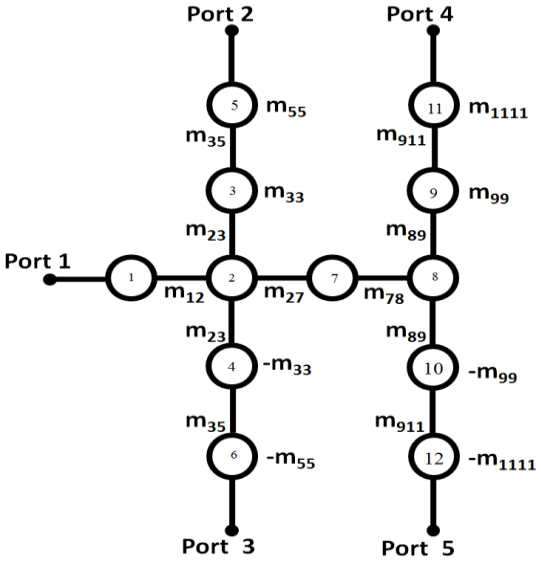

Figure (4.3): structure of multiplexer two.

The coupling coefficients between any adjacent resonators m_{ij} and frequency offsets m_{ii} are optimized using cost function in equation (3.14) to have final values $m_{12} = 1.0773$, $m_{23} = 0.2774$, $m_{27} = 0.7728$, $m_{33} = 0.4603$, $m_{35} = 0.0764$, $m_{55} = 0.4641$, $m_{78} = 0.7058$, $m_{89} = 0.3083$, $m_{99} = 1.3383$, $m_{911} = 0.0768$, $m_{1111} = 1.4201$. For symmetry, some conditions were taken in account to simplify the optimization, these conditions are $m_{23} = m_{24}$, $m_{35} = m_{46}$, $m_{89} = m_{810}$, $m_{911} = m_{1012}$, $m_{33} = -m_{44}$, $m_{55} = -m_{66}$, $m_{99} = -m_{1010}$ and $m_{1111} = -m_{1212}$.

The optimization started with ten initial values {0.1,0.2,.....,1} to get the best result to be optimized to get final values. This means that the initial values were put in loop to get the correct beginning. In this example only the second term in the cost function in equation (3.14), the term related to return zeros, was used in optimization and the others were neglected. The optimized coupling matrix is given in table (4.4) and the multiplexer prototype response is depicted in figure (4.4), where figure (4.4)(a) represents S_{11}, S_{21}, S_{31}, S_{41}, S_{51} while figure (4.4)(b) represents isolation between every two adjacent channels S_{23}, S_{24}, S_{35}. Table (4.5) displays the realized values that are achieved by optimization versus the targets.

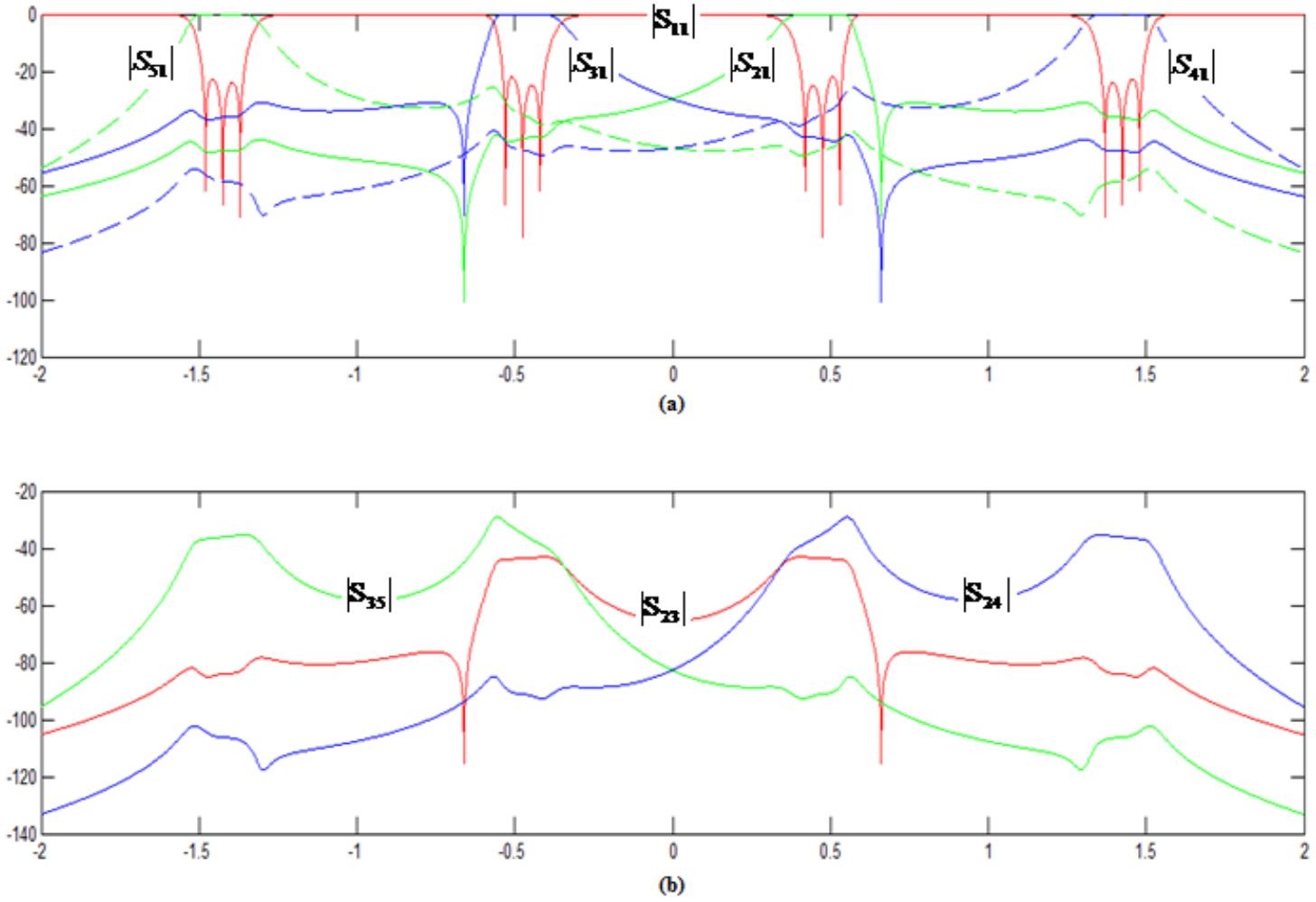

Figure (4.4): The theoretical response of multiplexer two: (a) Reflection loss and insertion loss, (b) The isolation between adjacent channels.

Table (4.4): The optimized coupling matrix of multiplexer two.

Resonators	1	2	3	4	5	6	7	8	9	10	11	12
1	0	1.0773	0	0	0	0	0	0	0	0	0	0
2	1.0773	0	0.2774	0.2774	0	0	0.7728	0	0	0	0	0
3	0	0.2774	0.4603	0	0.0764	0	0	0	0	0	0	0
4	0	0.2774	0	-0.4603	0	0.0764	0	0	0	0	0	0
5	0	0	0.0764	0	0.4641	0	0	0	0	0	0	0
6	0	0	0	0.0764	0	-0.4641	0	0	0	0	0	0
7	0	0.7728	0	0	0	0	0	0.7058	0	0	0	0
8	0	0	0	0	0	0	0.7058	0	0.3083	0.3083	0	0
9	0	0	0	0	0	0	0	0.3083	1.3383	0	0.0768	0
10	0	0	0	0	0	0	0	0.3083	0	-1.3383	0	0.0768
11	0	0	0	0	0	0	0	0	0.0768	0	1.4201	0
12	0	0	0	0	0	0	0	0	0	0.0768	0	-1.4201

Table (4.5): The Realized values versus the targets.

Item		Target	Realized values	Percentage of error
Return loss(L_R) in db		-20	-22.02	10.1%
boundaries	x_1	0.4	0.351	12.3%
	x_2	0.55	0.567	3.1%
	x_3	1.35	1.31	3.0%
	x_4	1.5	1.528	1.9%

4.1.3. Example 3: Non-contiguous band four channels multiplexer with $n = 12$, $r = 2$, $x_1 = 0.4$, $x_2 = 0.75$, $x_3 = 1.55$, $x_4 = 1.9$.

The multiplexer consists of four non contiguous channels as shown in figure (4.5), and it has twelve resonators in total with two resonators per arm. The specified return loss is 20 dB. The channels have an equal bandwidth with wider band width than previous examples and they are separated by equal guard bands. The edges of channels 1,2,3 and 4 are {-1.9,-1.55},{-0.75,-0.4},{0.4,0.75},{1.55,1.9} respectively. The normalized external quality factors are numerically calculated using equation (3.16) as $q_{e5} = q_{e6} = q_{e11} = q_{e12} = 4.8663$ and $q_{e1} = 1.2166$. The locations of return zeros are calculated using equation (3.15) as $\pm$ 1.8800i, $\pm$ 1.7250i, $\pm$ 1.5700i, $\pm$ 0.7300i, $\pm$ 0.5750i and $\pm$ 0.4200i. These locations are the initial locations and they may need optimization as in some next examples.

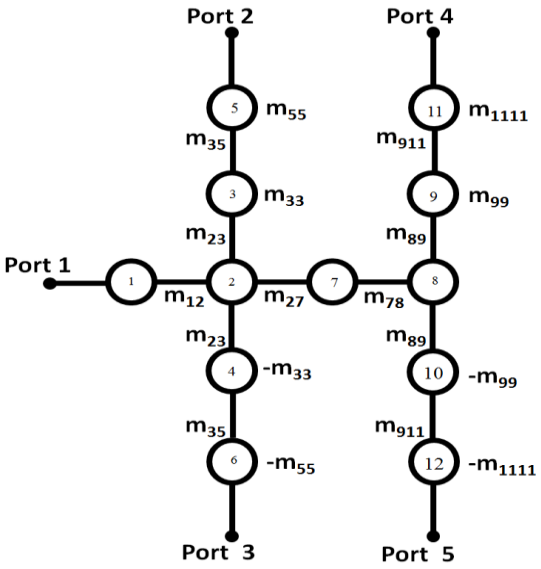

Figure (4.5): structure of multiplexer three.

The coupling coefficients between any adjacent resonators m_{ij} and frequency offsets m_{ii} are optimized using cost function in equation (3.14) to have final values $m_{12} = 1.3481$, $m_{23} = 0.5145$, $m_{27} = 0.8223$, $m_{33} = 0.5263$, $m_{35} = 0.1962$, $m_{55} = 0.5296$, $m_{78} = 1.0836$, $m_{89} = 0.5746$, $m_{99} = 1.4159$, $m_{911} = 0.2131$, $m_{1111} = 1.6879$. For symmetry, some conditions were taken in account to simplify the optimization, these conditions are $m_{23} = m_{24}$, $m_{35} = m_{46}$, $m_{89} = m_{810}$, $m_{911} = m_{1012}$, $m_{33} = -m_{44}$, $m_{55} = -m_{66}$, $m_{99} = -m_{1010}$ and $m_{1111} = -m_{1212}$.

The optimization started with example two coupling coefficients as initial to get final values. In this example only the second term in the cost function in equation (3.14), the term related to return zeros, was used in optimization and the others were neglected. The optimized coupling matrix is given in table (4.6) and the multiplexer prototype response is depicted in figure (4.6), where figure (4.6)(a) represents S_{11}, S_{21}, S_{31}, S_{41}, S_{51} while figure (4.6)(b) represents isolation between every two adjacent channels S_{23}, S_{24}, S_{35}. Table (4.7) displays the realized values that are achieved by optimization versus the targets.

Table (4.6): The optimized coupling matrix of multiplexer three.

Resonators	1	2	3	4	5	6	7	8	9	10	11	12
1	0	1.3481	0	0	0	0	0	0	0	0	0	0
2	1.3481	0	0.5145	0.5145	0	0	0.8223	0	0	0	0	0
3	0	0.5145	0.5263	0	0.1962	0	0	0	0	0	0	0
4	0	0.5145	0	-0.5263	0	0.1962	0	0	0	0	0	0
5	0	0	0.1962	0	0.5296	0	0	0	0	0	0	0
6	0	0	0	0.1962	0	-0.5296	0	0	0	0	0	0
7	0	0.8223	0	0	0	0	0	1.0836	0	0	0	0
8	0	0	0	0	0	0	1.0836	0	0.5746	0.5746	0	0
9	0	0	0	0	0	0	0	0.5746	1.4159	0	0.2131	0
10	0	0	0	0	0	0	0	0.5746	0	-1.4159	0	0.2131
11	0	0	0	0	0	0	0	0	0.2131	0	1.6879	0
12	0	0	0	0	0	0	0	0	0	0.2131	0	-1.6879

Table (4.7): The Realized values versus the targets.

Item		Target	Realized values	Percentage of error
Return loss(L_R) in db		-20	-17.65	12%
boundaries	x_1	0.4	0.242	40%
	x_2	0.75	0.781	4%
	x_3	1.55	1.418	9%
	x_4	1.9	1.969	4%

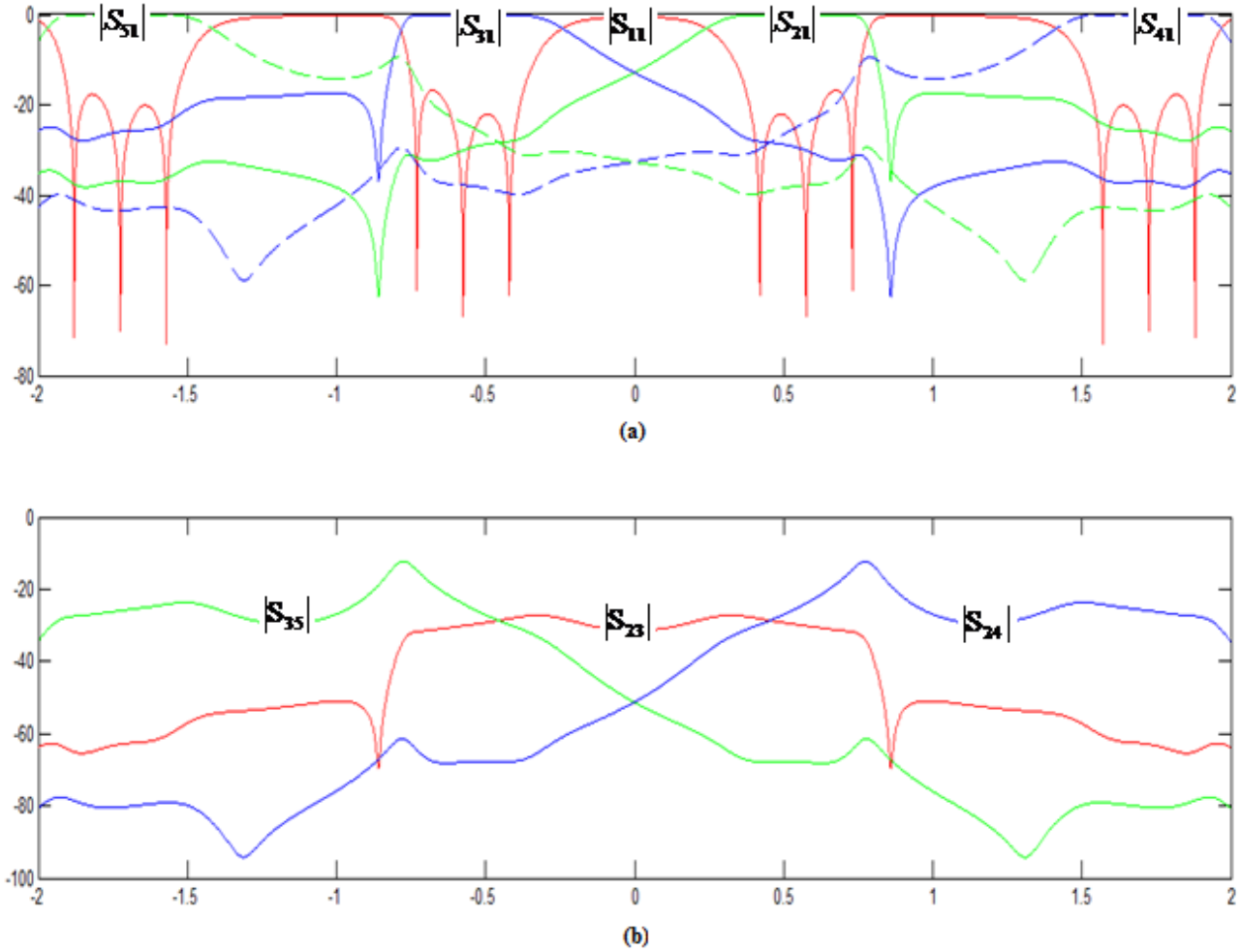

Figure (4.6): The theoretical response of multiplexer three: (a) Reflection loss and insertion loss, (b) The isolation between adjacent channels.

4.1.4. Example 4: Non-contiguous band four channels multiplexer with Quasi-Elliptic responses n = 20, r = 4, x_1 = 0.4, x_2 = 0.75, x_3 = 1.55, x_4 = 1.9.

The multiplexer consists of four non contiguous channels as shown in figure (4.7), and it has twenty resonators in total with four resonators per arm. The specified return loss is 20 dB. The channels have an equal bandwidth and they are separated by equal guard bands. The edges of channels 1, 2, 3 and 4 are {-1.9,-1.55},{-0.75,-0.4},{0.4,0.75},{1.55,1.9}, respectively. The eight transmission zeros locate at $\pm$ 0.3i, $\pm$ 0.85i, $\pm$ 1.45i and $\pm$ 2i. The normalized external quality factors are numerically calculated using equation (3.16) as $q_{e9} = q_{e10} = q_{e91} = q_{e20}$ = 5.5509 and q_{e1} = 1.3877. The locations of return zeros are calculated using equation (3.15) as $\pm$ 1.8800i, $\pm$ 1.8025i, $\pm$ 1.7250i, $\pm$ 1.6475i, $\pm$ 1.5700i, $\pm$ 0.7300i, $\pm$ 0.6525i, $\pm$ 0.5750i, $\pm$ 0.4975i and $\pm$ 0.4200i. These locations are the initial locations and they may need optimization as in some next examples. In figure (4.7), solid lines in the multiplexer represent direct coupling, and dashed lines represent cross coupling, and Quasi-Elliptic responses can be achieved.

The coupling coefficients between any adjacent resonators m_{ij} and frequency offsets m_{ii} are optimized using cost function in equation (3.14) to have final values m_{12} =1.3489, m_{23} = 0.4391, m_{33} = 0.5429, m_{35} = 0.1031, m_{39} = -0.0371, m_{55} = 0.5602, m_{57} = 0.1219, m_{77} = 0.5627, m_{79} = 0.1329, m_{99} = 0.5588, m_{211} = 0.8746, m_{1112} = 0.9734, m_{1213} = 0.5078, m_{1313} = 1.5098, m_{1315} = 0.1097, m_{1319} = -0.0271, m_{1515} =1.7157, m_{1517} = 0.1177, m_{1717} = 1.7213, m_{1719} = 0.1371, m_{1919} =1.7189. For symmetry, some conditions were taken in account to simplify the optimization, these conditions are $m_{23} = m_{24}$, $m_{35} = m_{46}$, $m_{57} = m_{68}$, $m_{79} = m_{810}$, $m_{39} = m_{410}$, $m_{1213} = m_{1214}$, $m_{1315} = m_{1416}$, $m_{1517} = m_{1618}$, $m_{1719} = m_{1820}$, $m_{1319} = m_{1420}$, $m_{33} = -m_{44}$, $m_{55} = -m_{66}$, $m_{77} = -m_{88}$, $m_{99} = -m_{1010}$, $m_{1313} = -m_{1414}$, $m_{1515} = -m_{1616}$, $m_{1717} = -m_{1818}$ and $m_{1919} = -m_{2020}$.

In this example the whole cost function in equation (3.14) has been used except the third term that optimizes the return zeros' locations to enforce return loss level of 20dB. The optimized coupling matrix is given in table (4.9) and the multiplexer prototype response is depicted in figure (4.8), where figure (4.8) (a) represents S_{11}, S_{21}, S_{31}, S_{41}, S_{51} while figure (4.8) (b) represents isolation between every two adjacent channels S_{23}, S_{24}, S_{35}. Table (4.8) displays the realized values that are achieved by optimization versus the targets.

Table (4.8): The Realized values versus the targets.

Item		Target	Realized values	Percentage of error
boundaries	x_1	0.4	0.381	5%
	x_2	0.75	0.745	1%
	x_3	1.55	1.534	1%
	x_4	1.9	1.906	0%
Transmission zeros	*t1*	0.3	0.317	6%
	t2	0.85	0.841	1%
	t3	1.45	1.437	1%
	t4	2	2.001	0%

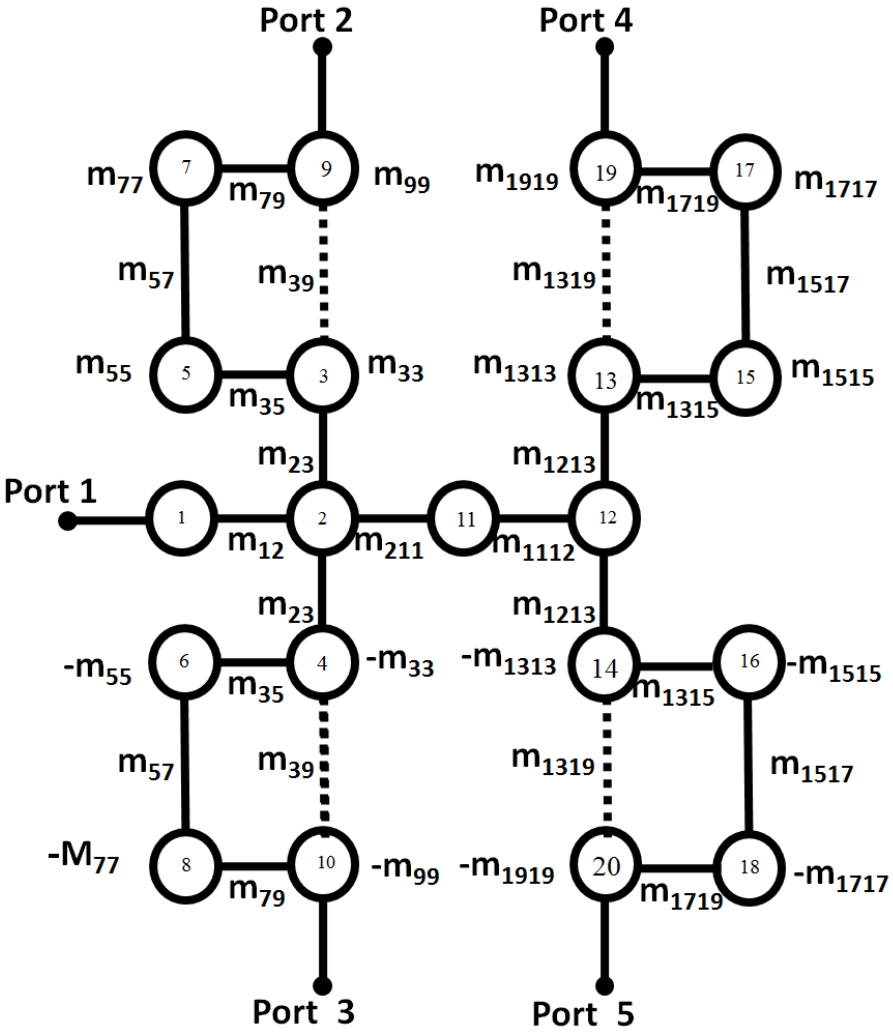

Figure (4.7): structure of multiplexer four.

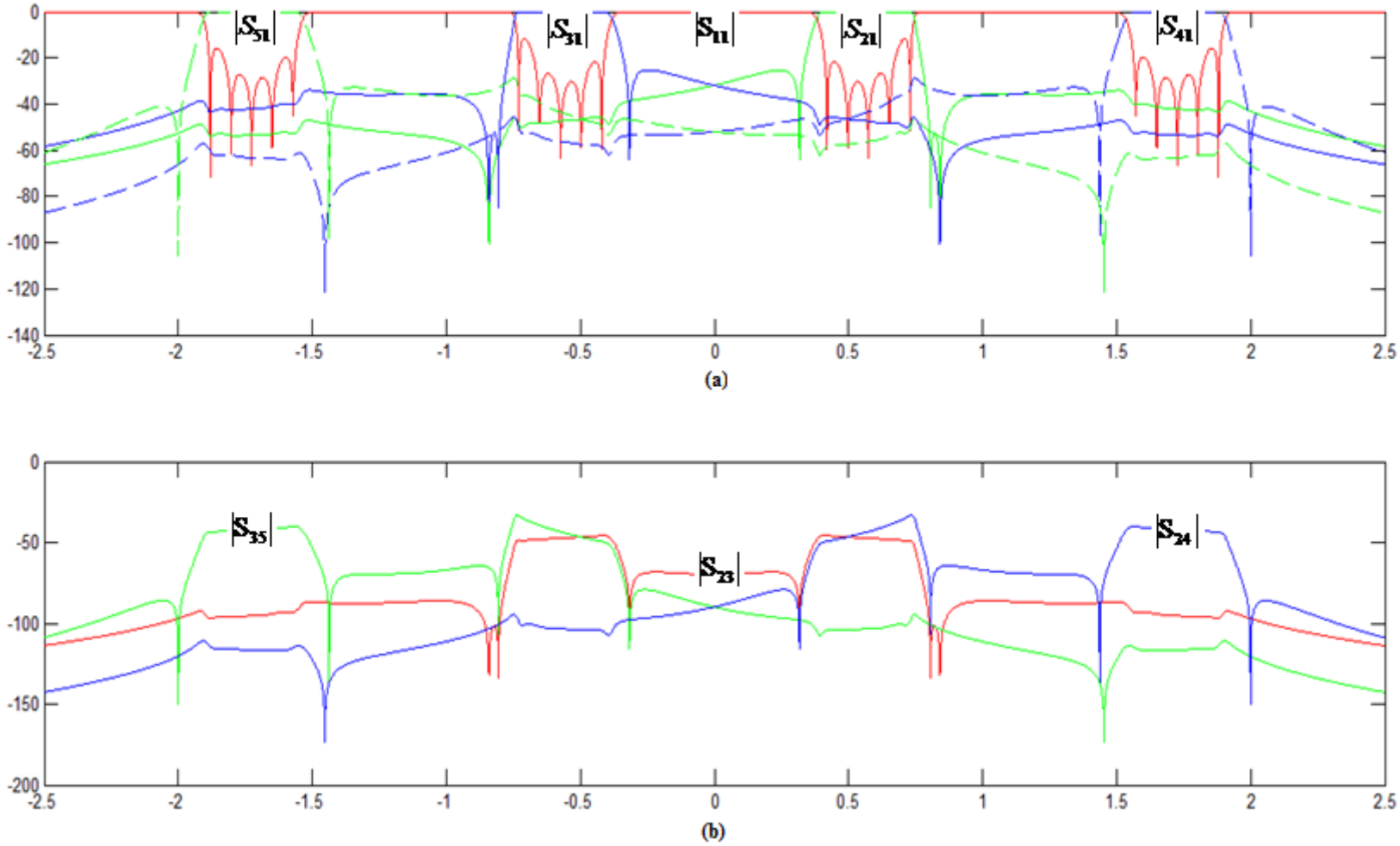

Figure (4.8): The theoretical response of multiplexer four: (a) Reflection loss and insertion loss, (b) The isolation between adjacent channels.

Table (4.9): The optimized coupling matrix of multiplexer four.

Resonator	1	2	3	4	5	6	7	8	9	10	11	12	13	14	15	16	17	18	19	20
1	0	1.3489	0	0	0	0	0	0	0	0	0	0	0	0	0	0	0	0	0	0
2	1.3489	0	0.4391	0.4391	0	0	0	0	0	0	0.8746	0	0	0	0	0	0	0	0	0
3	0	0.4391	0.5429	0	0.1031	0	0	0	-0.0371	0	0	0	0	0	0	0	0	0	0	0
4	0	0.4391	0	-0.5429	0	0.1031	0	0	0	-0.0371	0	0	0	0	0	0	0	0	0	0
5	0	0	0.1031	0	0.5602	0	0.1219	0	0	0	0	0	0	0	0	0	0	0	0	0
6	0	0	0	0.1031	0	-0.5602	0	0.1219	0	0	0	0	0	0	0	0	0	0	0	0
7	0	0	0	0	0.1219	0	0.5627	0	0.1329	0	0	0	0	0	0	0	0	0	0	0
8	0	0	0	0	0	0.1219	0	-0.5627	0	0.1329	0	0	0	0	0	0	0	0	0	0
9	0	0	-0.0371	0	0	0	0.1329	0	0.5588	0	0	0	0	0	0	0	0	0	0	0
10	0	0	0	-0.0371	0	0	0	0.1329	0	-0.5588	0	0	0	0	0	0	0	0	0	0
11	0	0.8746	0	0	0	0	0	0	0	0	0	0.9734	0	0	0	0	0	0	0	0
12	0	0	0	0	0	0	0	0	0	0	0.9734	0	0.5078	0.5078	0	0	0	0	0	0
13	0	0	0	0	0	0	0	0	0	0	0	0.5078	1.5098	0	0.1097	0	0	0	-0.0271	0
14	0	0	0	0	0	0	0	0	0	0	0	0.5078	0	-1.5098	0	0.1097	0	0	0	-0.0271
15	0	0	0	0	0	0	0	0	0	0	0	0	0.1097	0	1.7157	0	0.1177	0	0	0
16	0	0	0	0	0	0	0	0	0	0	0	0	0	0.1097	0	-1.7157	0	0.1177	0	0
17	0	0	0	0	0	0	0	0	0	0	0	0	0	0	0.1177	0	1.7213	0	0.1371	0
18	0	0	0	0	0	0	0	0	0	0	0	0	0	0	0	0.1177	0	-1.7213	0	0.1371
19	0	0	0	0	0	0	0	0	0	0	0	0	-0.0271	0	0	0	0.1371	0	1.7189	0
20	0	0	0	0	0	0	0	0	0	0	0	0	0	-0.0271	0	0	0	0.1371	0	-1.7189

4.1.5. Example 5: Non-contiguous band four channels multiplexer consists of two channels with Quasi elliptic response and the other two channels with Chebyshev response and $n = 20$, $r = 4$, $x_1 = 0.4$, $x_2 = 0.75$, $x_3 = 1.55$, $x_4 = 1.9$.

The multiplexer consists of four non contiguous channels as shown in figure (4.9), and it has twenty resonators in total with four resonators per arm. The specified return loss is 20 dB. The channels have an equal bandwidth and they are separated by equal guard bands. The edges of channels 1,2,3 and 4 are {-1.9,-1.55},{-0.75,-0.4},{0.4,0.75},{1.55,1.9} respectively. The four transmission zeros locate at ± 1.45i and ± 2i. The normalized external quality factors are numerically calculated using equation (3.16) as $q_{e9} = q_{e10} = q_{e91} = q_{e20} = 5.5509$ and $q_{e1} = 1.3877$. The locations of return zeros are calculated using equation (3.15) as ± 1.8800i, ± 1.8025i, ± 1.7250i, ± 1.6475i, ± 1.5700i, ± 0.7300i, ± 0.6525i, ± 0.5750i, ± 0.4975i and ± 0.4200i. These locations are the initial locations and they need optimization as in example six. In figure (4.9) , solid lines represent direct coupling, and dashed lines represent cross coupling, and both Quasi-Elliptic and Chebyshev responses can be achieved.

The coupling coefficients between any adjacent resonators m_{ij} and frequency offsets m_{ii} are optimized using cost function in equation (3.14) to have final values $m_{12} = 1.3470$, $m_{23} = 0.4458$, $m_{211} = 0.8663$, $m_{33} = 0.5448$, $m_{35} = 0.1129$, $m_{55} = 0.5589$, $m_{57} = 0.1043$, $m_{77} = 0.5618$, $m_{79} = 0.1419$, $m_{99} = 0.5614$, $m_{1112} = 0.9831$, $m_{1213} = 0.5032$, $m_{1313} = 1.5115$, $m_{1315} = 0.1100$, $m_{1319} = -0.0271$, $m_{1515} = 1.7149$, $m_{1517} = 0.1181$, $m_{1717} = 1.7202$, $m_{1719} = 0.1375$, $m_{1919} = 1.7174$. For symmetry, some conditions were taken in account to simplify the optimization, these conditions are $m_{23} = m_{24}$, $m_{35} = m_{46}$, $m_{57} = m_{68}$, $m_{79} = m_{810}$, $m_{1213} = m_{1214}$, $m_{1315} = m_{1416}$, $m_{1517} = m_{1618}$, $m_{1719} = m_{1820}$, $m_{1319} = m_{1420}$, $m_{33} = -m_{44}$, $m_{55} = -m_{66}$, $m_{77} = -m_{88}$, $m_{99} = -m_{1010}$, $m_{1313} = -m_{1414}$, $m_{1515} = -m_{1616}$, $m_{1717} = -m_{1818}$ and $m_{1919} = -m_{2020}$.

In this example the whole cost function in equation (3.14) has been used except the third term that optimizes the return zeros' locations to enforce return loss level of 20dB. Table (4.10) displays the realized values that are achieved by optimization versus the targets. The optimized coupling matrix is given in table (4.11) and the multiplexer prototype response is depicted in figure (4.10).

Table (4.10): The Realized values versus the targets.

Item		Target	Realized values	Percentage of error
boundaries	x_1	0.4	0.368	8.0%
	x_2	0.75	0.754	1%
	x_3	1.55	1.533	1.1%
	x_4	1.9	1.905	0. 3%
Transmission zeros	t_3	1.45	1.435	1.0%
	t_4	2	2	0%

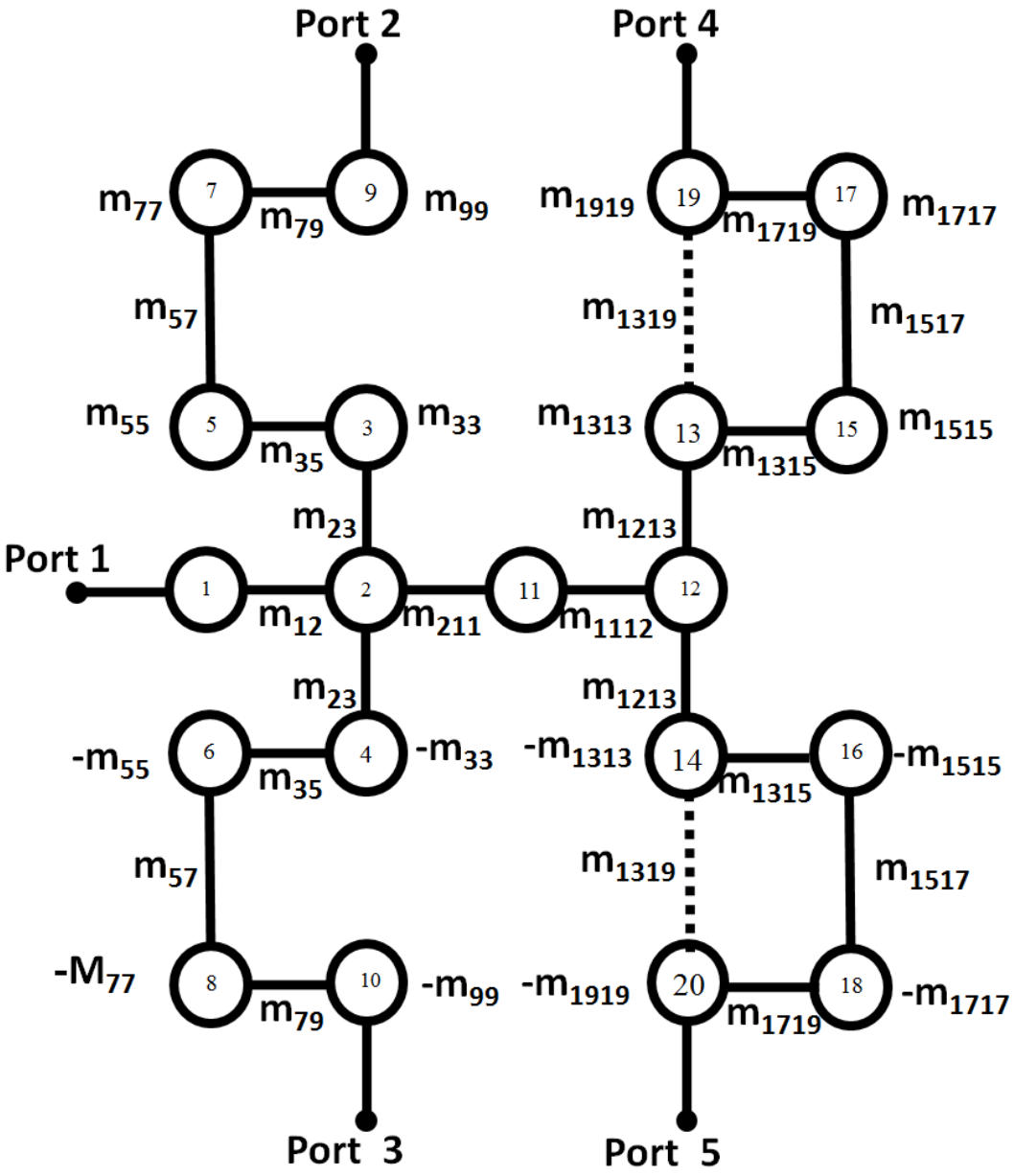

Figure (4.9): structure of multiplexer five.

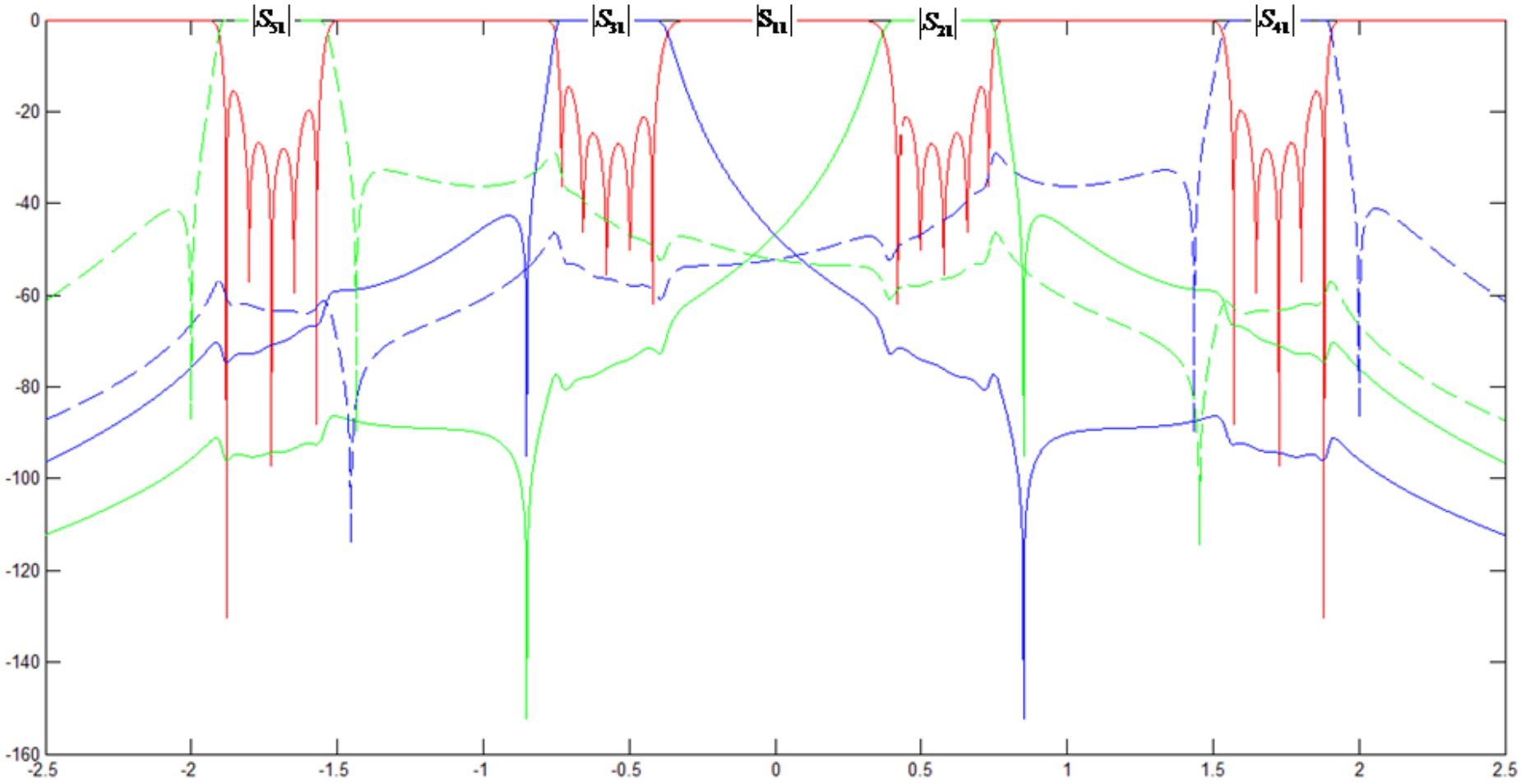

Figure (4.10): The theoretical response of multiplexer five.

Table (4.11): The optimized coupling matrix of multiplexer five.

Resonator	1	2	3	4	5	6	7	8	9	10	11	12	13	14	15	16	17	18	19	20
1	0	1.347	0	0	0	0	0	0	0	0	0	0	0	0	0	0	0	0	0	0
2	1.3470	0	0.4458	0.4458	0	0	0	0	0	0	0.8663	0	0	0	0	0	0	0	0	0
3	0	0.4458	0.5448	0	0.1129	0	0	0	0	0	0	0	0	0	0	0	0	0	0	0
4	0	0.4458	0	-0.5448	0	0.1129	0	0	0	0	0	0	0	0	0	0	0	0	0	0
5	0	0	0.1129	0	0.5589	0	0.1043	0	0	0	0	0	0	0	0	0	0	0	0	0
6	0	0	0	0.1129	0	-0.5589	0	0.1043	0	0	0	0	0	0	0	0	0	0	0	0
7	0	0	0	0	0.1043	0	0.5618	0	0.1419	0	0	0	0	0	0	0	0	0	0	0
8	0	0	0	0	0	0.1043	0	-0.5618	0	0.1419	0	0	0	0	0	0	0	0	0	0
9	0	0	0	0	0	0	0.1419	0	0.5614	0	0	0	0	0	0	0	0	0	0	0
10	0	0	0	0	0	0	0	0.1419	0	-0.5614	0	0	0	0	0	0	0	0	0	0
11	0	0.8663	0	0	0	0	0	0	0	0	0	0.9831	0	0	0	0	0	0	0	0
12	0	0	0	0	0	0	0	0	0	0	0.9831	0	0.5032	0.5032	0	0	0	0	0	0
13	0	0	0	0	0	0	0	0	0	0	0	0.5032	1.5115	0	0.1100	0	0	0	-0.0271	0
14	0	0	0	0	0	0	0	0	0	0	0	0.5032	0	-1.5115	0	0.1100	0	0	0	-0.0271
15	0	0	0	0	0	0	0	0	0	0	0	0	0.1100	0	1.7149	0	0.1181	0	0	0
16	0	0	0	0	0	0	0	0	0	0	0	0	0	0.1100	0	-1.7149	0	0.1181	0	0
17	0	0	0	0	0	0	0	0	0	0	0	0	0	0	0.1181	0	1.7202	0	0.1375	0
18	0	0	0	0	0	0	0	0	0	0	0	0	0	0	0	0.1181	0	-1.7202	0	0.1375
19	0	0	0	0	0	0	0	0	0	0	0	0	-0.0271	0	0	0	0.1375	0	1.7174	0
20	0	0	0	0	0	0	0	0	0	0	0	0	0	-0.0271	0	0	0	0.1375	0	-1.7174

4.1.6. Example 6: Non-contiguous band four channels multiplexer consists of two channels with Quasi elliptic response and the other two channels with Chebyshev response and $n = 20$, $r = 4$, $x_1 = 0.4$, $x_2 = 0.75$, $x_3 = 1.55$, $x_4 = 1.9$.

The multiplexer consists of four non contiguous channels as shown in figure (4.11), and it has twenty resonators in total with four resonators per arm. The specified return loss is 20 dB. The channels have an equal bandwidth and they are separated by equal guard bands. The edges of channels 1,2,3 and 4 are {-1.9,-1.55},{-0.75,-0.4},{0.4,0.75},{1.55,1.9} respectively. The four transmission zeros locate at ± 0.3i and ± 0.85i. The normalized external quality factors are numerically calculated using equation (3.16) as $q_{e9} = q_{e10} = q_{e91} = q_{e20}$ =5.5509 and q_{e1} = 1.3877. The locations of return zeros are calculated using equation (3.15) as ± 1.8800i, ± 1.8025i, ± 1.7250i, ± 1.6475i, ± 1.5700i, ± 0.7300i, ± 0.6525i, ± 0.5750i, ± 0.4975i and ± 0.4200i. These locations are the initial locations and they are optimized to get return zeros with return loss less than 20 dB. The final return zeros' locations are ± 1.8821i, ± 1.8240i, ± 1.7255i, ± 1.6203i, ± 1.5510i, ± 0.7275i, ± 0.6826i, ± 0.5934i, ± 0.4821i, ± 0.4121i. In figure (4.11) , solid lines represent direct coupling, and dashed lines represent cross coupling, and both Quasi-Elliptic and Chebyshev responses can be achieved.

The coupling coefficients between any adjacent resonators m_{ij} and frequency offsets m_{ii} are optimized using cost function in equation (3.14) to have final values m_{12} =1.3393, m_{23} = 0.4370, m_{211} =0.8821, m_{33} = 0.5400, m_{35} = 0.1079, m_{39} = -0.0286, m_{55} = 0.5569, m_{57} = 0.1213, m_{77} =0.5659, m_{79} =0.1424, m_{99} = 0.5669, m_{1112} = 1.0066, m_{1213} = 0.5069, m_{1313} = 1.5014, m_{1315} = 0.1238, m_{1515} =1.7062, m_{1517} = 0.1115, m_{1717} = 1.7126, m_{1719} = 0.1514, m_{1919} =1.7132. For symmetry, some conditions were taken in account to simplify the optimization, these conditions are $m_{23} = m_{24}$, $m_{35} = m_{46}$, $m_{39} = m_{410}$, $m_{57} = m_{68}$, $m_{79} = m_{810}$, $m_{1213} = m_{1214}$, $m_{1315} = m_{1416}$, $m_{1517} = m_{1618}$, $m_{1719} = m_{1820}$, $m_{33} = -m_{44}$, $m_{55} = -m_{66}$, $m_{77} = -m_{88}$, $m_{99} = -m_{1010}$, $m_{1313} = -m_{1414}$, $m_{1515} = -m_{1616}$, $m_{1717} = -m_{1818}$ and $m_{1919} = -m_{2020}$.

In this example all terms in the cost function in equation (3.14) are entered into optimization process. Table (4.12) displays the realized values that are achieved by optimization versus the targets. The optimized coupling matrix is given in table (4.13) and the multiplexer prototype response is depicted in figure (4.12).

Table (4.12): The Realized values versus the targets.

Item		Target	Realized values	Percentage of error
Return loss(L_R) in db		-20	-20.22	1.1%
boundaries	x_1	0.4	0.372	7.0%
	x_2	0.75	0.753	0.4%
	x_3	1.55	1.505	2.9%
	x_4	1.9	1.918	0.9%
Transmission zeros	t_1	0.3	0.279	7.0%
	t_2	0.85	0.844	0.7%

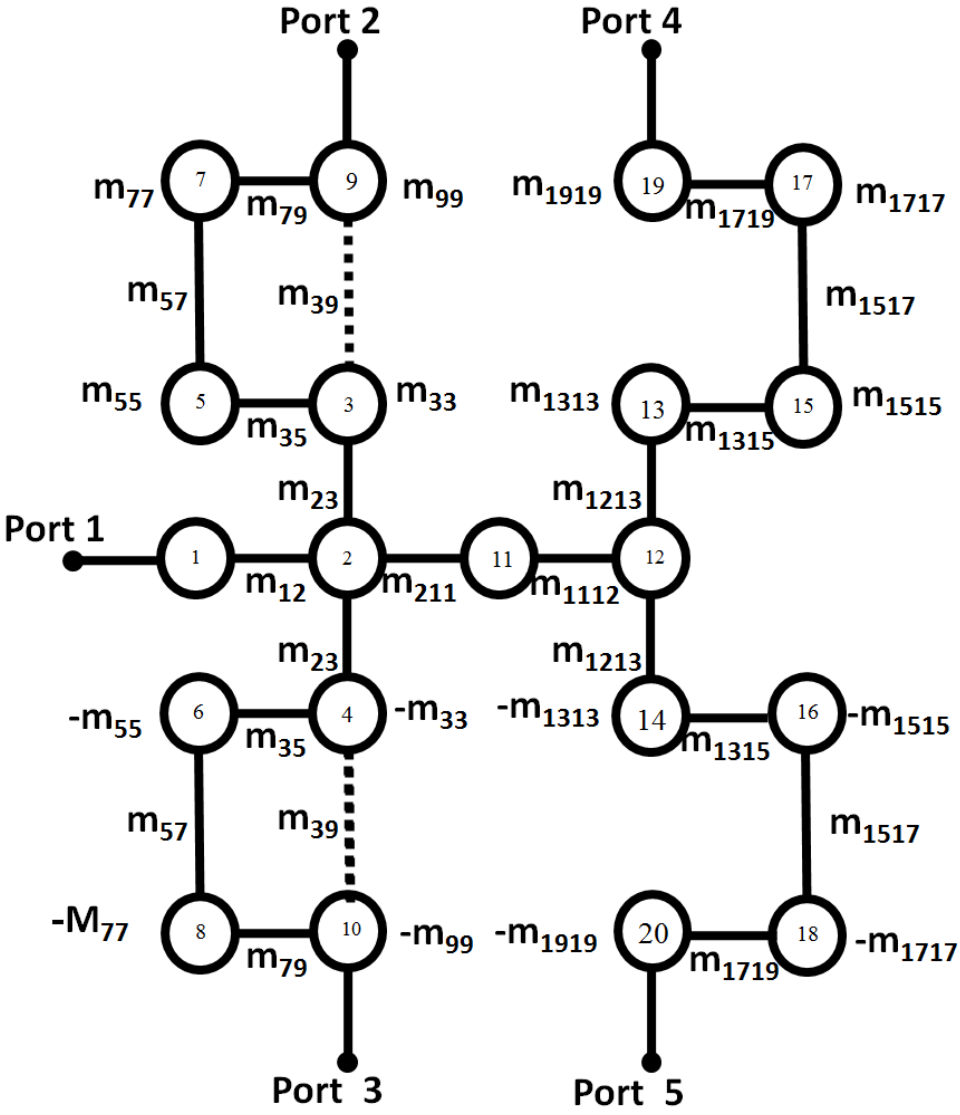

Figure (4.11): structure of multiplexer six.

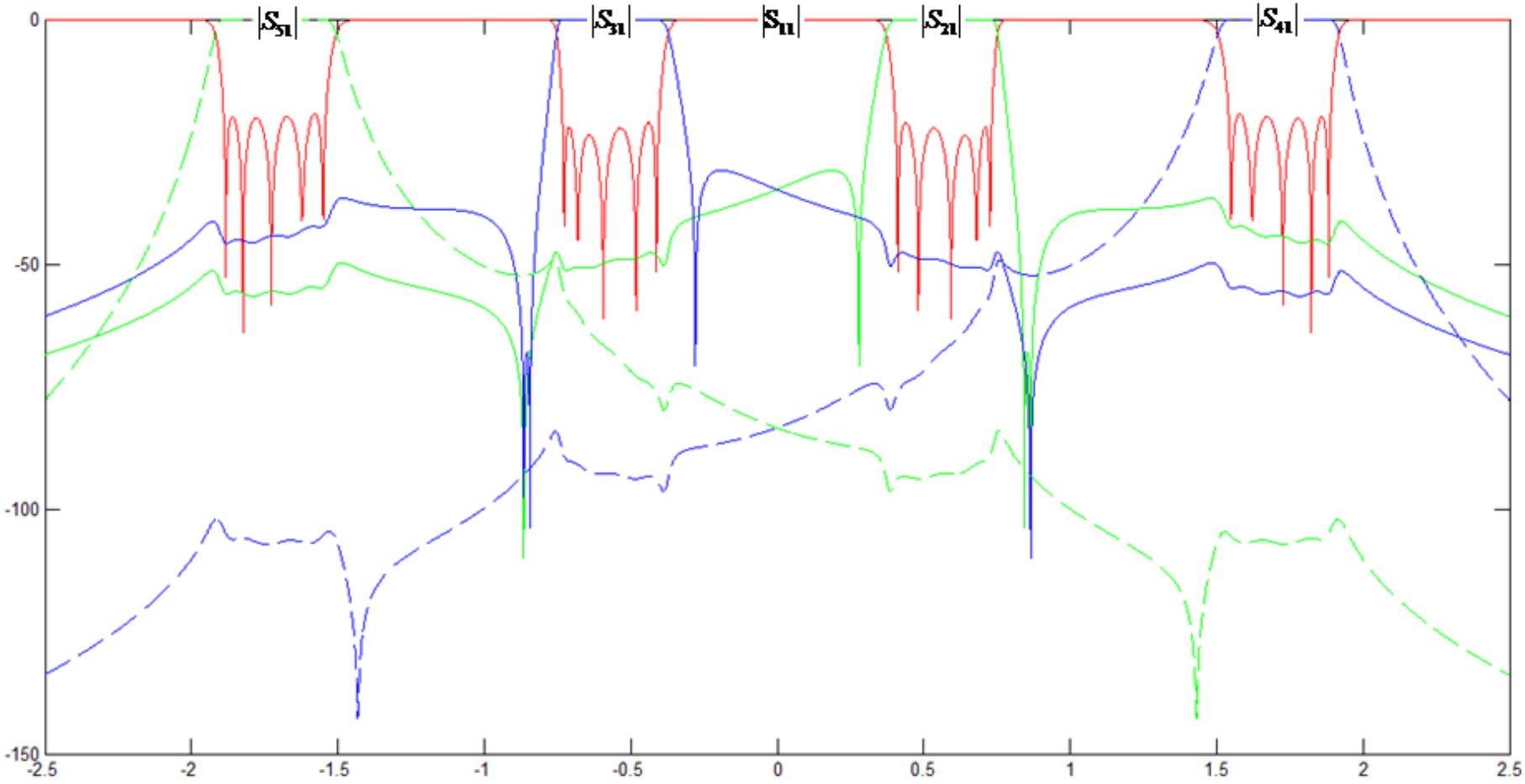

Figure (4.12): The theoretical response of multiplexer six.

Table (4.13): The optimized coupling matrix of multiplexer six.

Resonator	1	2	3	4	5	6	7	8	9	10	11	12	13	14	15	16	17	18	19	20
1	0	1.3393	0	0	0	0	0	0	0	0	0	0	0	0	0	0	0	0	0	0
2	1.3393	0	0.437	0.437	0	0	0	0	0	0	0.8821	0	0	0	0	0	0	0	0	0
3	0	0.437	0.54	0	0.1079	0	0	0	-0.0286	0	0	0	0	0	0	0	0	0	0	0
4	0	0.437	0	-0.54	0	0.1079	0	0	0	-0.0286	0	0	0	0	0	0	0	0	0	0
5	0	0	0.1079	0	0.5569	0	0.1213	0	0	0	0	0	0	0	0	0	0	0	0	0
6	0	0	0	0.1079	0	-0.5569	0	0.1213	0	0	0	0	0	0	0	0	0	0	0	0
7	0	0	0	0	0.1213	0	0.5659	0	0.1424	0	0	0	0	0	0	0	0	0	0	0
8	0	0	0	0	0	0.1213	0	-0.5659	0	0.1424	0	0	0	0	0	0	0	0	0	0
9	0	0	-0.0286	0	0	0	0.1424	0	0.5669	0	0	0	0	0	0	0	0	0	0	0
10	0	0	0	-0.0286	0	0	0	0.1424	0	-0.5669	0	0	0	0	0	0	0	0	0	0
11	0	0.8821	0	0	0	0	0	0	0	0	0	1.0066	0	0	0	0	0	0	0	0
12	0	0	0	0	0	0	0	0	0	0	1.0066	0	0.5069	0.5069	0	0	0	0	0	0
13	0	0	0	0	0	0	0	0	0	0	0	0.5069	1.5014	0	0.1238	0	0	0	0	0
14	0	0	0	0	0	0	0	0	0	0	0	0.5069	0	-1.5014	0	0.1238	0	0	0	0
15	0	0	0	0	0	0	0	0	0	0	0	0	0.1238	0	1.7062	0	0.1115	0	0	0
16	0	0	0	0	0	0	0	0	0	0	0	0	0	0.1238	0	-1.7062	0	0.1115	0	0
17	0	0	0	0	0	0	0	0	0	0	0	0	0	0	0.1115	0	1.7126	0	0.1514	0
18	0	0	0	0	0	0	0	0	0	0	0	0	0	0	0	0.1115	0	-1.7126	0	0.1514
19	0	0	0	0	0	0	0	0	0	0	0	0		0	0	0	0.1514	0	1.7132	0
20	0	0	0	0	0	0	0	0	0	0	0	0	0		0	0	0	0.1514	0	-1.7132

4.1.7. Example 7: Non-contiguous narrow band six channels multiplexer with $n = 12$, $r = 1$, $x_1 = 0.3$, $x_2 = 0.4$, $x_3 = 1$, $x_4 = 1.1$, $x_5 = 1.7$, $x_6 = 1.8$.

The multiplexer consists of six non contiguous channels as shown in figure (4.13), and it has twelve resonators in total with one resonator per arm. The specified return loss is 20 dB. The channels have an equal bandwidth and they are separated by equal guard bands. The edges of channels 1, 2, 3, 4, 5 and 6 are {-1.8,-1.7}, {-1.1,-1}, {-0.4,-0.3}, {0.3,0.4}, {1,1.1}, {1.8,1.7} respectively. The normalized external quality factors are numerically calculated using equation (3.16) as $q_{e3} = q_{e4} = q_{e7} = q_{e8} = q_{e11} = q_{e12} = 13.2960$ and $q_{e1} = 2.2160$. The locations of return zeros are calculated using equation (3.15) as ± 0.3200i, ± 0.3800i, ± 1.0200i, ± 1.0800i, ± 1.7200i and ± 1.7800i.

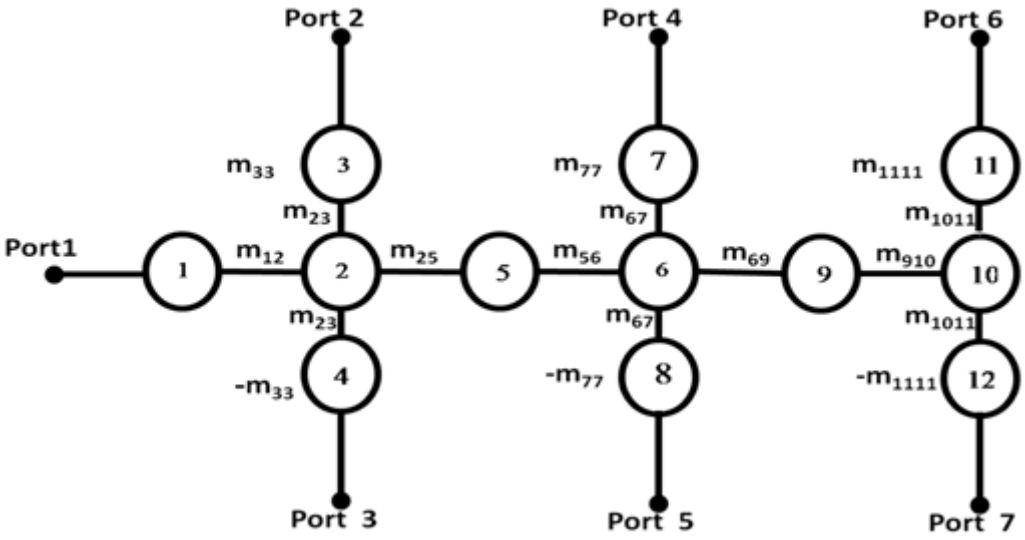

Figure (4.13): structure of multiplexer seven.

The coupling coefficients between any adjacent resonators m_{ij} and frequency offsets m_{ii} are optimized using cost function in equation (3.14) to have final values $m_{12} = 1.2153$, $m_{23} = 0.2082$, $m_{25} = 0.9936$, $m_{33} = 1.0437$, $m_{56} = 0.9328$, $m_{67} = 0.2013$, $m_{77} = 1.7119$, $m_{69} = 0.8311$, $m_{910} = 0.5839$, $m_{1011} = 0.122$, $m_{1111} = 0.3398$. For symmetry, some conditions were taken in account to simplify the optimization, these conditions are $m_{23} = m_{24}$, $m_{67} = m_{68}$, $m_{1011} = m_{1012}$, $m_{33} = -m_{44}$, $m_{77} = -m_{88}$ and $m_{1111} = -m_{1212}$.

In this example only the second term in the cost function in equation (3.14), the term related to return zeros, was used in optimization and the others were neglected. The optimized coupling matrix is given in table (4.14) and the multiplexer prototype response is depicted in figure (4.14). Table (4.15) displays the realized values that are achieved by optimization versus the targets.

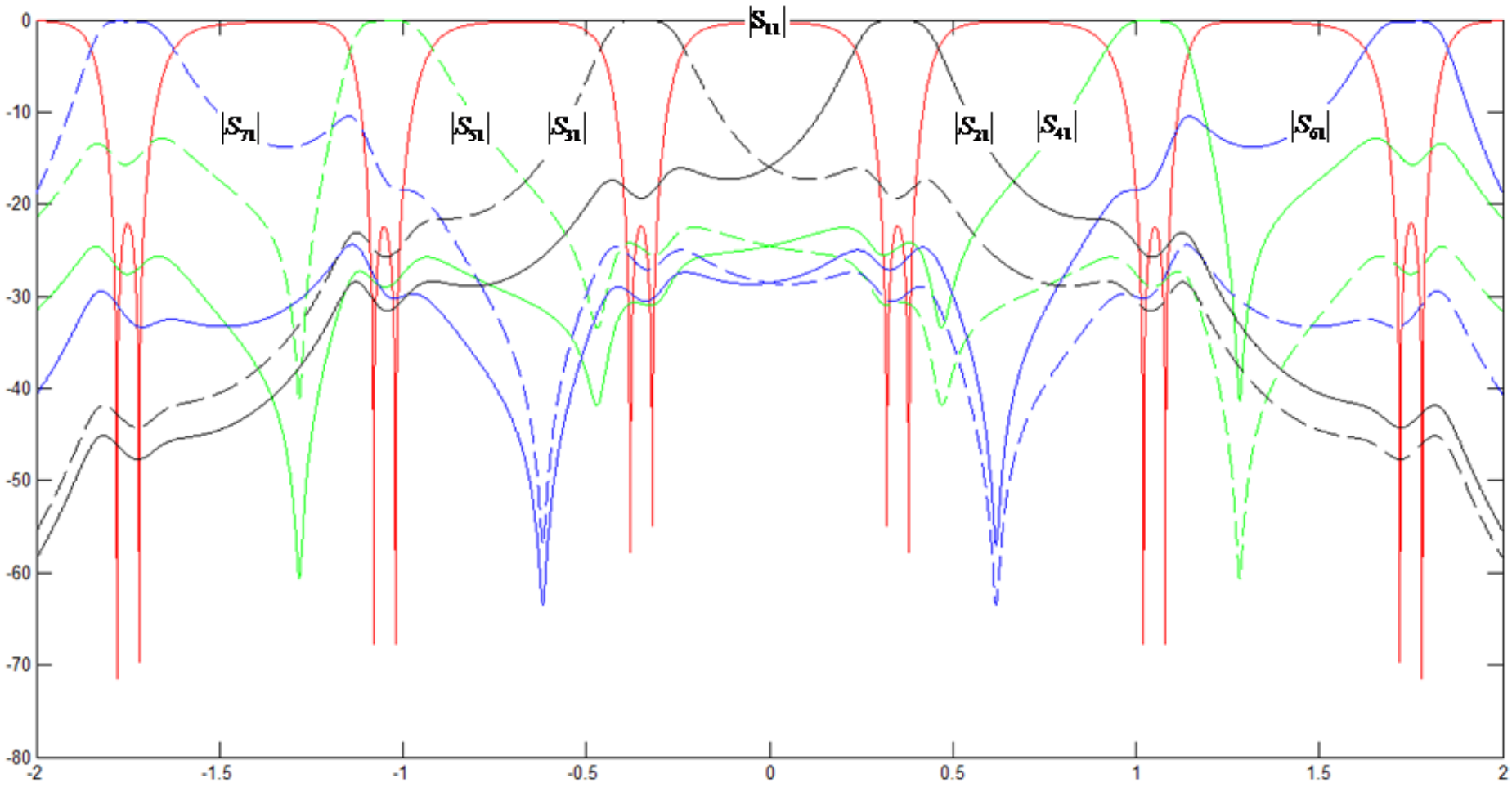

Figure (4.14): The theoretical response of multiplexer seven.

Table (4.14): The optimized coupling matrix of multiplexer seven.

Resonators	1	2	3	4	5	6	7	8	9	10	11	12
1	0	1.2153	0	0	0	0	0	0	0	0	0	0
2	1.2153	0	0.2082	0.2082	0.9936	0	0	0	0	0	0	0
3	0	0.2082	1.0437	0	0	0	0	0	0	0	0	0
4	0	0.2082	0	-1.0437	0	0	0	0	0	0	0	0
5	0	0.9936	0	0	0	0.9328	0	0	0	0	0	0
6	0	0	0	0	0.9328	0	0.2013	0.2013	0.8311	0	0	0
7	0	0	0	0	0	0.2013	1.7119	0	0	0	0	0
8	0	0	0	0	0	0.2013	0	-1.7119	0	0	0	0
9	0	0	0	0	0	0.8311	0	0	0	0.5839	0	0
10	0	0	0	0	0	0	0	0	0.5839	0	0.1227	0.1227
11	0	0	0	0	0	0	0	0	0	0.1227	0.3398	0
12	0	0	0	0	0	0	0	0	0	0.1227	0	-0.3398

Table (4.15): The Realized values versus the targets.

Item		Target	Realized values	Percentage of error
Return loss(L_R) in db		-20	-22.07	0.4%
boundaries	x_1	0.3	0.235	21.7%
	x_2	0.4	0.46	15.0%
	x_3	1	0.922	7.8%
	x_4	1.1	1.14	3.6%
	x_5	1.7	1.629	4.2%
	x_6	1.8	1.849	2.7%

4.1.8. Example 8: Non-contiguous narrow band four channels multiplexer with $n = 8$, $r = 1$, $x_1 = 0.5$, $x_2 = 0.6$, $x_3 = 1.6$, $x_4 = 1.7$.

Isolation between channels can be improved by increasing the number of resonator per arm. This example presents a new way to improve the isolation between channels. The example is based on the structures in figure (4.15). Figure (4.16) shows the response of the structure with the normal distribution of channels and table (4.17) shows the optimized coupling matrix of this structure. Figure (4.17) shows the response of the structure with interchanging the positions of channels in the same structure shown in figure (4.15) and table (4.18) shows the optimized coupling matrix of this structure.

The interchanging of the positions of channel 3 and channel 4 improves the isolation between the adjacent channels as appears in figure (4.17). Before interchanging the channels the isolation peaks is around -10 dB as shown in figure (4.16), but after interchanging the channels the isolation peaks is around -20 dB. This improvement in isolation occurs due to separating the channels by more frequency band. Table (4.16) displays the realized values that are achieved by optimization versus the targets.

Table (4.16): The Realized values versus the targets.

Item		Target	Realized values	Percentage of error
Return loss(L_R) in db		-20	-21.88	9.4%
Boundaries	x_1	0.5	0.413	17.4%
	x_2	0.6	0.628	4.7%
	x_3	1.6	1.529	4.4%
	x_4	1.7	1.75	2.9%

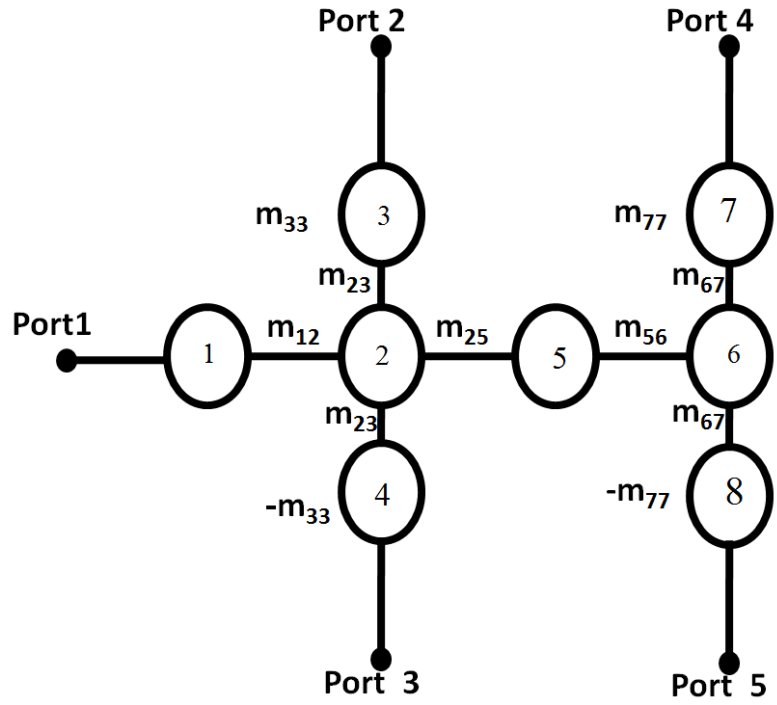

(a)

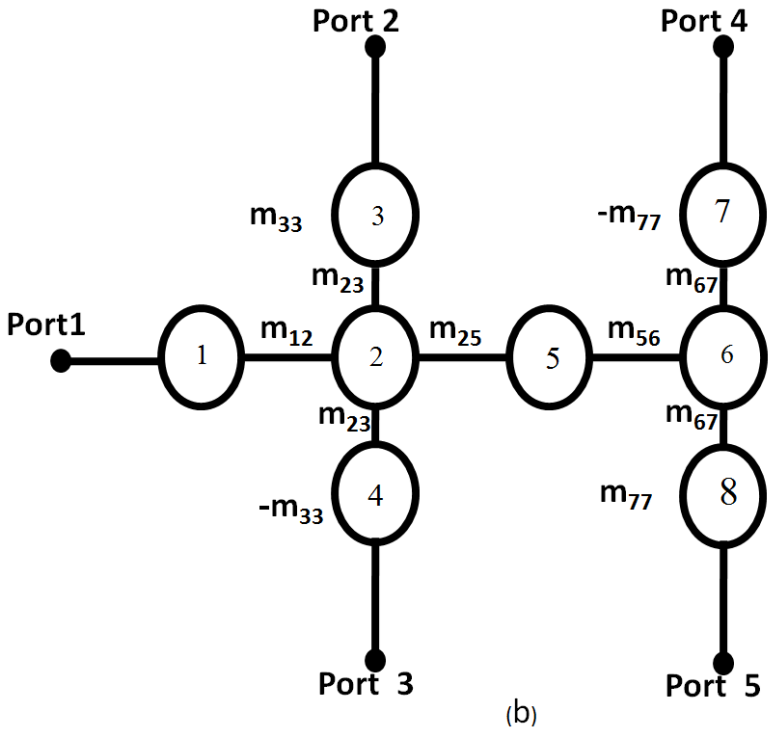

(b)

Figure (4.15): structure of multiplexer eight:

(a) before interchanging of channels.

(b) after interchanging of channels.

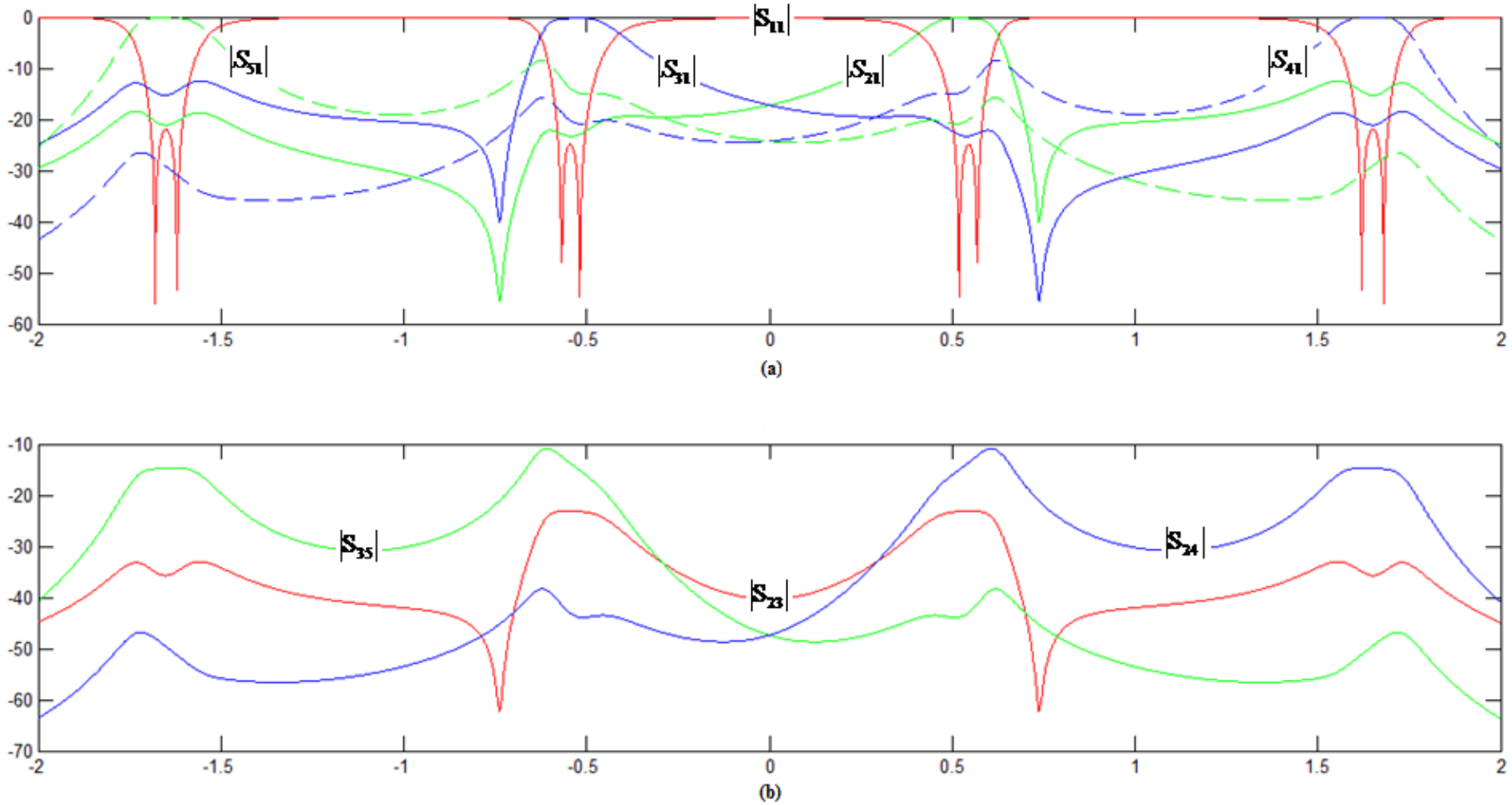

Figure (4.16): The theoretical response of multiplexer eight before interchanging of channels: (a) Reflection loss and insertion loss, (b) The isolation between adjacent channels.

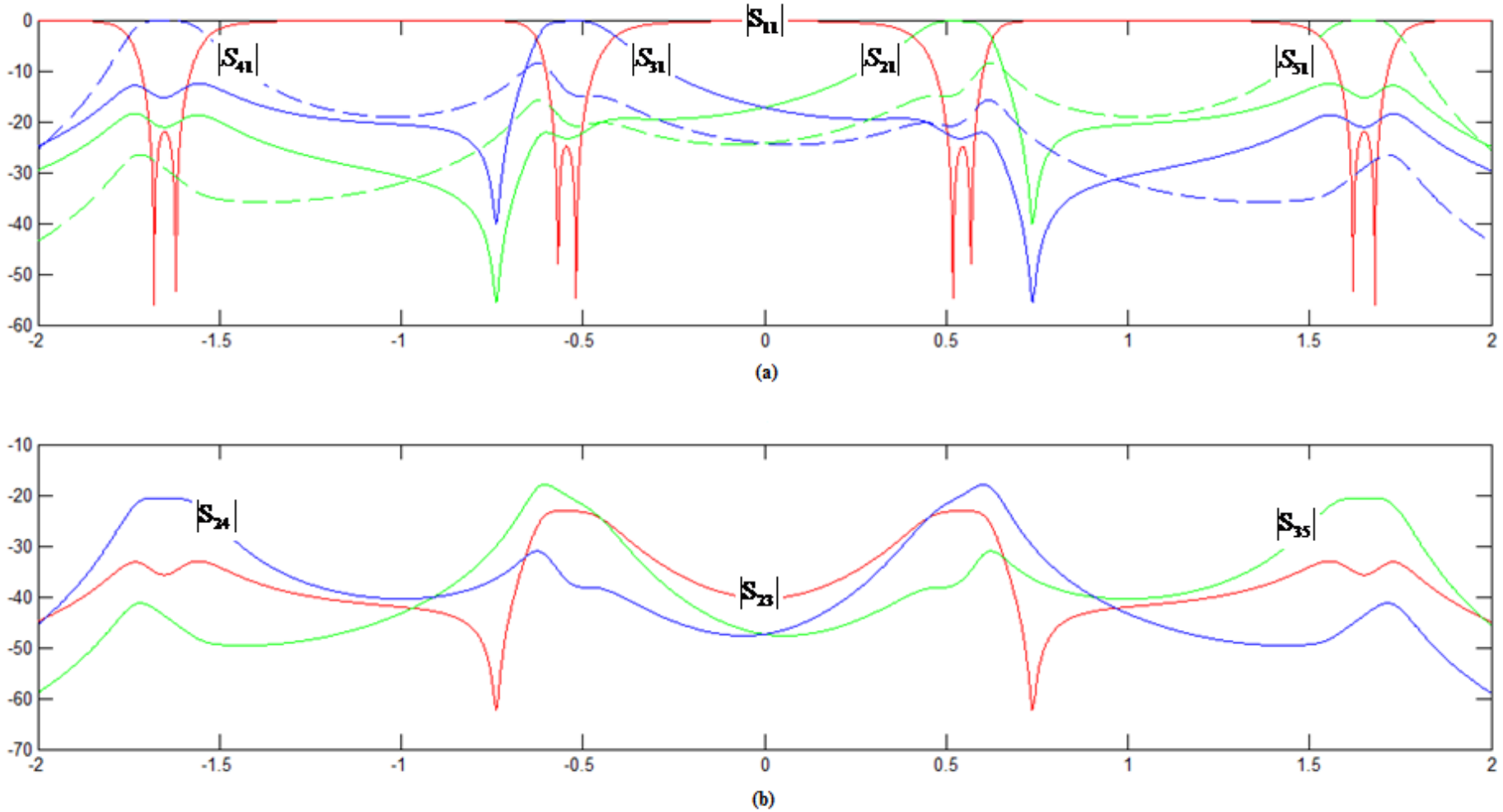

Figure (4.17): The theoretical response of multiplexer eight after interchanging of channels: (a) Reflection loss and insertion loss, (b) The isolation between adjacent channels.

Table (4.17): The optimized coupling matrix of multiplexer eight before interchanging of channels.

Resonators	1	2	3	4	5	6	7	8
1	0	1.2279	0	0	0	0	0	0
2	1.2279	0	0.3060	0.3060	0.9119	0	0	0
3	0	0.3060	0.5324	0	0	0	0	0
4	0	0.3060	0	-0.5324	0	0	0	0
5	0	0.9119	0	0	0	0.7809	0	0
6	0	0	0	0	0.7809	0	0.3390	0.3390
7	0	0	0	0	0	0.3390	1.5639	0
8	0	0	0	0	0	0.3390	0	-1.5639

Table (4.18): The optimized coupling matrix of multiplexer eight after interchanging of channels.

Resonators	1	2	3	4	5	6	7	8
1	0	1.2279	0	0	0	0	0	0
2	1.2279	0	0.3060	0.3060	0.9119	0	0	0
3	0	0.3060	0.5324	0	0	0	0	0
4	0	0.3060	0	-0.5324	0	0	0	0
5	0	0.9119	0	0	0	0.7809	0	0
6	0	0	0	0	0.7809	0	0.3390	0.3390
7	0	0	0	0	0	0.3390	-1.5639	0
8	0	0	0	0	0	0.3390	0	1.5639

4.1.9. Example 9: Non-contiguous band four channels multiplexer with $n = 16$, $r_1 = 2$, $r_2 = 4$, $x_1 = 0.4$, $x_2 = 0.65$, $x_3 = 1.45$, $x_4 = 1.95$, $t_1=1.35$, $t_2=2.05$.

This example is different from all previous examples because it has four channels and each two channels have different bandwidth, different response and different number of resonators per arm. This means that the general structure is able to synthesize multiplexers with massive scale of properties and characteristics. As shown in figure (4.18) the total number of resonators in the whole structure is sixteen resonators and the number of resonators in both channels one and two is two resonators but the number of resonators in both channels three and four is four resonators. Channels one and two have Chebyshev response while the channels three and four have quasi elliptic response due to the existence of cross coupling m_{915}.

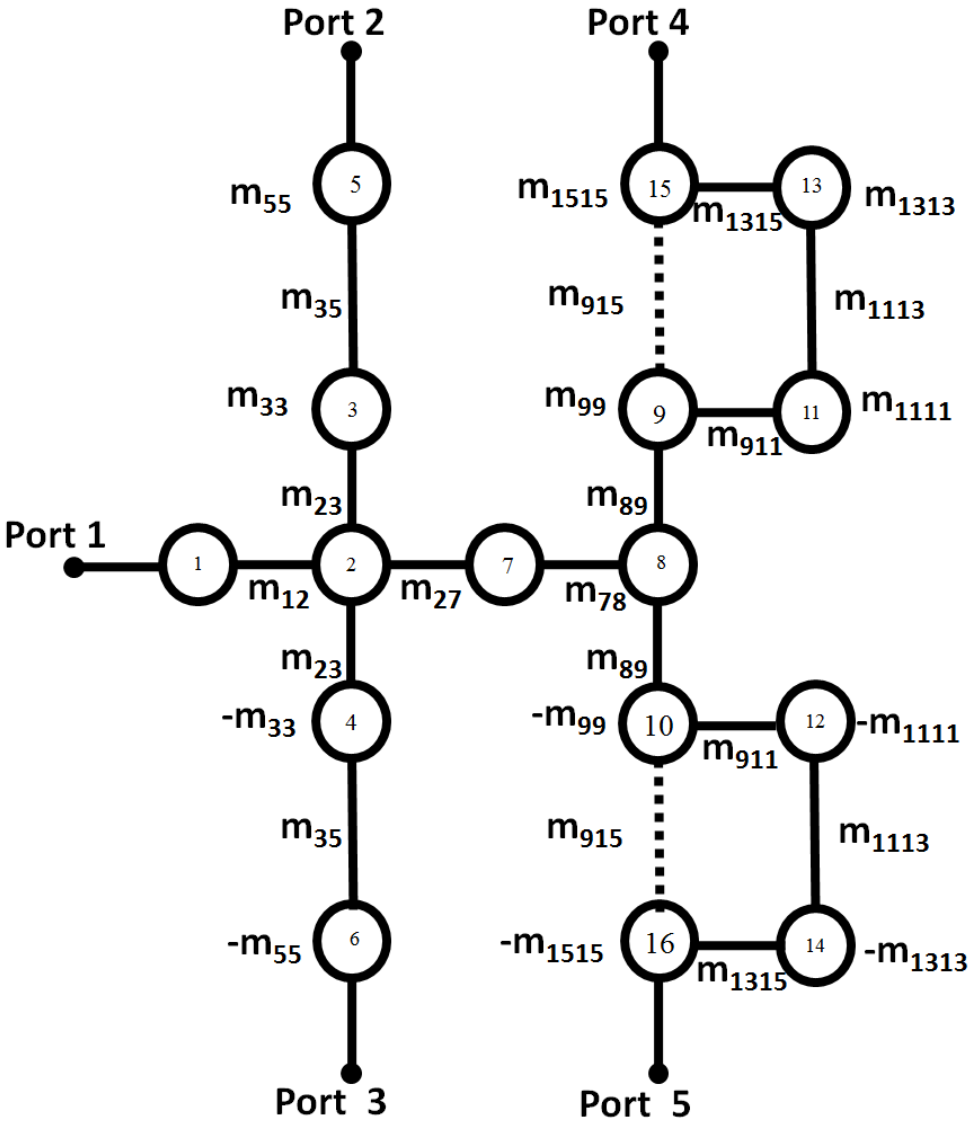

Figure (4.18): structure of multiplexer nine.

The optimization process in this example is different from the optimization processes in all previous examples because in the previous examples the optimization processes are done in one step where all coupling coefficients and reflection zeros' locations were entered into optimization process but in this example each diplexer (two arms) is optimized as an individual block then most of the results are taken as initial values in the optimization process for the whole multiplexer.

The first diplexer is optimized to get some of the coupling coefficients that are taken as initial values m_{33} =0.4963, m_{35} = 0.1293, m_{55} = 0.5180, and reflection zeros' locations as $\pm 0.4200i$, $\pm 0.5250i$, $\pm 0.6300i$. The second diplexer is optimized to get some of the coupling coefficients that are taken as initial values m_{99} = 1.6751, m_{911} = 0.1438, m_{915} = 0.0736, m_{1111} = 1.6986, m_{1113} = 0.2039, m_{1313} = 1.7015, m_{1315} = 0.2032, m_{1515} = 1.7007, and the optimized reflection zeros' locations $\pm$ 1.4533i, $\pm 1.5380i$, $\pm$ 1.7061i, $\pm 1.8697i$, $\pm 1.9496i$ will be entered into whole optimization process.

Table (4.19) displays the realized values that are achieved by optimization versus the targets. The final values of coupling coefficients, as shown in table (4.20), are m_{12} = 1.4543, m_{23} = 0.4798, m_{27} = 0.7550, m_{33} = 0.4951, m_{35} = 0.1409, m_{55} = 0.4942, m_{78} = 1.1151, m_{89} = 0.7059, m_{99} = 1.1479, m_{911} = 0.2044, m_{1111} = 1.6564, m_{1113} = 0.2029, m_{1313} = 1.7056, m_{1315} = 0.2048, m_{1515} = 1.6787, m_{915} = 0.0905. The normalized external quality factors q_{e5} = q_{e6} = 6.8128, q_{e15} = q_{e16} = 3.8856 and q_{e1} = 1.2372.

Table (4.19): The Realized values versus the targets.

Item		Target	Realized values	Percentage of error
Return loss(L_R) in db		-20	-18.2	9.0%
boundaries	x_1	0.4	0.289	27.8%
	x_2	0.65	0.671	3.2%
	x_3	1.45	1.397	3.7%
	x_4	1.95	1.98	1.5%
Transmission zeros	t_1	1.35	1.313	2.7%
	t_2	2.05	2.049	0%

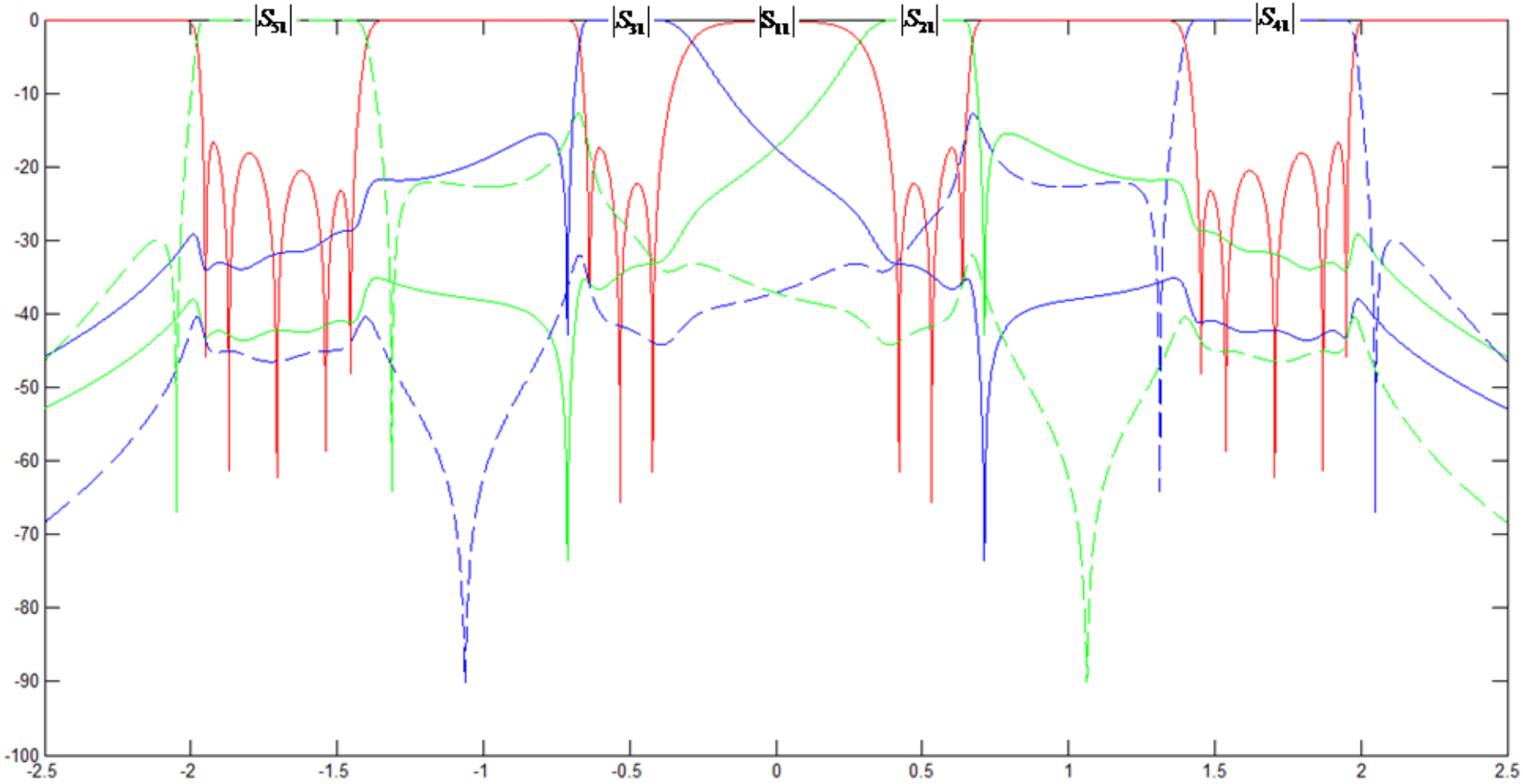

Figure (4.19): The theoretical response of multiplexer nine.

Table (4.20): The optimized coupling matrix of multiplexer nine.

Resonator	1	2	3	4	5	6	7	8	9	10	11	12	13	14	15	16
1	0	1.4543	0	0	0	0	0	0	0	0	0	0	0	0	0	0
2	1.4543	0	0.4798	0.4798	0	0	0.755	0	0	0	0	0	0	0	0	0
3	0	0.4798	0.4951	0	0.1409	0	0	0	0	0	0	0	0	0	0	0
4	0	0.4798	0	-0.4951	0	0.1409	0	0	0	0	0	0	0	0	0	0
5	0	0	0.1409	0	0.4942	0	0	0	0	0	0	0	0	0	0	0
6	0	0	0	0.1409	0	-0.4942	0	0	0	0	0	0	0	0	0	0
7	0	0.755	0	0	0	0	0	1.1151	0	0	0	0	0	0	0	0
8	0	0	0	0	0	0	1.1151	0	0.7059	0.7059	0	0	0	0	0	0
9	0	0	0	0	0	0	0	0.7059	1.1479	0	0.2044	0	0	0	0	0
10	0	0	0	0	0	0	0	0.7059	0	-1.1479	0	0.2044	0	0	0	0
11	0	0	0	0	0	0	0	0	0.2044	0	1.6564	0	0.2029	0	0	0
12	0	0	0	0	0	0	0	0	0	0.2044	0	-1.6564	0	0.2029	0	0
13	0	0	0	0	0	0	0	0	0	0	0.2029	0	1.7056	0	0.2048	0.2048
14	0	0	0	0	0	0	0	0	0	0	0	0.2029	0	-1.7056	0	0
15	0	0	0	0	0	0	0	0	0	0	0	0	0.2048	0	1.6787	0
16	0	0	0	0	0	0	0	0	0	0	0	0	0	0.2048	0	-1.6787

The validity of the last example is going to be checked. The band pass multiplexer starts from 2700 MHz to 3300 MHz. The smallest and the largest values in both range of values of normalized external quality factors and coupling coefficients have been chosen for implementation, so other values between them can be guaranteed to be realized. To achieve these values, the open loop resonators have been used and HFSS software has been used in simulation. The implementation is going to be done on RT/duroid 6006 substrate which has dielectric constant ε_r of 6.15 and thickness of 1.27mm. The equations needed for designed are stated in chapter eight in [1].

The normalized external coupling is calculated from equation (4.1)

$$k_e = \frac{1}{q_e} \tag{4.1}$$

where q_e is the normalized external quality factor. The external coupling K_e and coupling coefficients M_{ij} are calculated from equation (4.2)

$$K_e = \frac{k_e \times FBW}{x_n},$$

$$M_{ij} = \frac{m_{ij} \times FBW}{x_n} \tag{4.2}$$

where *FBW* is the fractional bandwidth which is calculated from equation (3.5), and x_n is the maximum normalized frequency in low-pass.

$|S_{21}|$ response for a resonator with a port with weak coupling should be found to extract the external coupling from physical structure, and $|S_{21}|$ response for two coupled resonators with two weak coupling ports should be found to extract the coupling coefficient for two coupled resonators. Equation (4.3) is used for calculations of external coupling where $\Delta\omega_{\pm 3dB}$ and ω_0 can be extracted from $|S_{21}|$ as shown in figure (4.20) and the coupling coefficient can be extracted for synchronous resonators by equation (4.4) where ω_2^2 and ω_1^2 are the frequency at peaks as shown in figure (4.21) [2].

$$K_e = \frac{\Delta\omega_{\pm 3dB}}{\omega_0} \tag{4.3}$$

$$M_{ij} = \pm\frac{\omega_2^2 - \omega_1^2}{\omega_2^2 + \omega_1^2} \tag{4.4}$$

Table (4.21) shows the specification of the band-pass frequencies and their transformations into low-pass using equations (3.1) and (3.5) and table (4.22) shows the calculations of FBW and center frequency using equation (3.5).

The minimum and maximum external coupling values have been calculated for example nine as shown in table (4.23) using equations (4.1) and (4.2). Figure (4.22) shows the physical structure used in achieving external coupling. Equation (4.3) is used to calculate the external coupling from physical structure as shown in table (4.24). Figures (4.23) and (4.24) represent response of $|S_{21}|$ for minimum and maximum normalized quality factor respectively.

The minimum and maximum coupling coefficient values have been calculated for example nine as shown in table (4.25) using (4.2). Figures (4.25) and (4.26) shows the physical structure for two coupled microstrip used in achieving minimum and maximum coupling coefficient respectively. Equation (4.4) is used to calculate the coupling coefficient for synchronous resonators from physical structure as shown in table (4.26). Figure (4.27) represent response of $|S_{21}|$ for maximum coupling coefficient.

It is noticed the *FBW* is relatively large which means that these values can be achievable for narrower multiplexers.

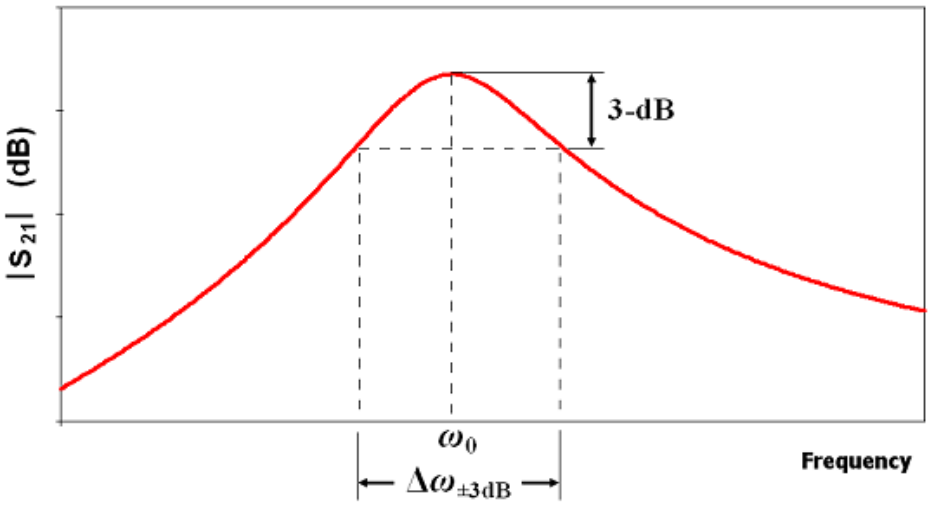

Figure (4.20): Response of $|S_{21}|$ for loaded resonator.

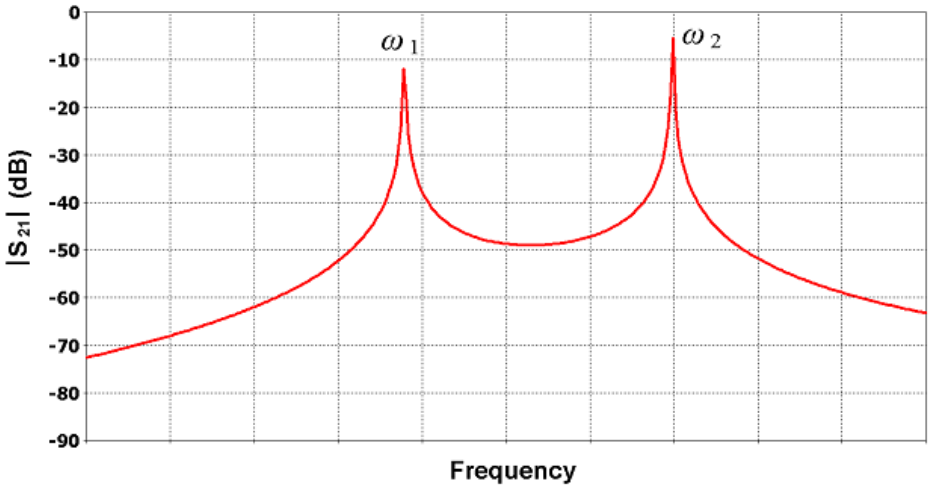

Figure (4.21): $|S_{21}|$ of two coupled resonators showing two frequency peaks.

Table (4.21): Normalization values of multiplexer's bands.

Band-pass (MHz)		Normalized	
W_1	2700	-1.95032	$-x_1$
W_2	2770	-1.451771	$-x_2$
W_3	2886	-0.654554	$-x_3$
W_4	2924	-0.400646	$-x_4$
W_5	3047	0.3989099	x_1
W_6	3087	0.6520629	x_2
W_7	3217	1.4536602	x_3
W_8	3300	1.9498272	x_4

Table (4.22): Calculation of *FBW* and center frequency.

upper frequency	3.3
lower frequency	2.7
center frequency	2.9849623
FBW	0.2010076

Table (4.23): Calculations of external coupling.

normalized quality factor			normalized external coupling	external coupling
max value	q_{e5}	6.8128	0.146782527	0.015130463
min value	q_{e1}	1.2372	0.808276754	0.083317831

Table (4.24): The physical dimensions and calculations of external coupling.

x (mm)	y (mm)	w (mm)	t (mm)	g (mm)	ω_0 (GHz)	$\Delta\omega_{\pm 3dB}$ (GHz)	K_e
6	8	1.838256836	3.9	1.2	2.951	0.043	0.014571332
6.5	7.5	1.838256836	2.25	1.5	2.932	0.2545	0.086800819
6.5	7.5	1.838256836	1.75	1.5	2.921	0.3616	0.123793221

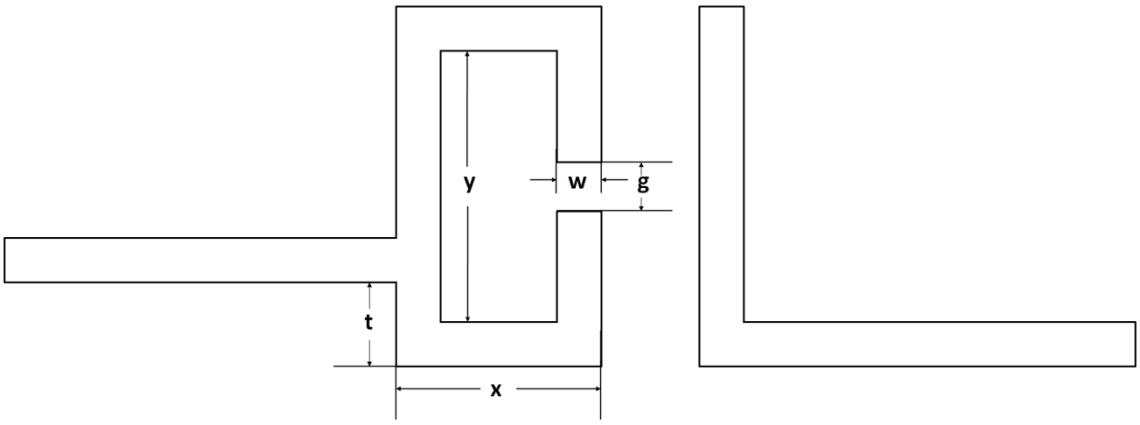

Figure (4.22): Externally coupled microstrip resonator .

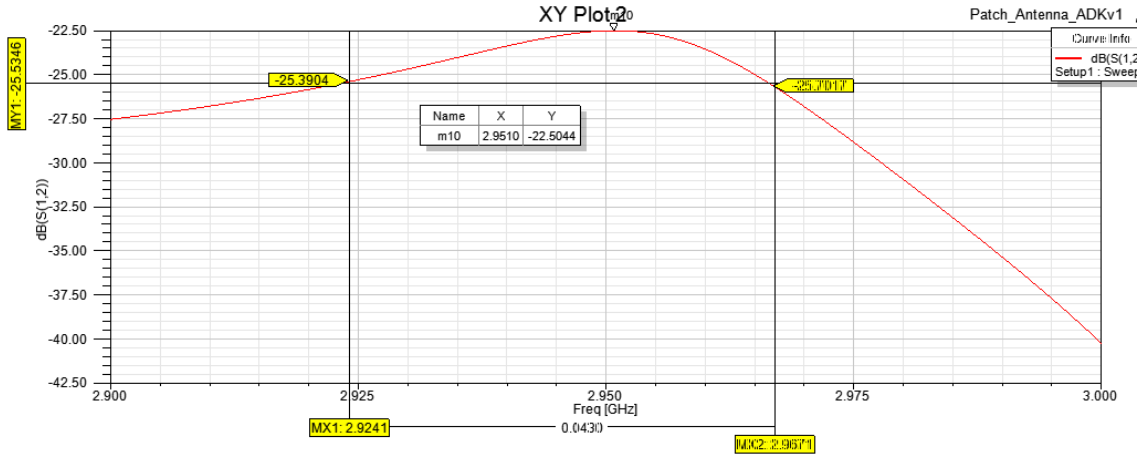

Figure (4.23): Response of $|S_{21}|$ for minimum quality factor.

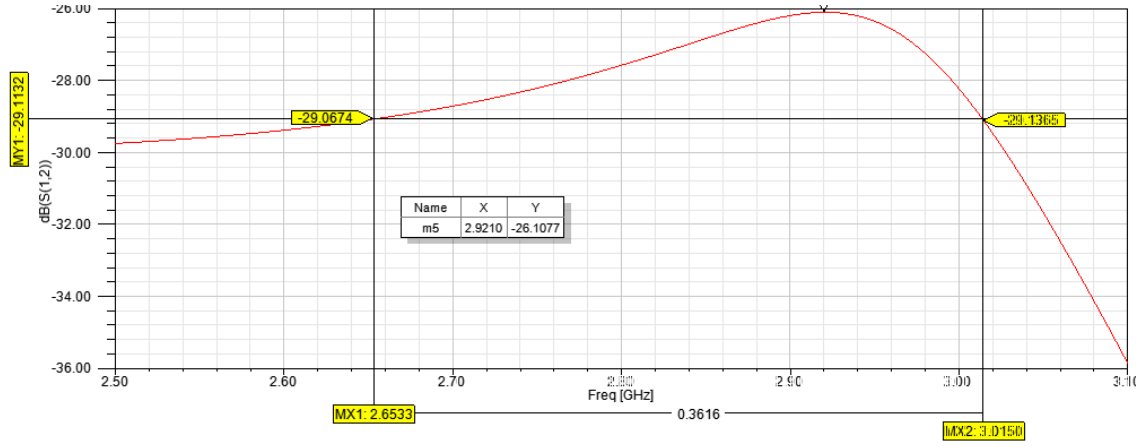

Figure (4.24): Response of $|S_{21}|$ for maximum quality factor.

Table (4.25): Calculations of coupling coefficients.

normalized quality factor			coupling coefficient
max value	m12	1.4543	0.149910437
min value	m46	0.1409	0.014524088

Table (4.26): The physical dimensions and calculations of coupling coefficients.

x(mm)	*y*(mm)	*w*(mm)	*g*(mm)	*s*(mm)	f_1(GHz)	f_2(GHz)	M_{ij}
18	7	1.838257	0.2	0.1	2.745	3.225	0.159771
6	8	1.838257	1.5	2.5	2.925	2.961	0.012232

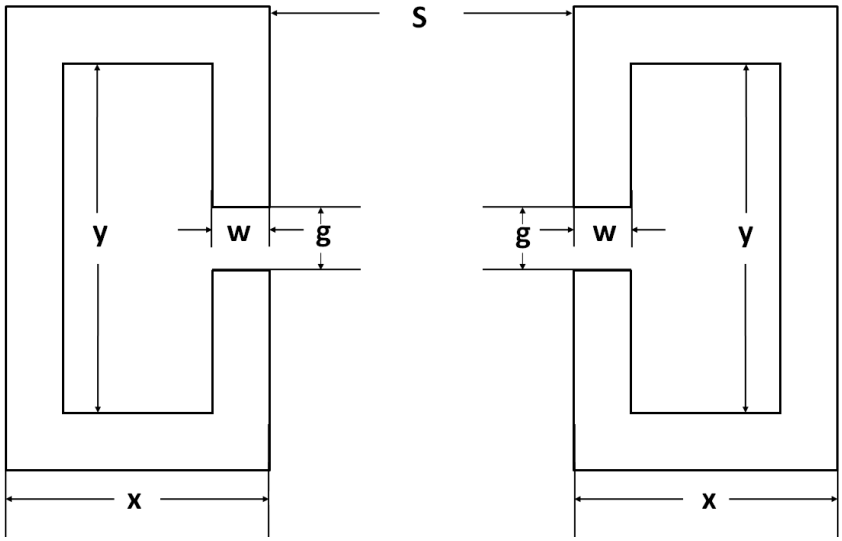

Figure (4.25): The physical structure of the minimum coupling coefficient in example nine.

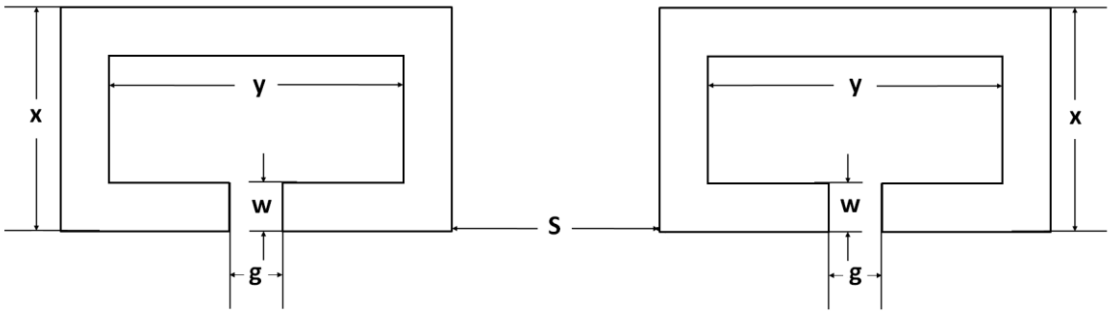

Figure (4.26): The physical structure of the maximum coupling coefficient in example nine.

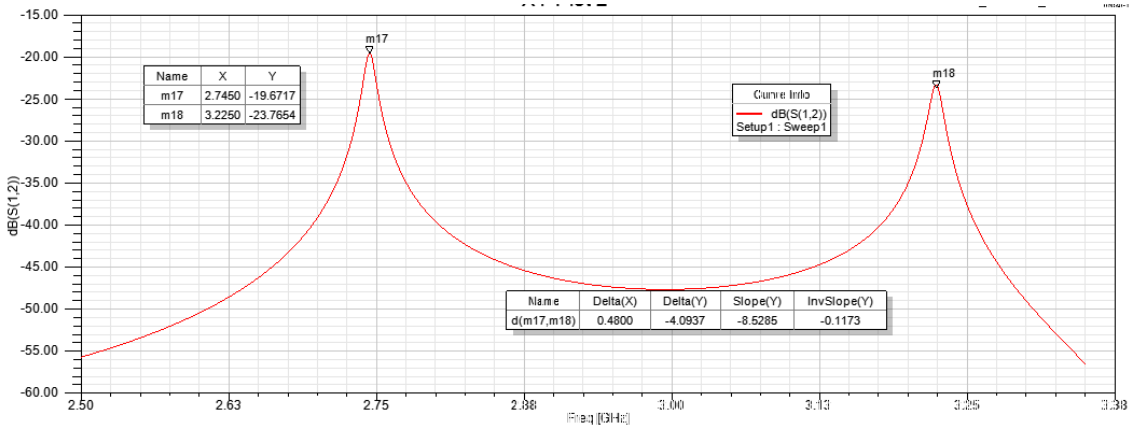

Figure (4.27): Response of $|S_{21}|$ for the maximum coupling coefficient.

4.2 Conclusion

In chapter three, the synthesis procedure of coupled resonator multiplexers is presented. The procedure has been applied to the proposed novel structure in nine examples in chapter four and the reality of results have been checked in last example. Each example is mentioned to advance an advantage of the structure and to prove the ability of structure to meet the interesting characteristics in multiplexers. A remarkable advantage of this novel structure is the ability of dividing the multiplexer into smaller blocks (diplexers) and optimizing each diplexer individually. This decreases the complexity of optimization process and save the time consumed in optimization. The main disadvantage in the novel structure is the degradation of isolation between channel compared with conventional multiplexer. Increasing the number of resonators per channel and interchanging the channels positions improves the isolation as shown in examples.

REFERENCES

1. J.S. Hong and M.J. Lancaster, "Microstrip filters for RF/microwave applications". New York: Wiley, 2001.
2. T. F. Skaik, "Synthesis of Coupled Resonator Circuits with Multiple Outputs using Coupling Matrix Optimization", PhD thesis, the University of Birmingham, 2011.

chapter 5

Conclusion and Future Work

5.1 Conclusion

This thesis talks about synthesis multiplexers based on coupled resonators circuits theory using optimization of coupling matrix. The multiplexers are N-port networks, so analysis of those networks has been introduced for both electrical and magnetic coupling. In magnetic coupling, each resonator in the network is represented by a series R-L-C circuit. Using Kirchoff's voltage law, the equations of network are written and the system or network is represented by impedance matrix. In electric coupling, each resonator in the network is represented by a parallel R-L-C circuit. Using Kirchoff's current law, the equations of network are written and the system or network is represented by admittance matrix. The general formula is derived to use for both types of coupling because the normalized impedance matrix is identical to that normalized admittance matrix, which means unified formulation is derived for an n-coupled resonators regardless of whether the couplings are magnetic or electric or even the combination of both. A General matrix [A] has been formulated in terms of the coupling matrix [M], and a cost function has been derived to be used in optimization.

The procedures of synthesis starts from determining the operation's bands to transform them from band pass to low pass. Then using derived equations, the external quality factors can be numerically calculated to reduce the parameters that need optimization. After that initial reflection zeros' frequency locations can be calculated. These locations have equal spaces between them. These initial locations, transmission zero, return loss and initial coupling coefficient are entered to the optimization algorithm to minimize the cost function to get the optimal values of reflection zeros' frequency location and the optimal coupling coefficients. Finally scattering parameters can be plotted using scattering parameters equations to view the response.

A generalized novel coupled resonator multiplexer is proposed in this thesis. It is based on coupled resonators circuit and the synthesis is based on optimization of coupling matrix. There is neither power distribution network nor extra resonating junction so the number of reflection zeros is equal to the number of total resonators, thus the novel structure can be miniaturized in comparison to the conventional multiplexers since it consists of only resonators without the need to use manifolds or circulators or an extra junction resonator.. The synthesis of the new structure is simple and it has less complexity in comparison to others, but is noted that the isolation between some channels degrades depending on the number of resonators between the ports of each corresponding channels. This thesis talks about two ways to improve the isolation. This first approach talks about increasing the number of resonators per channel. This will increase the isolation with low complexity but it will also increase the

size that is reduced by removing the external junctions. The other way talks about interchanging the positions of channels which can improve the isolation between overlapping channels.

The optimization processes are done by a MATLAB function "fminsearch" to return the minimum value of unconstrained multivariable function using derivative-free method. "fminsearch" uses the simplex search method of Lagarias et al where it is a direct search method that does not use numerical or analytic gradients. This function needs initial values and these initial values play a very important role in getting optimal solution in faster time. The initial values are given in different ways, sometime they are given equally and another time they are taken from previous design. This way is important when you need to update or improve the design.

The proposed structure can achieve Chebyshev response , Quasi elliptic response and both so direct coupling and cross coupling are existing in this structure. These responses and different characteristics have been achieved in this thesis.

5.2 Future Work

In the Chebyshev examples in the inner channels, a transmission zero appears without existing any cross coupling, and in the examples with Quasi elliptic response in the inner channel, an extra transmission zero appears in addition to the two transmission zeros coming from cross coupling to be three transmission zeros per inner channel. These extra transmission zeros need to be investigated to understand why they appear. Another future work can be done by implementation of the proposed structure or by designing and implementation more complex multiplexers by adding more channels and more cross coupling to improve selectivity. Further work can also be conducted by introducing new methods to improve the isolation between the multiplexer channels, as it has been shown that the isolation performance of the proposed coupled resonator multiplexers degrades in comparison with the conventional multiplexers.

The initial values of coupling coefficients and the locations of the reflection zeros play an important role in optimization processes. Future work can be conducted by finding equations that calculate the exact coupling coefficients and locations of the reflection zeros and hence the parameters in optimization process can be reduced and the optimization becomes faster.